

**SMART FOOD WASTE RECYCLING SYSTEM USING BLACK SOLDIER FLY  
LARVAE: DESIGN OF CIRCUIT AND INTEGRATION OF SENSORS**

MOK JIA LUO

INNOVATION & DESIGN PROGRAMME  
NATIONAL UNIVERSITY OF SINGAPORE

2024

**SMART FOOD WASTE RECYCLING SYSTEM USING BLACK SOLDIER FLY  
LARVAE: DESIGN OF CIRCUIT AND INTEGRATION OF SENSORS**

**MOK JIA LUO**

**A THESIS SUBMITTED FOR THE DEGREE OF  
BACHELOR OF ENGINEERING (ELECTRICAL ENGINEERING)  
INNOVATION & DESIGN PROGRAMME  
NATIONAL UNIVERSITY OF SINGAPORE**

## DECLARATION

I hereby declare that this thesis is my original work and it has been written by me in its entirety.

I have duly acknowledged all the sources of information which have been used in this thesis.

Except for the use of ChatGPT to rephrase some of the content.

A handwritten signature in black ink, appearing to read "Mok Jia Luo". It is written in a cursive style with a horizontal line underneath it.

Mok Jia Luo

6 April 2024

## ACKNOWLEDGEMENTS

Throughout the duration of this project, I have received a great deal of support and assistance which I would like to acknowledge in this section.

First and foremost, I would like to thank my supervisors, Dr Elliot Law and Miss Wong Kah Wei for their invaluable advice, continuous support, and patience throughout this project. Your insightful feedback and expert guidance on how to conduct research has broadened my perspective in the realm of research in the engineering field.

I would also like to thank Fuhrmann Adrian, a researcher from the Singapore-ETH Centre, for his invaluable expertise and generous provision of access to both his knowledge and facilities, which greatly benefited my research in this project.

I would like to thank the technicians and administrative staff who have helped me greatly during the prototyping phase. From the iDP electronics workshop, I would like to thank Miss Annie Tan for her advice and guidance on the design and fabrication of the electronics components.

Last but not least, I would like to thank my group mates, Ashley Chua Jun Hong, Man Chun Hang, Lim Ying Min Alica and Lee Wai Seng for their hard work and dedication throughout this project - from the ideation stage to prototyping and finally, reporting our findings in our individual dissertations.

# Table of Contents

<b>1. Food Waste Management in Singapore .....</b>	<b>1</b>
1.1    Food Waste Management .....	1
1.2    Negative Impact of Incineration Plants .....	2
1.3    Government's Plans to Manage Food Waste .....	3
1.4    Other Solutions Currently being Explored in Singapore.....	4
1.4.1        Anaerobic Digestion.....	4
1.4.2        Insects .....	5
<b>2. Using Black Soldier Fly Larvae to Treat Heterogenous Food Waste .....</b>	<b>6</b>
2.1    What is Black Soldier Fly (BSF).....	6
2.2    Why BSFL .....	7
2.3    Contributions to Food Security.....	8
2.4    Existing research with BSFL .....	9
2.5    Project Objective and Scope.....	13
2.5.1        Project Objectives .....	13
2.5.2        Project Vision .....	14
2.5.3        Value Proposition.....	15
<b>3. Concept Development Process.....</b>	<b>16</b>
3.1    Design Requirements .....	16
3.2    Concept Design.....	17
3.3    Scope of Work .....	20
<b>4 Testing of Various Sensors .....</b>	<b>22</b>
4.1    Moisture Content of the Substrate .....	23
4.2    Light Intensity .....	28
4.3    Temperature in the Substrate .....	31
4.4    Internal Air Temperature.....	33
4.5    Relative Humidity .....	35
4.6    Carbon Dioxide Emissions.....	38
4.7    Ammonia .....	41
4.8    Methane .....	42
4.9    pH Value .....	42
4.10    Mass of the Substrate.....	44
<b>5. Hardware and Software Integration .....</b>	<b>45</b>
5.1 Hardware Integration.....	46
5.1.1        Phase 1 .....	47

5.1.2	Phase 2 .....	55
5.1.3	Phase 3 (Full System Assembly Test) .....	61
5.1.3.1	Preparation at the BSFL Research facility .....	62
5.1.3.2	Installation and Assembly of the Electronics Components into Prototype .....	64
5.1.3.3	Placing the containers with substrate into the prototype.....	72
5.2.	Software Integration .....	74
<b>6.</b>	<b>Conclusion and Future Work.....</b>	<b>77</b>
<b>References.....</b>		<b>79</b>
<b>Appendix .....</b>		<b>87</b>
Appendix A:	List of Design Concepts.....	87
Appendix B:	Solution Principles .....	90
Appendix C:	Lift and Passageways Considerations in NUS .....	91
Appendix D:	Explanation for the Weight of the Reactor .....	94
Appendix E:	Explanation for the Dimensions of the Reactor.....	95
Appendix F:	Calculations to support the use of 6 fans in one 8-way extension safety socket.....	96

## **Summary**

In 2022, Singapore produced 813 million kg of food waste which equated to more than 2 bowls of rice per person per day. With food waste rank amongst the lowest in recycling rate, it has become a focal point for the local government, prompting exploration of methods to reduce food wastage. With the current trend of waste growth and minimal improvement in recycling rate, Singapore's sole landfill is projected to reach capacity by 2035, a decade earlier than anticipated.

Due to Singapore's consistently high waste generation and heavy reliance on incineration for waste management, the government is seeking alternative solutions that focus on environmental sustainability. It is now exploring the concept of a circular economy to repurpose food waste into valuable resources. Among the various technologies for processing food waste, the utilization of insects in organic waste bioconversion processes has garnered interest due to their capacity to convert low-value substrates into cost-effective, environmentally sustainable high-quality feed. One such insect is the Black Soldier Fly larvae. The Black Soldier Fly Larvae is regarded as the optimal choice due to its highly efficient feeding capability and capacity to process various waste streams.

However, a drawback of insect-based waste bioconversion is that the growth of insects is contingent upon the type of organic substrate. Although extensive research has been dedicated to utilizing the Black Soldier Fly Larvae for managing municipal food waste streams, most studies have investigated homogeneous waste streams within controlled environments. There is little research on municipal food waste of high degree of heterogeneity.

The problem statement is as follows: In order to efficiently treat and recycle Singapore's heterogenous food waste, more research is required to define the optimal parameters for maximizing BSFL utilization in this specific waste stream.

Therefore, the objective of this project is **to design a scale-up version of a deployable reactor that does on-site treatment process with minimal human labor.**

To evaluate the concept design, a one-third scale prototype of the proposed solution is developed. To enable the optimization of internal conditions within the reactor during the bioconversion process, sensors that measure conditions in the substrate and environment conditions in the reactor are needed.

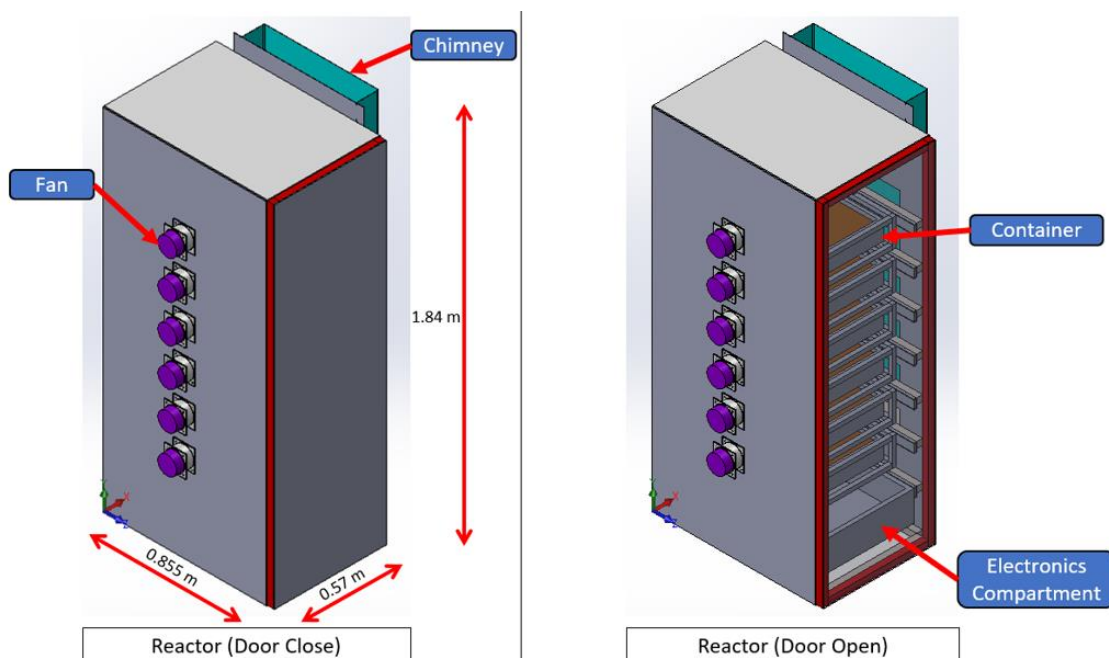


Fig. 9. A CAD showing the overall dimensions of the one-third scale prototype reactor, Door Close (left) and Door Open (right)

## List of Tables

Tab. 1. 2022 Waste Statistics in Singapore .....	1
Tab. 2. 2022 Recycling Rate Statistics in Singapore.....	1
Tab. 3. Singapore's Recycling Rate over a five-year period .....	2
Tab. 4. Overview of the Design Requirements .....	16
Tab. 5. 10 Parameters that will affect the development of the BSFL and the Location of the corresponding sensors.....	18
Tab. 6. Scope of Work Allocation.....	21
Tab. 7 Overview of the Two types of Sensors for each Corresponding Parameter.....	22
Tab. 8. Overview of the working Sensors and the their quantity planned to be used in each phase..	46
Tab 9. Overview of the Electrical Components and their Pinouts.....	71

## List of Figures

Fig. 1. Lifecycle of Black Soldier Fly .....	6
Fig. 2. Closing the Food Waste Loop with BSFL .....	8
Fig. 3. Climate Respiration Chamber.....	10
Fig. 4. Research Reactors for BSFL bioconversion by ETH Zurich, Singapore-ETH Centre, NUS funded by the National Research Foundation of Singapore at Block S4A .....	11
Fig. 5. Reactors that does On-Site Treatment Deployed at Hawker Centers around Singapore.....	14
Fig. 6. Key Stakeholders in the BSFL Bioconversion Process.....	15
Fig. 7. A Computer-Aided Design (CAD) of Reactor, Door Close (left) and Door Open (right) .....	17
Fig. 8. Functional Block Diagram (FBD) of the Reactor .....	19
Fig. 9. A CAD showing the overall dimensions of the one-third scale prototype reactor, Door Close (left) and Door Open (right) .....	20
Fig. 10. Resistive Soil Moisture Sensor (left) and Capacitive Soil Moisture Sensor (right) .....	23
Fig. 11. Oven (left), Frass Placed Inside Oven before Drying (middle), Frass after Drying for 48 hours at 80 °C (right) .....	25
Fig. 12. Frass Type #1 (top row) and Frass Type #2 (bottom row) with Three Moisture Content Levels each. 0% (left), 50% (middle), 80% (right) .....	25
Fig. 13. Soil Moisture Sensors In-direct Contact with Dry Frass .....	26
Fig. 14. Data from the Resistive Sensor in Frass Type #1 (Relationship Plotted on a Scatter Graph) ..	26
Fig. 15. Data from the Resistive Sensor in Frass Type #2 (Relationship Plotted on a Scatter Graph) ..	26
Fig 16. Data from the Capacitive Sensor in Frass Type #1 (Relationship Plotted on a Scatter Graph).).	27
Fig. 17. Data from the Capacitive Sensor in Frass Type #2 (Relationship Plotted on a Scatter Graph)	27
Fig. 18. Digital Luminosity Lux Light Sensor BH1750 .....	28
Fig. 19. Laboratory-Style Bioconversion Reactor with Two Cover Opening Angle, 10° (left), Greater than 50° (middle), Location of Protractor (right).....	29
Fig. 20. Location of BH1750 Light Sensor Inside the Laboratory-Style Reactor, away from the Opening (left), Middle of box (right) .....	29
Fig. 21. Data from BH1750 Lux Light Sensor inside the Laboratory-Style Reactor, positioned in the Middle and at Location farther away from opening (Plotted on a Scatter Graph) .....	30
Fig. 22. Digital Temperature Sensor DS18B20 Waterproof with JST Header .....	31

Fig. 23. Digital Pocket Thermometer (top), Sensor and Thermometer in Boiling Water (bottom left), Sensor and Thermometer in Chilled Water (bottom right) .....	32
Fig. 24. Comparison of the Readings against the Reference Device in Boiling Water and Chilled Water .....	32
Fig. 25. Digital Temperature Sensor DS18B20 .....	33
Fig. 26. Laboratory-Style Reactor (left), Inside the Reactor (middle), Fan (right) .....	34
Fig. 27. Readings from DS18B20 Digital Temperature Sensor inside the Laboratory-Style Reactor compared against Anemometer readings (top), Temperature dropped when the fan was turned on (bottom) .....	34
Fig. 28. Temperature Humidity Sensor DHT11 (left) and DHT22 (right) .....	35
Fig. 29. Top View of relative humidity sensors inside a container (top left), Front view relative humidity sensors inside a container (bottom left), To further prevent exposure to external environments (right) .....	36
Fig. 30. Readings from the DHT22 Humidity Sensors .....	36
Fig. 31. Specification Comparison between DHT11 and DHT22 .....	37
Fig. 32. 10,000ppm MH-Z16 NDIR CO <sub>2</sub> Sensor .....	38
Fig. 33. MH-Z16 CO <sub>2</sub> Sensor inside a Glass Jar with another CO <sub>2</sub> measuring device attached to reference machine .....	39
Fig. 34. Data from MH-Z16 CO <sub>2</sub> Sensor inside of Glass Jar .....	39
Fig. 35. SGP30 Air Quality Sensor .....	40
Fig. 36. MQ137 Ammonia Gas Sensor .....	41
Fig. 37. Gravity: Analog CH4 Gas Sensor .....	42
Fig. 38. Gravity Analog pH sensor .....	43
Fig. 39. Four 50 Kg Load with HX711 Amplifier Module .....	44
Fig. 40. Standalone reactor for BSFL bioconversion by ETH Zurich, Singapore-ETH Centre, NUS funded by the National Research Foundation of Singapore at Block S4A .....	45
Fig. 41. Timeline of Phase 1 .....	47
Fig. 42. Plastic Container in the center of large bin (left) and Plastic Container before start of experiment (right) .....	48
Fig. 43. Arduino Uno compatible Data Logging Shield V1.0 .....	49
Fig. 44. Plastic Container with sensors mounted (left) and Placement of Capacitive Soil Moisture Sensors in container (right) .....	50
Fig. 45. Plastic Container with sensors mounted (left) and Placement of DS18B20 Sensors in container (right) .....	50
Fig. 46. Data from the four Capacitive Sensor in open-air configuration setup (Plotted on a Line Graph) .....	51
Fig. 47. Data from Six DS18B20 Temperature Sensor in open-air configuration setup (Plotted on a Line Graph) .....	52
Fig. 48. Plastic Container with sensors mounted (left) and Placement of Analog pH Sensor in container (right) .....	53
Fig. 49. Data from two Gravity: Analog pH Sensor in open-air configuration setup (Plotted on a Line Graph) .....	54
Fig. 50. Timeline of Phase 2 .....	55
Fig. 51. Food waste, 5-DOL and Peanut Skin (left) and Top view after pouring the peanut skin over the food waste (right) .....	56
Fig. 52. Top view after pouring the 5-DOL over food waste in the center (left) and Larvae sitting above food waste (right) .....	56

Fig. 53. Top view before food container with substrate is placed inside standalone reactor (left) and Overview of the general locations of the various electronics (right) .....	57
Fig. 54. Location of sensors to measure conditions in the substrate in the standalone reactor .....	57
Fig 55. Fan mounted on the outside of reactor (left), Location of sensors to measure environmental conditions inside standalone reactor, outlet (middle), inlet (right) .....	58
Fig. 56. NUS Protoboard shield for Arduino Mega before soldering (top left), Components soldered onto protoboard (bottom left) and Micro SD Card Module connect to shield .....	59
Fig. 57. Modifications made to Protoboard Shield .....	60
Fig 58. Phase 3, Ongoing Experiment Timeline (Subject to Change) .....	61
Fig 59. (From left to right) Unprepared Food Waste, Food Waste on weighing scale, Before Food Waste is mixed with cocopeat, After Food Waste is mixed with cocopeat.....	62
Fig. 60. Food Plastic Container being weigh on weighing scale (left) and Substrate ready for BSFL (right) .....	62
Fig. 61. Height of the substrate measured with a ruler (left) and Substrate wrapped in clear plastic (right) .....	63
Fig. 62 General locations for sensors in the one-third scale prototype .....	64
Fig. 63. (left to right) Female Dupont Connections to ensure reliable connection from sensors to Arduino board .....	65
Fig. 64. Overview of the all the Electronics components Part #1 (Exclude the fans) .....	66
Fig. 65. Overview of the all the Electronics components Part #2 (Exclude sensors) .....	67
Fig. 66. Sensors mounted on aluminum profile at Top Container (left) and Sensors mounted inside the chimney (right) .....	68
Fig. 67. Electronic compartment view from the back of reactor, Electrical considerations to protect the electronics below from the substrate above.....	69
Fig. 68. Side view of Prototype where air vents are located (left) and Installation of wire mesh (right) .....	70
Fig. 69. Pictorial Diagram of Electronic Circuit showing the connections of the Sensors, Fans and 5 V Power supply.....	70
Fig. 70. Location of Phase 3 Experiment (left), View of the bioconversion process, door open (middle), Each level containing substrate (right).....	72
Fig. 71. pH sensor removed from middle and bottom container .....	73
Fig. 72. Flowchart of the Various Sensors Integrated Together .....	74
Fig. 73. Overview of Logical Flow for Storing of data and Regulating Air flow rate .....	75

# 1. Food Waste Management in Singapore

## 1.1 Food Waste Management

Singapore, a tropical island in Southeast Asia, has a total land area of 734.4 km<sup>2</sup> [1]. In 2022, this urban city, with a total population of 5.64 million people, generated about 7.39 million tonnes of solid waste [2]. Of the total solid waste, 12 percent or 813,000 tonnes was contributed by food waste which is equivalent to more than 2 bowls of rice per person per day [3], [4].

*Tab. 1. 2022 Waste Statistics in Singapore*

Waste Type	Total Generated ('000 tonnes)
Ferrous Metal	1,338
Paper/ Cardboard	1,064
Construction & Demolition	1,424
Plastics	1,001
Food	813
Horticultural	221

Source: Adapted from [2]

*Tab. 2. 2022 Recycling Rate Statistics in Singapore*

Waste Type	Recycling Rate (%)
Textile/ Leather	2
Plastics	6
Ash & Sludge	11
Glass	14
Food	18
Paper/ Cardboard	37

Source: Adapted from [2]

Although food wastage is rank fifth in the total waste generated and fifth in the lowest recycling rate, as presented in [2, Tab. 1] and [2, Tab. 2], the local government has been exploring various methods to minimize food wastage at the source as well as implement initiatives to increase the recycling rate [3]. However, with several initiatives launched such as the “Food Waste Reduction (FWR) outreach programme” in 2015 and the “3R Fund” co-funding scheme, the total food waste

generation, and the recycling rate, from 2018 to 2022, has shown extremely little improvement [3], [5]. With the current rate of waste growth and a recycling rate persisting at around 18 percent, as seen in [3, Tab. 3], not only has it contributed to a shortened lifespan of Singapore's only offshore landfill, but it has also contributed to an increase in carbon emissions, contributing to global warming [3], [4].

*Tab. 3. Singapore's Recycling Rate over a five-year period*

Year	Recycling Rate (%)
2022	18
2021	19
2020	19
2019	18
2018	17

Source: Adapted from [3]

## 1.2 Negative Impact of Incineration Plants

In the late 1970s, to reduce the volume of solid waste that was being transported to Pulau Semakau Landfill, the National Environment Agency (NEA) adopted the waste-to-energy (WTE) incineration technology [6]. With the process of incineration able to reduce the original volume of waste by up to 90%, a total of four WTE plants have been built in Singapore as of the year 2023 [6], [7]. Despite its effectiveness in waste disposal, which includes food waste, incineration has two main issues.

The first issue is related to the available space left at the landfill. Due to Singapore's growing population and thriving economy, the increase in solid waste, including food waste, has significantly increased the amount of waste transported over [7]. With only 2,000 tonnes of WTE incinerated ash and non-incinerable waste transported daily, the landfill is expected to be filled by 2035, 10 years earlier than initially planned [8], [9]. In a land scarce Singapore, with the current rate of waste growth, it is not sustainable to create another landfill as a new offshore landfill would be needed every 30 to 35 years [8].

The second issue is regarding carbon dioxide (CO<sub>2</sub>) emissions. Incinerating waste for energy production results in the emission of toxic pollutants including Methane (CH<sub>4</sub>), oxides of nitrogen (NO<sub>x</sub>) and most prominently, CO<sub>2</sub> [10], [11], [12]. Even though Singapore's WTE plants are equipped with a flue gas cleaning system, greenhouse gases like CO<sub>2</sub> continues to be released [13], [14]. With about 791,434 tonnes of CO<sub>2</sub> emitted in 2020 and 629,170 tonnes of CO<sub>2</sub> emitted in 2021, the incineration process continues to contribute to global warming and climate change [15]. As Singapore shifts towards a more sustainable waste and resource management nation, there is a need to increase the overall recycling rate of the solid waste, including food waste, to reduce both the amount of waste sent to the landfill as well as CO<sub>2</sub> emissions from WTE plants [16].

### **1.3 Government's Plans to Manage Food Waste**

Given Singapore's historically high waste output and a waste management system that heavily relies on waste incineration as the primary means of disposal, Singapore made a national commitment towards protecting the environment [17]. In 2019, it embarked on its journey towards becoming a Zero Waste Nation [18]. Amongst the various waste streams, food waste is known to be one of the biggest [4]. In the same year, Singapore generated around 744 million kg of food waste which is equivalent 51,000 double decker buses [4]. To minimize this waste, there were both FWR outreach programs to reduce food wastage at its source as well as extensive awareness campaigns encouraging organizations and consumers to adopt smart food waste practices [4], [5]. Through legislation, under the landmark Resource Sustainability Act (RSA), there are two requirements related to treating food waste [3], [19]. Firstly, from 2021 onwards, developers of new industrial and commercial premises, such as food caterers and malls, are required to allocate and designate approximately two carpark lots for on-site food waste treatment in their design plans [3], [19]. Secondly, from 2024 onwards, industrial food waste generators such as food manufacturers and supermarkets, will need to not only segregate their food waste, but also implement a suitable treatment method to recycle their food waste [3], [19].

With various initiatives underway, to further enhance their capacity in addressing future challenges concerning resource security and scarcity, the government proceeded to drive the transition to a circular economy [18]. Instead of discarding food to be incinerated, there is potential to recycle the waste into valuable resources [19]. With the implementation of on-site food waste treatment systems, store owners and premises operators can convert their food waste into compost for landscaping purposes or water for non-potable uses, depending on the chosen treatment system [5]. Therefore, aligning with national goals and ongoing push for environmental sustainability, the adoption of a circular economy approach for the treatment and recycling of food waste becomes imperative to manage high waste growth and a low recycling rate.

## **1.4 Other Solutions Currently being Explored in Singapore**

According to Singapore's food waste management hierarchy, the highest priority is placed on prevention and reduction of food waste at its source, rather than on mitigation [3]. Nonetheless, in the context of a circular economy, innovation and developments in recycling and treating food waste hold equal importance. Among the numerous technologies available to process food waste and convert it into reusable resources, two technologies have demonstrated significant effectiveness in their unique ways.

### **1.4.1 Anaerobic Digestion**

The first technology is Anaerobic Digestion (AD). AD is a process that decomposes organic matter, such as agricultural and food waste, with the help of various anaerobic microorganisms in the absence of oxygen [20]. At the end of the AD process, the output is left with organic residue as well as biogas which generally consist of CH<sub>4</sub> and CO<sub>2</sub> [10], [20]. Given its potential in the production of biofertilizer and biogas for energy generation, an AD system is being piloted at the East Coast Lagoon Food Village [20], [21]. With this on-site food waste treatment system, the food waste loop can be closed at the source as the biogas produced is converted into electricity while the biofertilizer is used for NParks' landscaping application around East Coast Park [21]. However, with the methanogenic

reaction in the biogas production necessitating 20 to 40 days for each cycle, it is a common challenge associated with the use of AD [10]. This extended duration, together with other challenges including the process's sensitivity to acidity changes, is what makes AD a challenging technology to manage [10], [20], [22]. Furthermore, depending on the initial composition of the feedstock, the quality of the digestate (material that remains after the anaerobic digestion) and other by-products may not be environmentally safe and will require further treatment before it can be re-used [20]. Despite the various challenges, AD remains an efficient waste management technology [22]. This is evident in Singapore's plan to integrate AD technology into Tuas Nexus, Singapore's first integrated water and solid waste treatment facility, scheduled for completion in 2025 [23].

#### **1.4.2 Insects**

The second technology is the use of insects in organic waste bioconversion processes. Insects, for example yellow mealworm, housefly, and black soldier fly larvae (BSFL), have gained attention for their ability to transform low-value substrates into affordable, sustainable high-quality feed and organic fertilizers [24]. With their short life cycle, low gas emission, limited land and water requirements, when these insects are fed with organic waste, they will also generate biomass rich in proteins, fats and other minerals [24]. The utilization of insects, which are more sustainable and have a low impact on the environment, would not only effectively treat food waste but also provide a sustainable and circular livestock feed [24]. One disadvantage with insect-based waste bioconversion is that because the insect's growth depends on the type of organic substrate, depending on the type of insects, the type of organic waste will have to differ to ensure effective waste management [24].

## 2. Using Black Soldier Fly Larvae to Treat Heterogenous Food Waste

There are many insects that are considered highly versatile and adaptable to a variety of organic waste with high conversion rates [24]. Insects such as the mealworms, common houseflies, and black soldier fly (BSF) are currently among the most extensively studied insects in organic waste conversion, as well as their ability to serve as alternative protein source for animal feed [25]. Among the various insect species, the potential of BSFL to process organic waste has garnered increased attention [25].

### 2.1 What is Black Soldier Fly (BSF)

The BSF (*Hermetia illucens*) is an insect species belonging to the Dipteran family, Stratiomyidae. Their habitat lies within warm temperatures and tropical regions, spanning between the latitudes of 40°S and 45°N, making it survivable in Singapore conditions [26], [27], [28].

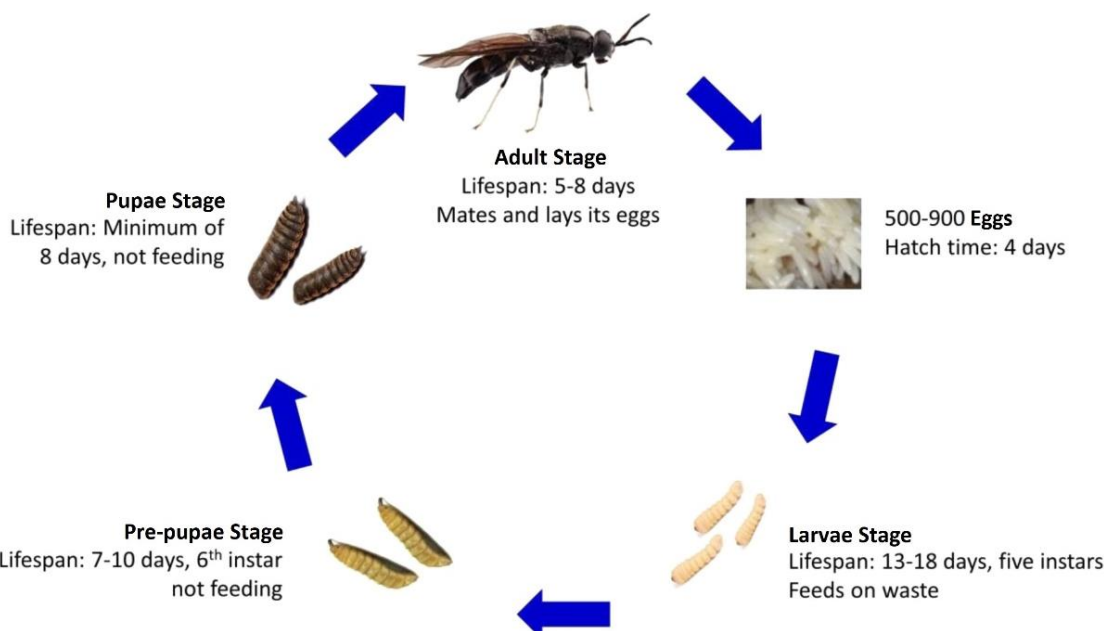


Fig. 1. Lifecycle of Black Soldier Fly  
Source: Adapted from [28]

The life cycle of the BSF consists of five major stages as illustrated in [28, Fig. 1] namely, egg, larvae, pre-pupae, pupae, and adult [28]. The larvae and pre-pupae stages make up the majority of the BSF lifecycle, while the relatively short stages of the BSF include the adults and egg hatching stages

[28]. When the files reach the adult stage, they will not be able to digest any food and can only take in liquid supplements [26]. Therefore, after hatching, the BSFL will voraciously consume various types of organic waste, while storing significant quantities of fat and protein in its body for subsequent life stages [26]. The feeding duration of the BSFL typically spans two to four weeks, depending on various factors such as environmental conditions, food availability, amongst others [26]. If the organic waste lacks proper nutrients or if the environmental conditions are unfavorable, the larvae are known to slow their feeding rate, thereby prolonging their transition to the pre-pupae stage, which can extend to anywhere between six to eight weeks [26], [28].

## 2.2 Why BSFL

In the insect industry, where rapid growth and a high conversion rate from cheap organic waste to high-quality animal feed and soil fertilizers are sought after, the BSFL is considered the top choice [28]. This is because the BSFL has: highly efficient feeding capability, ability to treat multiple waste streams, and high profitability from converting low-value organic waste into high-value resources.

Firstly, an attribute of the BSFL is its ability to efficiently reduce organic waste [29]. The BSFL can consume up to four times its body weight in food waste daily, potentially resulting in an 80% reduction by the end of the bioconversion process [29], [30]. By having a high waste reduction, the BSFL has been discovered to have the ability to neutralize disease-causing bacteria like *Salmonella spp* [29]. Thus, as an adult BSF, this insect species poses no threat in transmitting dangerous diseases to animals or humans [29], [31].

Secondly, acknowledging that various types of organic substrates will influence insect growth, the BSFL has shown versatility in their feedstock preferences and has been found to be able to effectively treat a variety of organic waste streams [31]. Among the 11 substrates tested, abattoir waste, food waste, human feces, and a mixture of abattoir waste with fruits and vegetables were identified as highly suitable for BSFL treatment [31]. The study, which analyzed parameters such as biomass conversion ratio, larval development time, and waste reduction, highlighted protein and

volatile solid content as key substrate properties which will affect larval development [31]. Hence, given the BSFL's adaptability to various waste streams, if the food waste or substrate is heterogeneous in nature, the BSFL would likely still be effective in treating the waste.

Thirdly, BSFL are efficient in converting low quality decaying organic waste into high-quality products [25]. Not only can the BSFL break down organic waste, but it can also convert the waste into larval biomass while enhancing the quality of the substrate by reducing the heavy metal concentration in the waste stream [25], [26]. In addition to reducing municipal solid waste, the BSF system also aligns seamlessly with a circular economy model. After reducing the weight of the food waste, the BSF pupae can be used for commercial purposes such as protein-rich animal feed, lipid and chitin extraction, among others [26]. At the end of the bioconversion process, the residue or frass can be collected and re-used as high-quality soil fertilizers, ensuring a complete bioconversion process with zero waste remaining [25]. The utilization of the BSFL offers numerous advantages, including a significant national benefit in the form of enhanced food security.

## 2.3 Contributions to Food Security

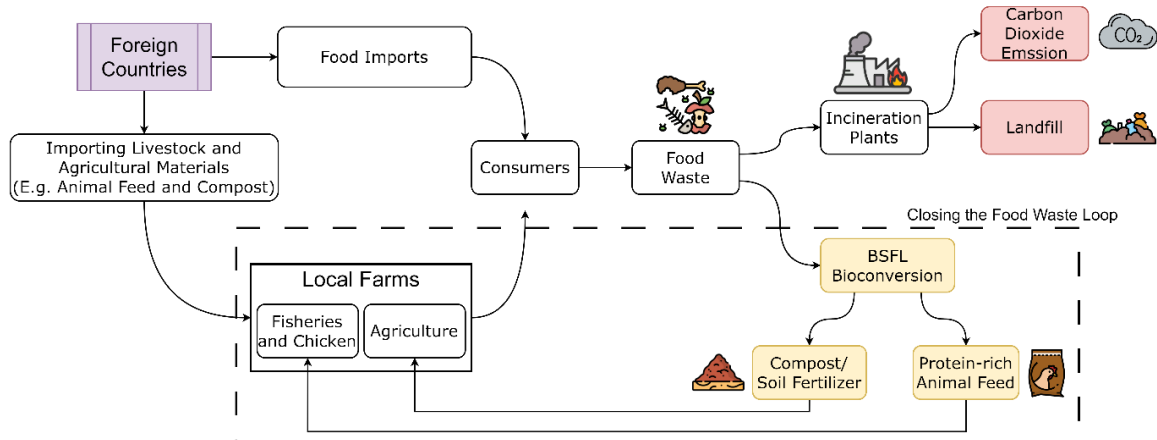


*Fig. 2. Closing the Food Waste Loop with BSFL*

Source: Adapted from [30]

According to the Singapore Food Agency (SFA), there is a heavy reliance on food imports given that more than 90 percent of Singapore's food is imported and only one percent of Singapore's land is set aside for farming [32], [33]. Due to land and resource constraints, Singapore is also dependent

on imports for agricultural purposes such as livestock feed and fertilizers [30], [33], [34]. As stated in 'Singapore Green Plan 2030', the government is looking for a more resilient food future and is committed to the '30 by 30' initiative [33], [35]. This initiative aims to develop Singapore's agricultural food industry to meet 30 percent of the country's nutritional requirements by the year 2030 [33], [35]. Therefore, with the BSFL ability to produce compost as well as serve as an alternative protein source, the BSFL is an ideal candidate in nutrient recovery while strengthening Singapore's food security via closing the food waste loop, as illustrated in [30, Fig. 2]. With food waste as the feedstock, the BSFL can not only convert the waste into valuable resources, but there will also be a reduction in the total amount of waste sent to the WTE plants, leading to a reduction in CO<sub>2</sub> emissions and incinerated ash from being transported over to the landfill.

## 2.4 Existing research with BSFL

Numerous research has been conducted on the utilization of the BSFL to address waste management issues at both local and global level [26], [28]. Among the various research areas, which range from investigating environmental factors to studying the impact of waste with diverse elements like metals, feed quality has surfaced as one of the most extensively studied subjects [26]. Without proper nutrition, which is an essential element in the development to pre-pupae, the development time will be severely affected, potentially extending to as long as two months [26]. However, an area of research that appears to be lacking is the study of how heterogeneous types of municipal food waste can affect the growth of BSFL.

During the experiments, although various types of substrates such as dog food, food waste, slaughterhouse waste and human faeces were tested, most of them were refined to achieve a homogeneous nature [31], [36], [37]. This homogeneity refers to either a uniform mixture, where the components are evenly distributed, or a single mixture where the composition is constant throughout [36], [37]. The reason behind this is likely to ensure accurate results by minimizing variability in the experiment. By achieving homogeneity in the substrate, the various findings including ideal substrate

conditions to achieve optimal larvae growth would likely be reliable and replicated in other BSFL laboratory experiments. However, these parameters may not be the same or applicable when dealing with heterogenous food waste, which can vary in the size of the food particles, nutritional quality within the waste as well as the uneven mixture of elements in the waste stream.

Besides the gap in the research field concerning optimal growth parameters in heterogenous food waste, most current experiments are conducted in laboratory settings [31], [37], [38]. These settings primarily employ the use of simple plastic containers or plastic cups and rely heavily on human intervention [31], [38], [39]. Although researchers are moving towards utilizing more advanced equipment in their experiments, these tools are likely specifically designed to be set up within their own laboratory environments [37]. An example of such equipment is the Climate Respiration Chamber in [37, Fig. 3]. This equipment has been specifically designed to connect to various gas pipes, allowing for precise control over gas variables [37]. Despite its unique characteristics, this chamber still requires human assistance to load and unload three plastic crates, each measuring 0.5 x 0.3 x 0.1m and filled with four kg of substrate, into and out of the chamber [37]. Handling four crates, each weighing about four kg, may not seem challenging initially. However, over time and with the potential expansion of the set-up, the repetitive loading and unloading tasks could pose long-term risks.

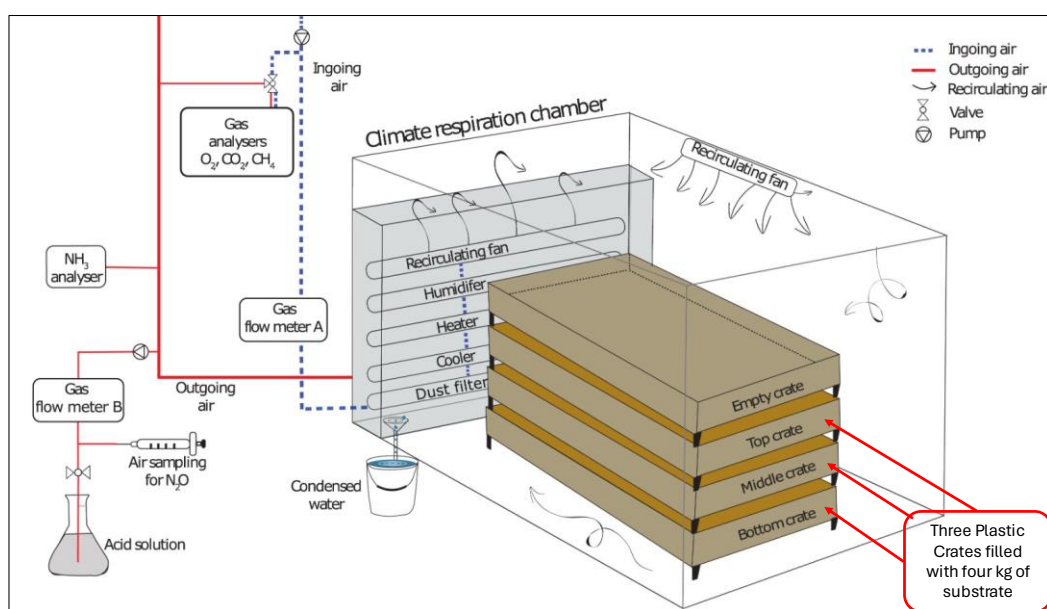


*Fig. 3. Climate Respiration Chamber*  
Source: Adapted from [37]



Fig. 4. Research Reactors for BSFL bioconversion by ETH Zurich, Singapore-ETH Centre, NUS funded by the National Research Foundation of Singapore at Block S4A

Another example of a laboratory style set-up is shown in [Fig. 4]. These reactors are currently being used to facilitate the treatment process of the BSFL in research areas surrounding food waste management and sustainable food production in urban systems. However, due to constraints related to the physical design, these reactors are not optimized for large-scale deployment outside of a laboratory environment. These constraints include handling of multiple containers, each containing 8 kg of food waste, in and out of the reactor, as well as having a footprint length of approximately 3 m, which includes the 0.1 m diameter grey pipes (A. Fuhrmann, personal communication, March 27, 2024).

Should a portable BSFL bioconversion chamber or reactor, optimized for large-scale deployment, be developed, there is still the question of identifying the ideal environmental parameters. As mentioned above, [31], [37], [38], most of the experiments conducted have been in laboratory settings where the BSFL would be reared in a generally well-controlled environment with constant external conditions. The optimum internal environmental conditions (i.e., inside the bioconversion chamber or reactor) identified are most likely determined in laboratory settings with the current setup. A portable bioconversion reactor intended for larger-scale deployment would likely require substantially larger dimensions.

In addition, if a BSFL-based solution is to be deployed at a wider scale, it is likely that such a reactor may need to be deployed outdoors which will have a higher variability in external environmental conditions such temperature and relative humidity. These two environmental factors are just a few of the many parameters that have been known to affect the survival rate of the BSFL [25], [26]. The optimum internal conditions found in previous lab-scale studies may not be fully applicable anymore and hence warrants further investigation in larger-scale setups.

As such, given the aforementioned research gaps, there is a need to determine to what extent the various parameters, from the laboratory, can be extrapolated to a scaled-up implementation for achieving optimal larvae growth with municipal food waste with high degree of heterogeneity.

## **2.5 Project Objective and Scope**

### **2.5.1 Project Objectives**

The process of incineration not only generates greenhouse gases, leading to global warming and other environmental issues, but the incineration ash, that is transported over to the landfill daily, is causing Singapore's only landfill to fill up more quickly than projected. Despite various government initiatives aimed at reducing food wastage at the source, the volume of generated food waste has remained high, with no significant improvement in the recycling rates of food waste. Amid the push for circular economy to recycle food waste, the BSFL stands out as an ideal candidate for reducing and treating municipal food waste, particularly in light of Singapore's land scarcity and limited resources, while providing high-quality by-products. While considerable research has focused on the utilization of the BSFL to address municipal food waste streams, most studies have examined homogeneous waste streams within controlled environments. Further research is necessary to address municipal food waste characterized by high levels of heterogeneity in a setting with higher variability in external environmental conditions.

The problem statement is as follows: In order to efficiently treat and recycle Singapore's heterogeneous food waste, more research is required to define the optimal parameters for maximizing BSFL utilization in this specific waste stream. Therefore, the objective of this project is **to design a scale-up version of a deployable reactor that does on-site treatment process with minimal human labor**. The scope of the project is to develop a proof-of-concept prototype for such a solution.

## 2.5.2 Project Vision

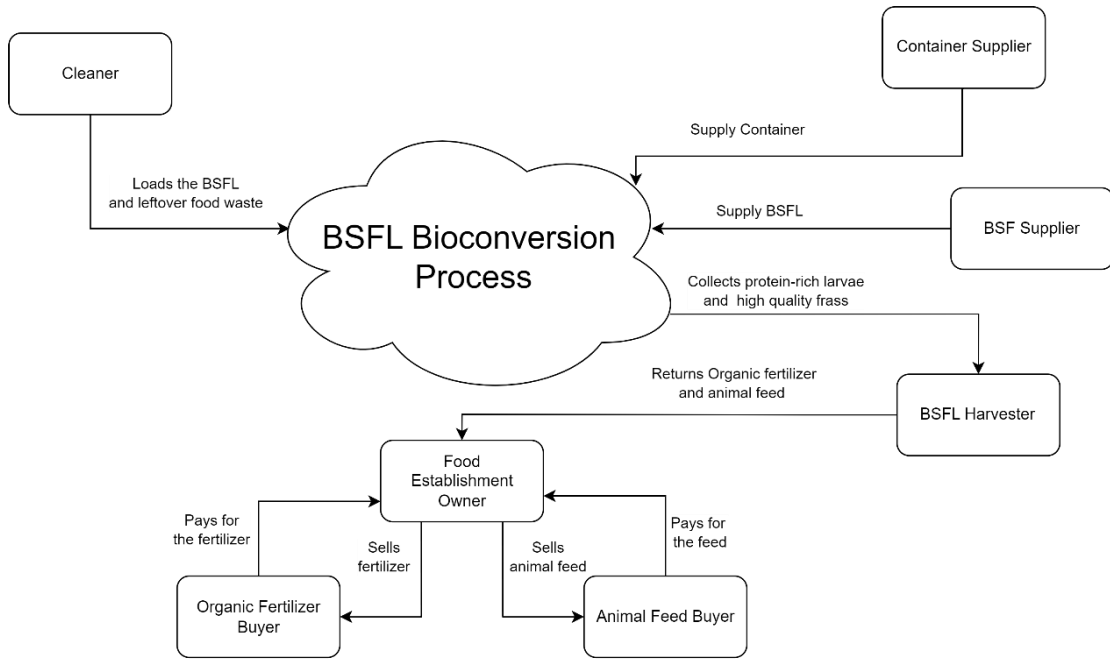


Fig. 5. Reactors that does On-Site Treatment Deployed at Hawker Centers around Singapore.

As of September 28, 2023, according to NEA, there exist over 110 hawker centers situated throughout Singapore [40]. While each hawker center's food waste output varies based on factors like visitor count and volume of food cooked, collectively, these centers will produce significant amounts of food waste. For instance, East Coast Lagoon Food Village, with 60 occupied stalls, was recorded to produce 150 kg of edible food waste daily [41]. Using this figure, we can estimate that in Singapore, solely from hawker centers, approximately 16,500 kg or 16.5 tonnes of heterogenous food waste are produced daily, collected, and sent to the four WTE plants for incineration.

By utilizing a reactor that uses BSFL to treat food waste at its source, not only would it reduce waste transportation costs, but it would also contribute to a decrease in CO<sub>2</sub> emissions from both food waste collection trucks and WTE plants. With reactors deployed in a decentralized manner, as illustrated in [Fig. 5], the reduction in food waste sent for incineration would aid in slowing the filling rate of the Pulau Semakau Landfill. Installing these reactors at hawker centers should not pose a significant problem, considering that the government has planned for commercial venues to assign specific areas for on-site food waste treatment, as mentioned in Section 1.3.

### 2.5.3 Value Proposition



*Fig. 6. Key Stakeholders in the BSFL Bioconversion Process*

To achieve the project vision outlined in Section 2.4.2, cooperation among the various stakeholders is necessary, as illustrated in [Fig. 6]. Seven key stakeholders have been identified: cleaners, container supplier, BSF supplier, BSFL harvester, food establishment owners, fertilizer, and feed buyer.

The involvement of cleaners is crucial as they would be the main operators for the reactor. Furthermore, considering that the reactor is planned to be situated within a food marketplace, it is important to provide incentives to encourage its adoption and integration. After the bioconversion process, where valuable resources like organic fertilizer and animal feed are generated, the plan is for food establishment owners to gain an additional means of generating income by selling fertilizers and animal feeds.

### 3. Concept Development Process

A total of 4 design concepts (Appendix A) had been generated based on functional analysis and refined using solution principles (Appendix B). The rest of the report will focus on the selected design discussed below.

#### 3.1 Design Requirements

A summary of the design requirements and the derivation of how these values were determined can be found in [Tab. 4].

*Tab. 4. Overview of the Design Requirements*

Criteria	Requirements	Rational
Size of Reactor	Does not have a footprint of more than Length: <b>1.4 m</b> Breadth: <b>1.2 m</b> Height: <b>2.1 m</b>	The size of the reactor will be constrained to fit within the dimensions of lifts in Singapore (Appendix C).
Weight	Weight of the reactor cannot exceed <b>280 kg</b>	The reactor needs to be transportable to different hawker centers in Singapore. The reactor's weight must remain below the maximum weight capacity of lifts (Appendix D).
Survival	Ensure internal air temperature remains between <b>25 °C and 35 °C</b>	Unfavorable conditions will prevent the larvae from feeding regularly [25], [26].
	Ensure Environmental Humidity does not drop below <b>40 % RH</b>	Mortality for the BSFL is 62, 26, and 3 % at a relative humidity of 25, 40, and 70 %, respectively [26].
	Light intensity inside the reactor ideally should be <b>0 lux</b> .	During feeding, the larvae will avoid sources of light and search for a shaded environment to feed. Unfavorable conditions will prevent the larvae from feeding [27].
	Prevent accumulation of toxic gas within the reactor during bioconversion (E.g., CO <sub>2</sub> , NH <sub>3</sub> and CH <sub>4</sub> )	During the bioconversion process, small quantities of toxic gases are produced as a result of feeding [25], [36]. Without adequate aeration, these gases can accumulate over time.
	Moisture content of the substrate is within <b>40 % and 80 %</b>	Moisture content affects the growth of the BSFL [25], [26].
	Temperature in the substrate is within <b>25 °C and 47 °C</b>	Temperature above <b>47 °C</b> is seen as lethal [42].
Ensure BSFL remains in the feeding container	Cannot have more than <b>5 %</b> of the BSFL escape from the feeding pod	The quality of valuable resources that will be harvested is affected by the efficiency of the bioconversion process (A. Fuhrmann, personal communication, March 27, 2024).
Ease of separation between frass and BSFL	Moisture Content of the substrate falls below <b>50 %</b> after the bioconversion process	Moisture content above 50 % will hinder the separation process during product harvesting [42].

Pest Prevention	Ensure rodents, insects and other animals do not enter the reactor during the bioconversion process	The presence of foreign animals will affect the efficiency of the bioconversion process (A. Fuhrmann, personal communication, March 27, 2024).
-----------------	---	--

### 3.2 Concept Design

A Computer-Aided Design (CAD) of the reactor is shown in [Fig. 7]. This reactor will utilize BSFL to efficiently treat and recycle municipal food waste which contains high degrees of heterogeneity, including variations in the size of food particles and an uneven mixture of elements in the food waste stream.

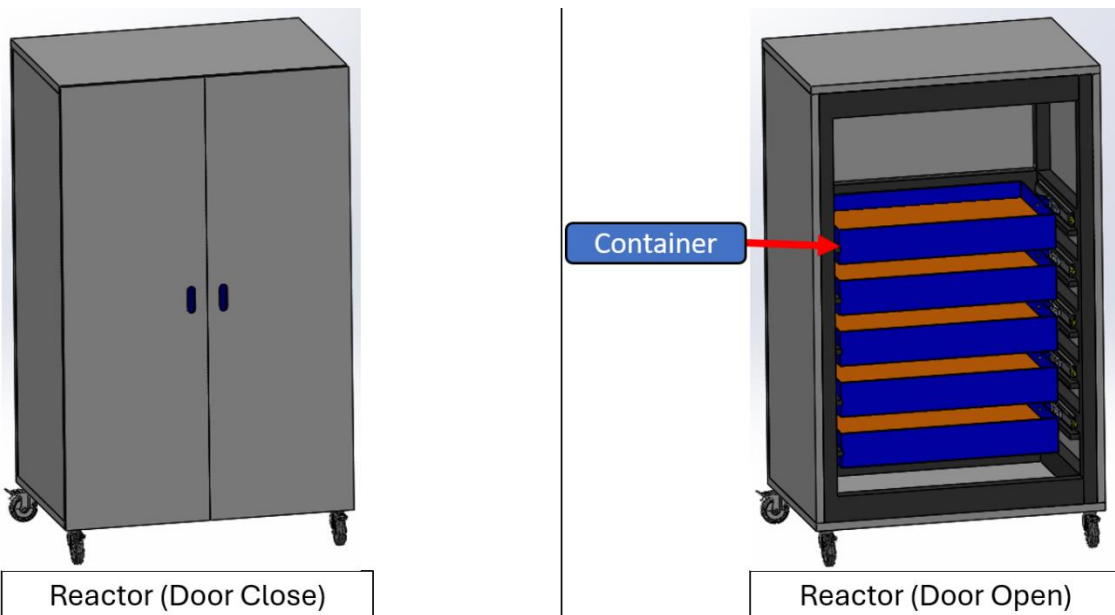


Fig. 7. A Computer-Aided Design (CAD) of Reactor, Door Close (left) and Door Open (right)

Five custom containers will be fabricated to accommodate approximately 150 kg of food waste in total. Within the reactor, it will be divided into two sections. The lower section will provide space for the five containers to be stacked in a vertical manner with a slight gap between them for aeration while the upper section will accommodate the bulk of the electronic components.

Although the containers are positioned at the lower section, considering the substantial amount of waste intended for treatment and recycling, the reactor will be designed in a way that facilitates easy loading and unloading of the food waste. In addition, due to the impact of environmental factors

on the growth of BSFL as well as bioconversion efficiency, various types of sensors will need to be placed within the reactor [26], [27].

*Tab. 5. 10 Parameters that will affect the development of the BSFL and the Location of the corresponding sensors*

Parameters	Rational	Location of the Sensors
<b>Moisture Content of the Substrate</b>	Survival and Separation	Inside the Food Waste
<b>Light Intensity</b>		Around the Containers
<b>Temperature in the Substrate</b>		Inside the Food Waste
<b>Internal Air Temperature</b>	Survival	Around the Containers
<b>Relative Humidity</b>		Around the Containers
<b>Gas Emission (CO<sub>2</sub>, NH<sub>3</sub>, CH<sub>4</sub>)</b>	Survival and Indication for Harvesting	Around the Containers
<b>pH Value of the Substrate</b>	Indication for Harvesting	Inside the Food Waste
<b>Mass of the Food Waste in each container</b>	Growth of BSFL and Indicator for bioconversion	Inside the Reactor
<b>Air Flow Rate</b>	Ensure proper airflow and adequate ventilation inside	Inside the Reactor
<b>Larval Density per container</b>	Availability of Nutrients	Inside the reactor

Depending on specific parameters, as listed in [Tab. 5], certain sensors will be embedded within the food waste (which is henceforth referred to as substrate), while others will be positioned either around the containers or somewhere inside the reactor. As shown in [Tab. 4], it is indicated that for survival, it is necessary to prevent the accumulation of toxic gases within the reactor during the bioconversion process. As such, a fan shall be utilized to generate the airflow and meet this requirement. A fan is chosen due to its simplicity and versatility, as it can be controlled by a microprocessor through pulse width modulation (PWM). Besides preventing stagnant air, the fan will also serve as the primary method for controlling the temperature, humidity, and moisture content inside of the reactor. The air flow rate parameter, regulated by the fan, will be adjusted according to the readings provided by the other sensors installed within the reactor. For example, if the

temperature in the substrate exceeds 47 °C, the fan will increase its speed to amplify the air flow rate inside the reactor and lower the substrate temperature to a safer level.

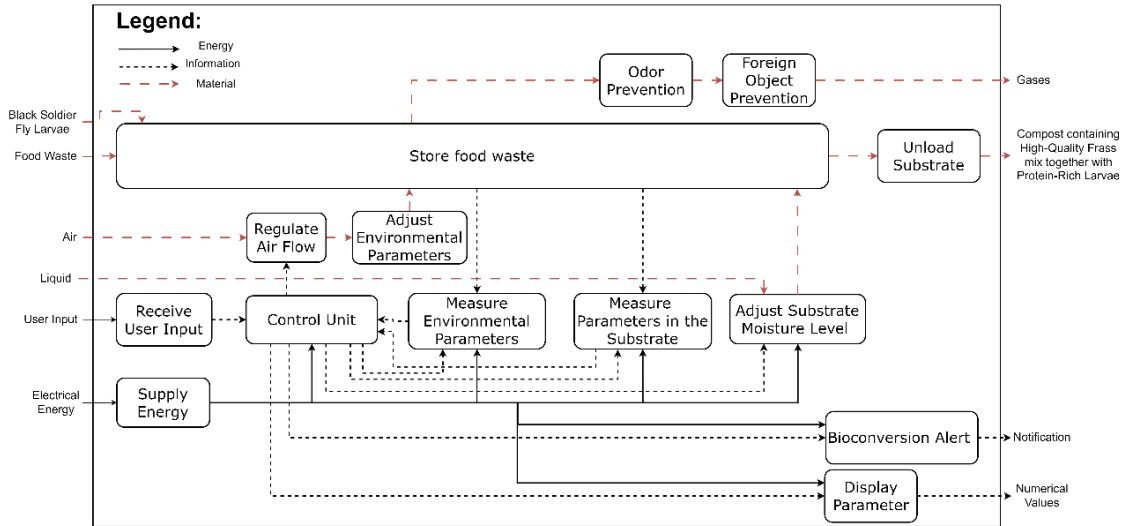


Fig. 8. Functional Block Diagram (FBD) of the Reactor

[Fig. 8] shows the functional block diagram of the reactor. Food waste will be loaded and stored inside the reactor. After the BSFL is placed into the food waste, various sensors will begin to monitor and track their respective parameters, either in the environment or the substrate. Based on the measured readings, the control unit will send PWM signals to adjust the fan speed. This adjustment will regulate the airflow, thereby controlling the environmental parameters within the reactor.

With the help of sensors to monitor substrate moisture level, pH value of the substrate and CO<sub>2</sub> emissions, these parameters can be used to determine the ideal point in time for product harvesting. When the desired point for harvesting is reached, for instance when the CO<sub>2</sub> reading plateau, the reactor will send a notification to the BSFL harvester, informing them that the BSFL is ready for harvesting. The reason for utilizing the plateauing of CO<sub>2</sub> readings can be elucidated by referring to the lifecycle of the BSFL, as illustrated in Section 2.1. As the BSFL reaches the pre-pupae stage, the conversion from substrate to compost will stop as the larvae would have stopped feeding [28]. The BSFL harvester is needed to collect the larvae for harvesting as well as to resume the bioconversion process with a new batch of larvae.

### 3.3 Scope of Work

To evaluate the concept design, a one-third scale prototype of the proposed solution, shown in [Fig. 9] will be built. Scaling down is necessary to manage the constraints of limited resources and available time. To conduct any experiments, larvae will be sourced from the BSFL research facility at Block S4A. The research team prepares batches of roughly 10,000 five-day-old larvae (5-DOL) for their experiments, adhering to specific practices conducted by the research team (A. Fuhrmann, personal communication, March 27, 2024). These preparations are limited to certain times of the month in line with the BSFL lifecycle. Considering the project vision outlined in Section 2.5.2, which envisions the treatment of approximately 150 kg of food waste, obtaining the required quantity of about 1,875,000 larvae for experimentation will present a significant challenge.

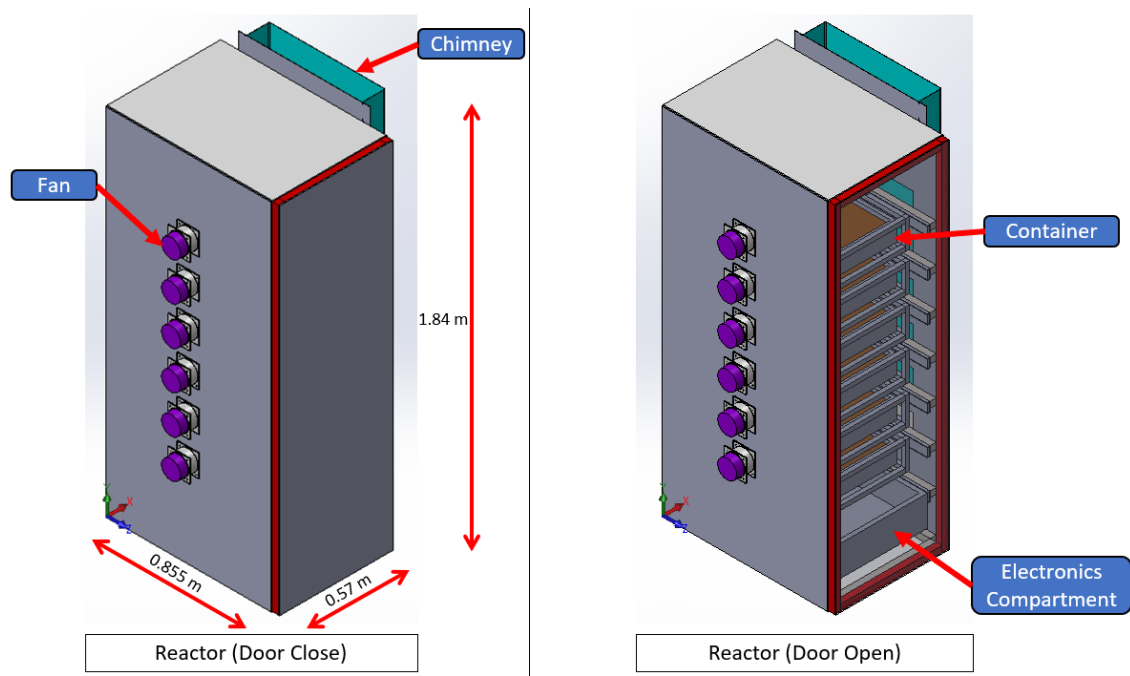


Fig. 9. A CAD showing the overall dimensions of the one-third scale prototype reactor, Door Close (left) and Door Open (right)

Note: 1.84 m is the total height of the reactor with wheels attached

As shown in [Fig. 9], the dimensions of the one-third scale reactor are **0.885 (L) x 0.57 (B) x 1.84 (H) m**. Air will be drawn in via the utilization of fans and subsequently, exit through the chimney situated on the opposite side. Rather than fabricating custom containers, which would reduce the flexibility and adaptability of a deployable reactor, the reactor will utilize a standard food plastic

containers of dimensions **0.435 (L) x 0.292 (B) x 0.09 (H) m**, obtained from the BSFL research facility.

To facilitate ease of maintenance, the electronic components will be repositioned to the bottom of the reactor.

To realize the proposed solution, the work has been divided into 2 main sub-teams and 5 supporting subsystems as listed in [Tab. 6], with this report focusing on **sensors** and **data and software**. The mechanical team aims to streamline the labor-intensive task of handling heavy food waste for the loaders and unloaders. Meanwhile, the electronics team will focus on enabling the optimization of the internal conditions within the reactor during the bioconversion process. This design should allow for some form of control over the internal conditions, including but not limited to internal air temperature, CO<sub>2</sub>, and moisture content of the substrate, outside of a laboratory setting.

In order for the internal conditions within the reactor to be efficiently controlled, the following questions will need to be investigated: the number of sensors for each parameter, the placement of the various sensors, procedure for the storage of the collected data and whether filtering of the data, to a certain extent, is required.

Tab. 6. Scope of Work Allocation

		Lim Ying Min, Alicia	Ashley Chua Jun Hong	Man Chun Hang	Lee Wai Seng	Mok Jia Luo
Mechanical	Ventilation	✓				
	Chassis and Container	✓	✓	✓		
Electronics	Sensors and data				✓	✓
	Software			✓		✓
	Power and Integration		✓		✓	

## 4 Testing of Various Sensors

[Tab. 5] shows a total of 10 parameters known to influence the development and growth of the BSFL. To monitor these parameters, various sensors will need to be installed inside the reactor. The sensors, in [Tab. 7], have been identified due to their availability in stores in Singapore and their compatibility with student-level projects, such as those involving Arduino or Raspberry Pi.

*Tab. 7 Overview of the Two types of Sensors for each Corresponding Parameter*

Parameters	Sensors Classification	Type of Sensors Identified	
		#1	#2
<b>Moisture Content of the Substrate</b>	Contact	Resistive Soil Moisture	Capacitive Soil Moisture
<b>Light Intensity</b>	Non-Contact	Ambient Light (BH1750)	-
<b>Temperature in the Substrate</b>	Contact	DS18B20 1-Wire Digital	-
<b>Internal Air Temperature</b>	Non-Contact	DS18B20 1-Wire Digital	DHT22 Module
<b>Relative Humidity</b>	Non-Contact	DHT11 Module	DHT22 Module
<b>Gas Emission (CO<sub>2</sub>)</b>	Non-Contact	MH-Z16 NDIR	SGP30
<b>Gas Emission (NH<sub>3</sub>)</b>	Non-Contact	MQ137	-
<b>Gas Emission (CH<sub>4</sub>)</b>	Non-Contact	MQ2	MQ4
<b>pH Value of the Substrate</b>	Contact	Analog pH	-
<b>Mass of the substrate in each container</b>	Contact	50kg Load Cells with HX711 amplifier module	-
<b>Air Flow Rate</b>	Non-Contact	Wind Speed (Adafruit Anemometer) <sup>1</sup>	-
<b>Larval Density per container</b>	Non-Contact	-	-

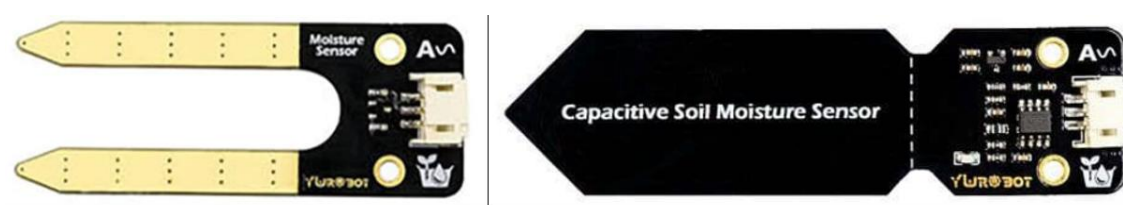
Note: <sup>[1]</sup> Sensor was not purchased due to its operating voltage of 7V, which exceeds the operating voltages of Arduino and Raspberry Pi. The additional cost required to provide specialized power for a single device is deemed unwarranted during this initial prototyping.

Parameters such as moisture content, substrate temperature, and pH value will utilize contact sensors, while the remaining parameters will be monitored using non-contact sensors. For the 'Air Flow Rate' parameter, a handheld anemometer will be utilized instead of a microcontroller-compatible device. Constant monitoring of the "Air Flow Rate" parameter is deemed unnecessary due

to the fixed structure of the reactor. This parameter will only need to be measured during the initial testing phase of the project. Once the reactor is deployed for on-site food waste treatment, tracking of this parameter will no longer be needed. In addition, although the "Larval Density per container" parameter holds significance due to nutrient availability, its meticulous tracking is not deemed crucial at this stage of prototyping. Unlike other parameters, the necessity to precisely count or monitor larvae spread within each container is relatively less pressing. As such, this parameter will no longer be discussed in the remainder of the report.

#### 4.1 Moisture Content of the Substrate

The growth rate of the larvae, substrate conversion rate, and larval survival rate are all impacted by moisture levels [25], [26]. In conditions of high moisture, although it promotes faster BSFL growth with the softening of solids in the substrate, the excess moisture tends to decrease the nutritional concentration in the substrate [25], [26]. In addition, the need for the BSFL to expand extra energy to remain afloat may result in a higher mortality rate, while simultaneously slowing down the substrate conversion rate [25], [26]. Conversely, at low moisture levels, not only does the amount of readily available dissolved organic nutrients decrease, thereby slowing down larval growth, but the substrate conversion rate will be slowed due to the larvae's inability to easily assimilate the drier substrate [26], [42]. Furthermore, to ensure that the substrate can be easily sieved at the end of the bioconversion process, the moisture content needs to be lower than 50 % [42]. As such, the generally recommended moisture content range for BSFL, during feeding, is between 60 % and 80 %, with an acceptable lower threshold typically falling between 40 % and 55 % [25], [26].



Source: <https://kuriosity.sg/collections/temperature-air-wind-gas-soil>

*Fig. 10. Resistive Soil Moisture Sensor (left) and Capacitive Soil Moisture Sensor (right)*  
Source: Adapted from [43]

[43, Fig. 10] shows two different types of soil moisture sensors that were tested. The selection of these sensors was based not only on their availability but also on the difference in their operational principles. The **resistive sensor** utilizes two exposed conductors which act as variable resistors. They will measure the substance's resistance, which varies according to its moisture content [44]. In contrast, the **capacitive sensor** only has a single probe and utilizes an integrated chip, a 555 timer, to measure how quickly a capacitor charges through a resistor. The capacitor, formed by two printed circuit boards (PCB) located within the probe, undergoes varying charging rate in response to the moisture level surrounding the probe [45]. With food waste comprising of different properties in contrast to soil, it became necessary to test these two sensors to determine which sensors would be able to accurately measure moisture content in this particular waste stream.

To create specimens of substrate with zero moisture content, frass obtained from a past bioconversion experiment in the BSFL research facility at Block S4A was placed in an oven for approximately 48 hours at temperature of 80 °C to ensure complete drying as shown in [Fig. 11]. Following this, small amounts of water were added to the initial dried frass to achieve the various desired moisture levels. For example, to achieve a frass with 20 % moisture content, 15 g of water would need to be added into 60 g of the oven-dried frass. In this experiment, a digital weighing scale, as seen in [Fig. 12], was employed to measure the necessary water mass for 20 %, 40 %, 50 %, 60 %, 70 %, and 80 % moisture levels. To determine how well the sensors perform under diverse conditions, such as in municipal food waste with a high degree of heterogeneity, two types of frass were used: one with cocopeat and the other without cocopeat. Cocopeat is a dry powdery material obtained from the processing of coconut fiber, primarily known for its capacity to absorb moisture [39]. Utilizing different substrate types offers the opportunity to compare the two sets of data readings and observe variations in the sensors' performance under different conditions.



Fig. 11. Oven (left), Frass Placed Inside Oven before Drying (middle), Frass after Drying for 48 hours at 80 °C (right)

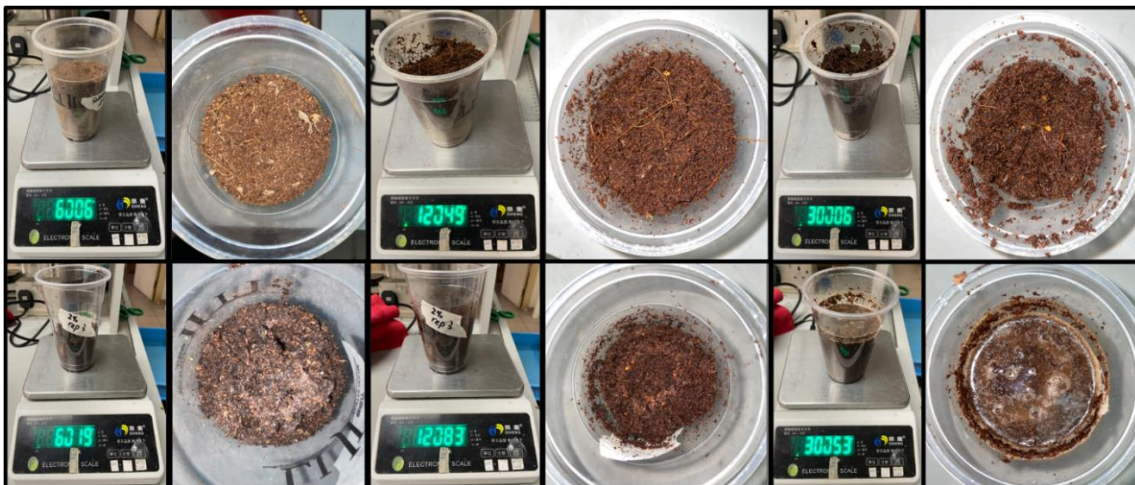


Fig. 12. Frass Type #1 (top row) and Frass Type #2 (bottom row) with Three Moisture Content Levels each. 0% (left), 50% (middle), 80% (right)

As shown in [Fig. 13], the resistive and capacitive soil moisture sensors were embedded into the specimens of frass. The sensors were embedded just below the dotted lines as seen in [Fig. 13] to prevent the frass from contacting with the electronics above, thus reducing the risk of potential short circuits.

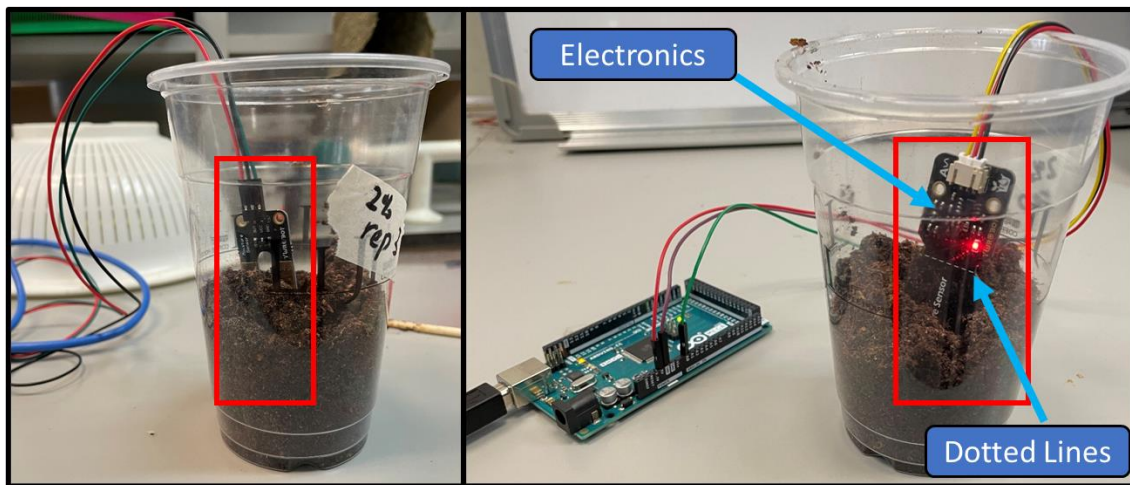


Fig. 13. Soil Moisture Sensors In-direct Contact with Dry Frass

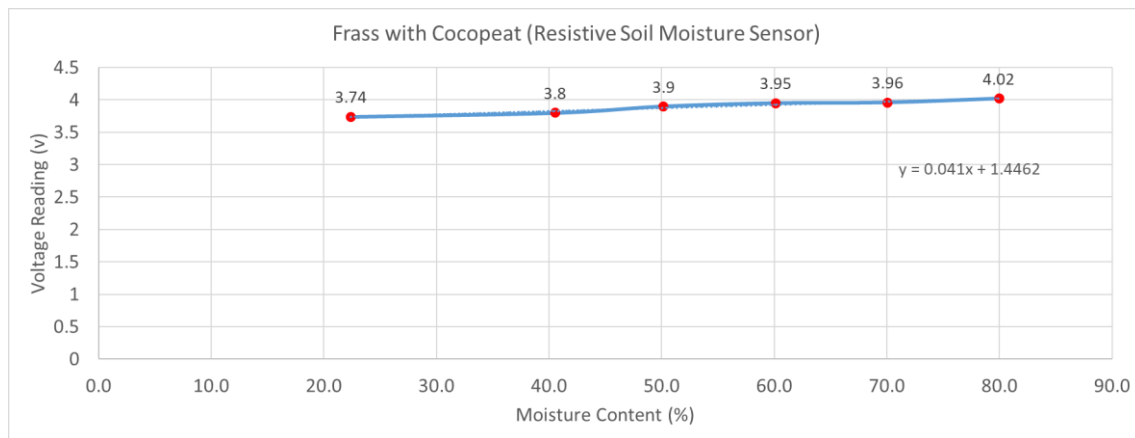


Fig. 14. Data from the Resistive Sensor in Frass Type #1 (Relationship Plotted on a Scatter Graph)

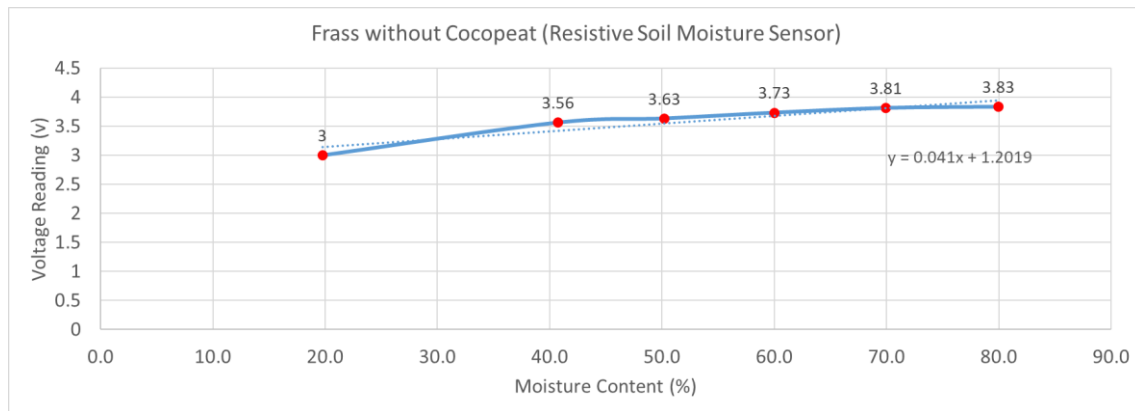


Fig. 15. Data from the Resistive Sensor in Frass Type #2 (Relationship Plotted on a Scatter Graph)

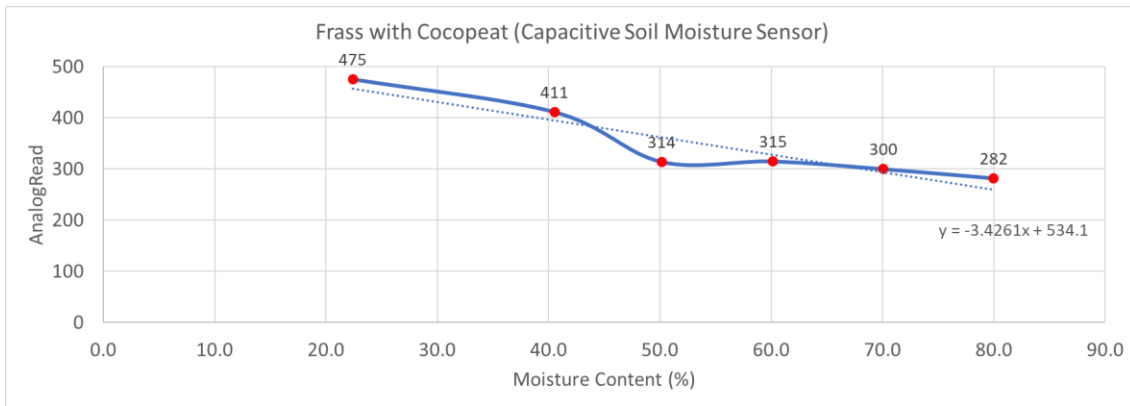


Fig 16. Data from the Capacitive Sensor in Frass Type #1 (Relationship Plotted on a Scatter Graph)

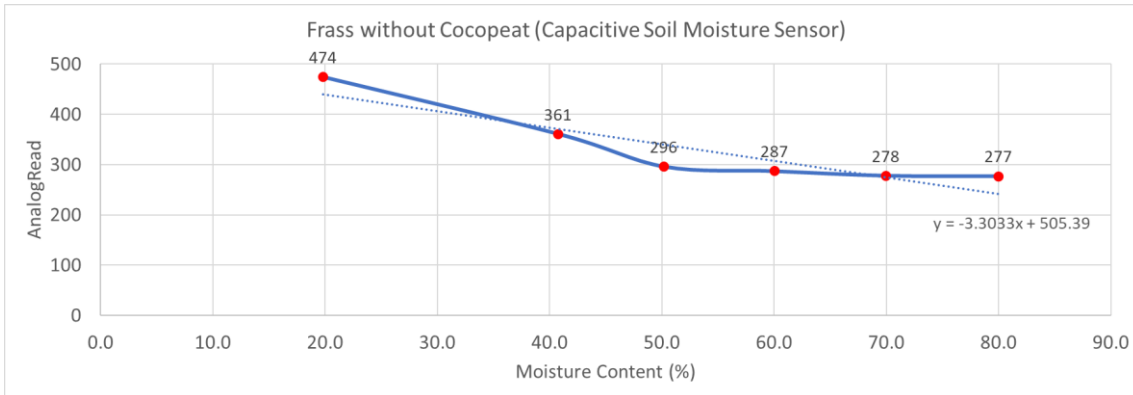


Fig. 17. Data from the Capacitive Sensor in Frass Type #2 (Relationship Plotted on a Scatter Graph)

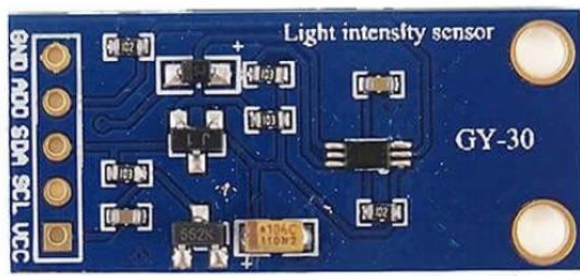
Since the moisture content of the substrate in the reactor is unlikely to drop below 20 %, leading to a high mortality rate of the BSFL [25], [26], the scatter plot is generated using moisture content readings ranging from 20 % to 80 %. Based on the data presented in the four figures, it can be concluded that, of the two substrate types, the readings from both sensors exhibit minimal variation, as indicated by the similarity in the equations derived from the data points for each respective sensor.

Despite the resistive sensor having a much more minimal variation, the capacitive sensor will be chosen to measure the moisture content of the substrate for one specific reason. Due to the foreseeable measurement errors that will occur because of rust. Rust formation on the exposed copper conductors can compromise the accuracy of readings from the resistive sensor, which will necessitate additional maintenance work to rectify the issue. These supplementary efforts for maintenance might not be sustainable in the long term, especially with the vision of deployment of multiple reactors in a decentralized setup across Singapore.

Therefore, the moisture content in the substrate will be determined using the equation of the line ( $y = -3.03033x + 505.39$ ) found in [Fig. 17] as a starting point, under the assumption that municipal food waste is not likely to contain cocopeat.

## 4.2 Light Intensity

The BSFL are known to avoid light and will actively seek out shaded areas away from sunlight [27]. Should the food source become exposed to light, the BSFL will burrow deeper into the substrate layer to escape the light [27]. The bioconversion process may potentially be affected for the following two reasons. Firstly, nutrient availability: if the majority of BSFL are feeding at the bottom of the substrate, the rate at which the nutrients at the bottom are depleted, would increase. Without sufficient nutrients, the BSFL, like any other living organism, cannot grow [25]. With a smaller form factor, the substrate conversion rate would likely be slower. Secondly, heat: if the BSFL are crowded below, the continues heat release during the bioconversion process may lead to an increase in the substrate temperature [26], [42]. If the temperature exceeds the lethal temperature of 47 °C, the larval survival rate would fall rapidly [42]. With a lower quantity of BSFL feeding, the substrate conversion rate would likely be slower. As such, it is recommended that the BSFL feed in the absence of light [27].



Source: <https://kuriosity.sg/collections/light-line-ir-colour/products/digital-luminosity-lux-light-sensor-bh1750>

*Fig. 18. Digital Luminosity Lux Light Sensor BH1750*

Source: Adapted from [46]

[46, Fig. 18] shows the **BH1750 lux light sensor** that was tested to measure the amount of ambient light entering the laboratory-style reactor shown in [Fig. 19]. This light sensor, which uses a photodiode to detect light, was chosen for its diverse features, including a wide range of 1 – 65535

lux and multiple measurement modes that can be digitally selected [47]. With the ability to switch between continuous and one-time modes, the sensor can be easily deactivated, reducing its power consumption.

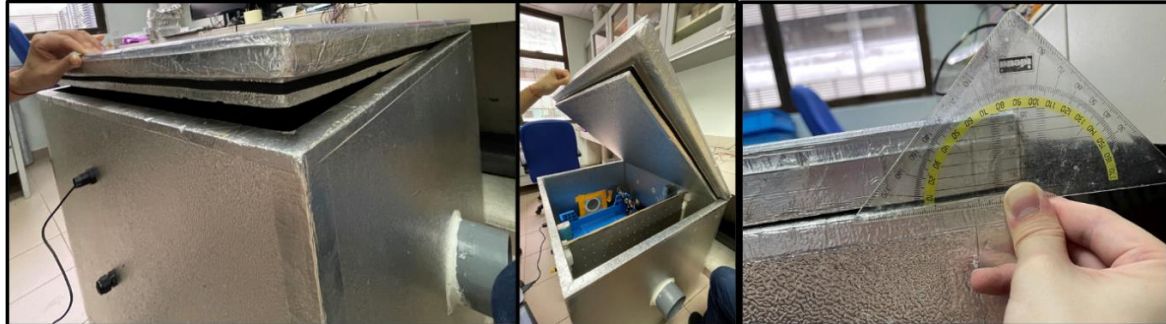


*Fig. 19. Laboratory-Style Bioconversion Reactor with Two Cover Opening Angle, 10° (left), Greater than 50° (middle), Location of Protractor (right)*

[Fig. 20] shows the location in which the light sensor was placed to assess its ambient light detection capability. The sensor was initially positioned in the middle as the reference point. The second location, farther from the opening, was selected to investigate variations in light intensity. The reactor's cover was opened at various angles from 5 ° to 50 ° as shown in [Fig. 19].

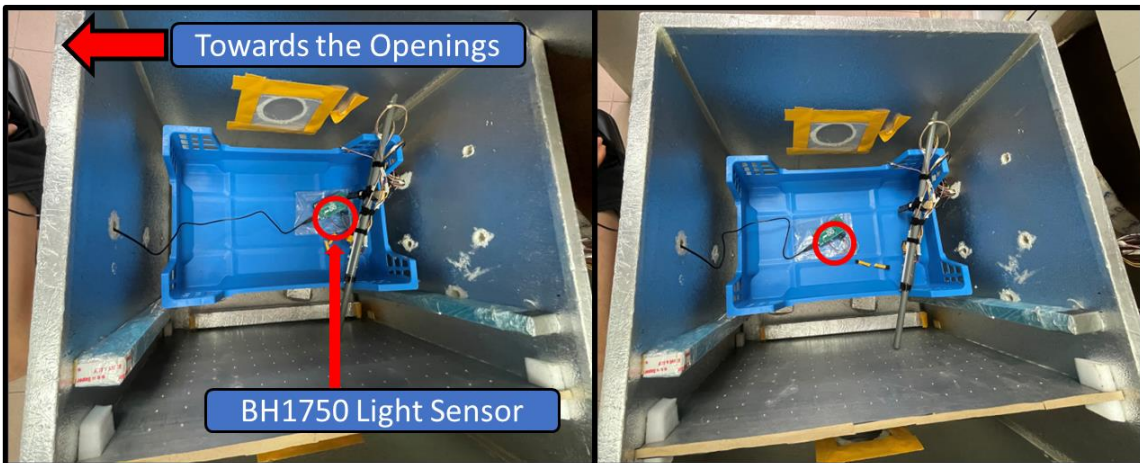


*Fig. 20. Location of BH1750 Light Sensor Inside the Laboratory-Style Reactor, away from the Opening (left), Middle of box (right)*

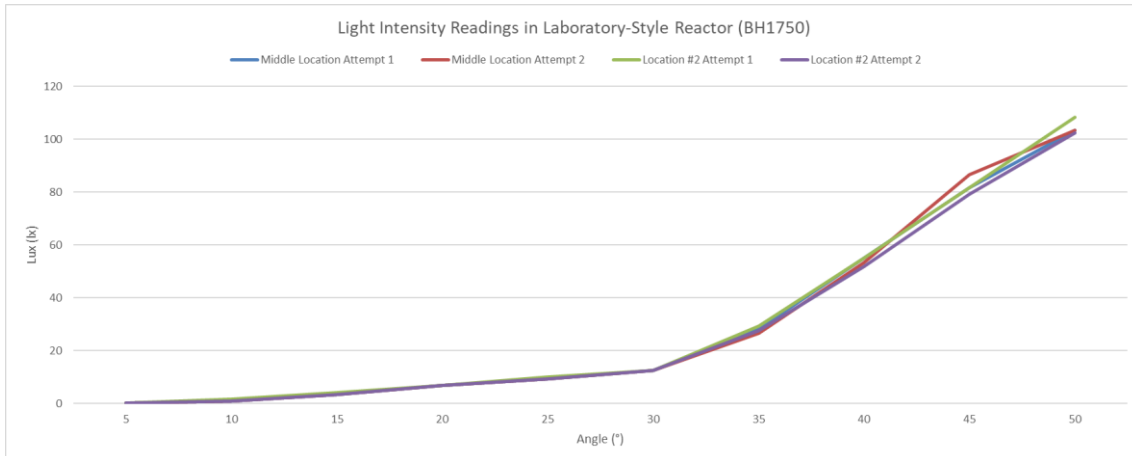


Fig. 21. Data from BH1750 Lux Light Sensor inside the Laboratory-Style Reactor, positioned in the Middle and at Location farther away from opening (Plotted on a Scatter Graph)

After conducting the experiment, no significant variation in readings was observed when the light sensor was positioned in the middle of the box compared to when it was placed farther away from the opening. According to the graph displayed in [Fig. 21], the BH1750 light sensor demonstrates a significant consistency in its measurements, highlighting the reliability of this sensor.

The experiment conducted with this light sensor has only been performed within the laboratory-style reactor shown in [Fig. 20]. To confirm the suitability of this sensor, another round of testing needs to be conducted with the BH1750 light sensor mounted inside the one-third scale prototype reactor.

### 4.3 Temperature in the Substrate

Temperature is crucial for the growth of BSFL, as it is for any other living organism [26]. Ensuring that the BSFL do not overheat is crucial, as high temperatures can result in a low larvae survival rate, consequently slowing down the substrate conversion rate [42]. On the contrary, while BSFL may not perish at low temperatures, their growth rate notably declines [26]. The larvae's development time has been observed to require up to an additional 50 days compared to warmer temperatures [26]. With a slow growth rate, the conversion rate will also be negatively impacted. Therefore, it is recommended that the larvae feed within temperature ranges of 25 °C to 30 °C, with an acceptable upper threshold limit at 47 °C [25], [26], [42].



---

Source: <https://kuriosity.sg/collections/temperature-air-wind-gas-soil/products/digital-temperature-sensor-ds18b20-waterproof-with-jst-header>

*Fig. 22. Digital Temperature Sensor DS18B20 Waterproof with JST Header*  
Source: Adapted from [48]

[48, Fig. 22] shows the **DS18B20 digital temperature sensor with waterproof probe** which uses a simple transistor. This sensor was chosen for its waterproof probe [49]. To assess its performance, it was placed in boiling and chilled water as shown in [Fig. 23], and a digital pocket thermometer as shown in [Fig. 23] was used as a reference device. To test the temperature of the boiling water, the temperature sensor and thermometer were directly inserted into the kettle.

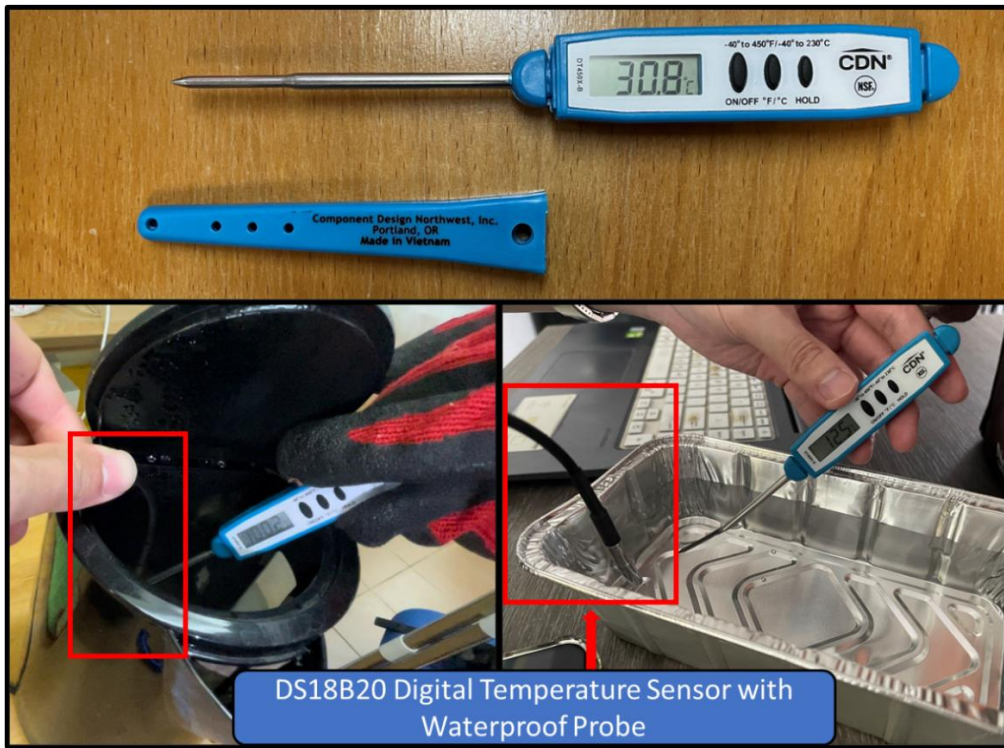


Fig. 23. Digital Pocket Thermometer (top), Sensor and Thermometer in Boiling Water (bottom left), Sensor and Thermometer in Chilled Water (bottom right)

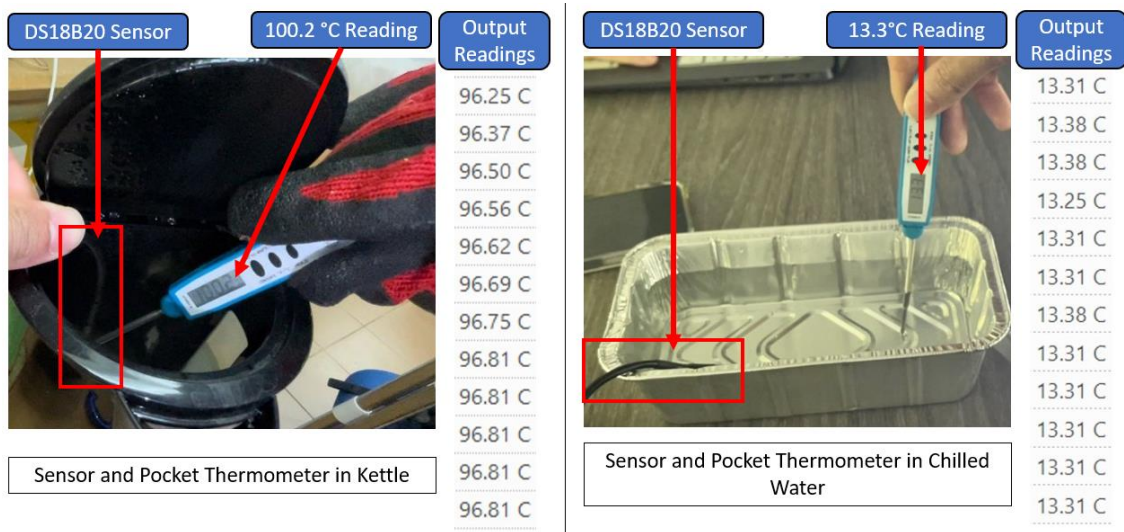


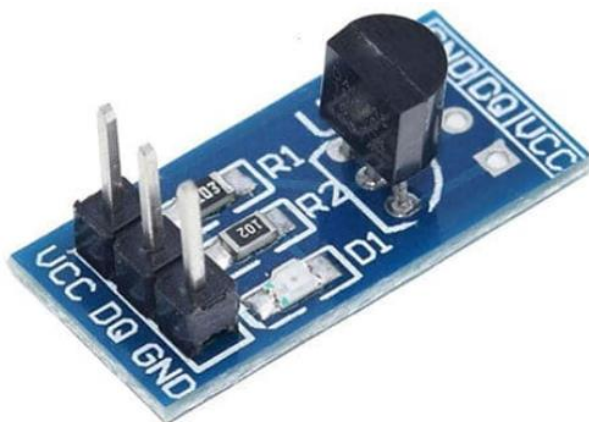
Fig. 24. Comparison of the Readings against the Reference Device in Boiling Water and Chilled Water

Given the low probability of the substrate temperature exceeding 47 °C and the sensor's accuracy of  $\pm 0.5$  °C [49], the experiment conducted with chilled water in [Fig. 24] illustrates the sensor's ability to provide relatively accurate readings at lower temperatures. This sensor is suitable and chosen for the one-third scale prototype reactor for two main reasons. Firstly, it can coexist alongside multiple DS18B20 sensors on the same 1-wire bus [49]. Each DS18B20 sensor comes pre-programmed with a unique 64-bit serial code, allowing multiple DS18B20 to be connected without the

need for additional pins on the microcontroller [49]. The second reason is the availability of sensors with waterproofing features. Among the available options, the DS18B20 sensor stands out as the only one equipped with waterproof capabilities. With its temperature range of -55 °C to 125 °C [49], this sensor will allow the reactor to accurately measure the temperature of the substrate.

#### 4.4 Internal Air Temperature

How the internal air temperature affects the bioconversion process is the same as temperature in the substrate. At high temperature, the larvae survival rate decreases significantly, leading to a slower conversion rate [42]. On the other hand, at lower temperatures, rather than impacting the survival rate, the larvae growth rate decreases, also resulting in a slower conversion rate [26]. There is a difference in the temperature ranges. It is recommended that the larvae feed within temperature ranges of 25 °C to 30 °C, with an acceptable upper threshold limit at 35 °C.



---

Source: <https://kuriosity.sg/collections/temperature-air-wind-gas-soil/products/digital-temperature-sensor-ds18b20>

Fig. 25. Digital Temperature Sensor DS18B20

Source: Adapted from [50]

[50, Fig. 25] shows the **DS18B20 digital temperature sensor** that was tested. This sensor has the same working principle as the DS18B20 temperature sensor with waterproof probe [49]. The experiment was conducted inside a controlled environment, as shown in [Fig. 26], where an anemometer was utilized as the reference device. Conducting the experiment within an enclosed box minimizes external influences while ensuring the acquisition of accurate results. Additionally, a fan was used to introduce ambient air into the box to change the temperature in the box.

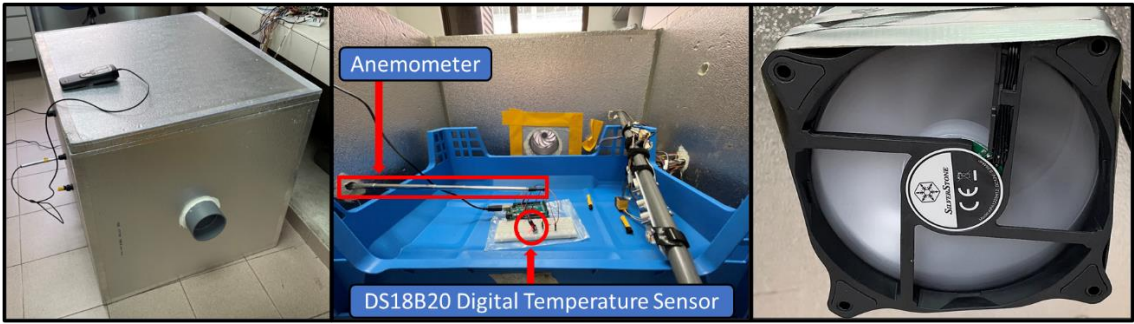
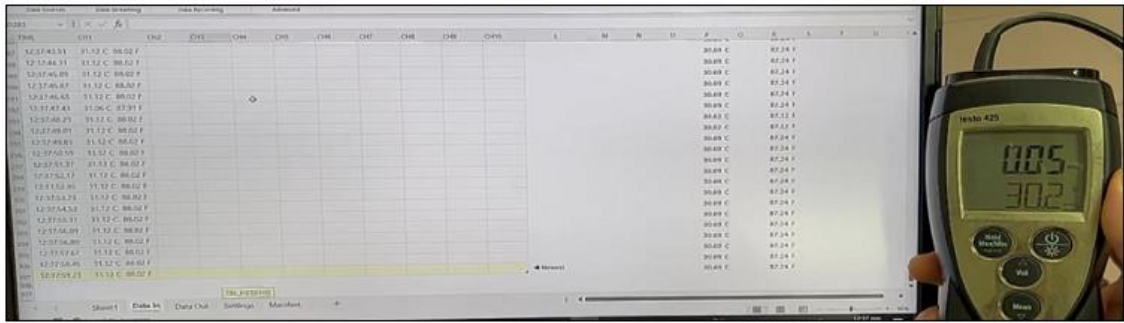


Fig. 26. Laboratory-Style Reactor (left), Inside the Reactor (middle), Fan (right)



Internal Air Temperature

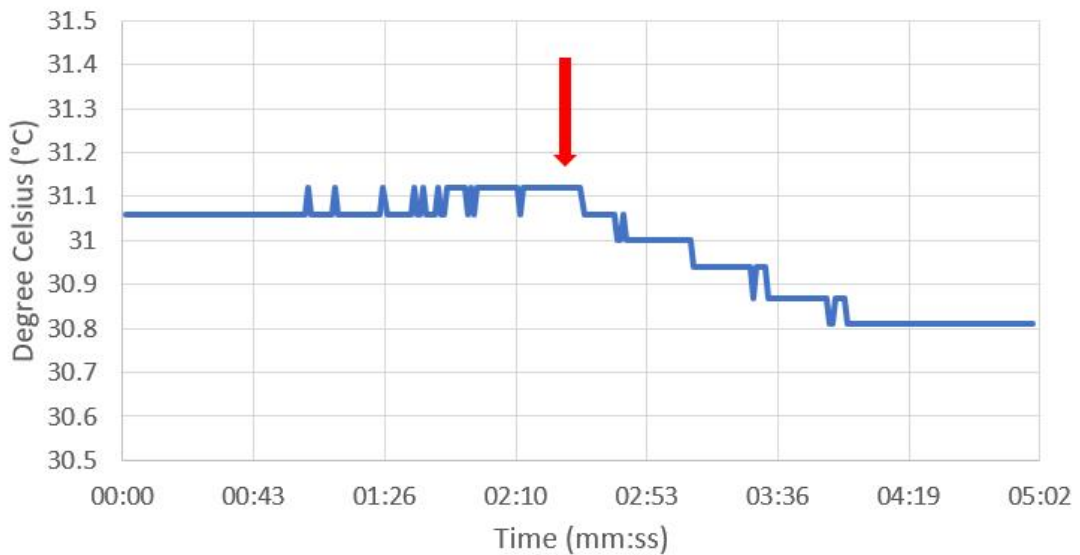


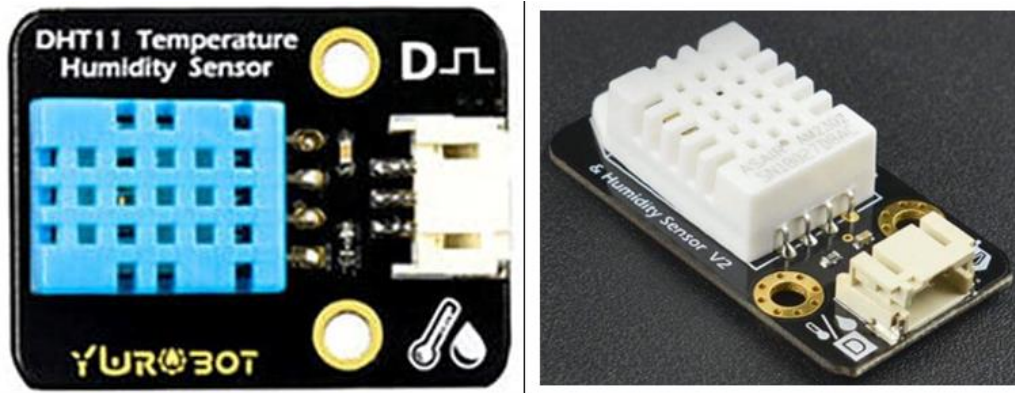
Fig. 27. Readings from DS18B20 Digital Temperature Sensor inside the Laboratory-Style Reactor compared against Anemometer readings (top), Temperature dropped when the fan was turned on (bottom)

[Fig. 27] shows that when the fan was turned on at around the 2 min 20 seconds mark, the sensor was able to measure a drop in internal air temperature. The change in temperature could be attributed to the presence of the Arduino Mega located inside the box. Since the microcontroller remained inside the box throughout the experiment, the heat generated by the board likely increased the internal temperature. Consequently, after the fan was turned on, the accumulated heat was expelled from inside, resulting in a drop in temperature to room temperature. While the sensor's

readings exhibit slight variations from the anemometer's measurements over a period of 5 minutes, the DS18B20's unique ability to coexist alongside multiple DS18B20 on the same 1-wire bus makes it an ideal choice for the reactor. Since various sensors will need to be installed inside the reactor, having the ability to utilize fewer pins on the microcontroller is a strong advantage.

## 4.5 Relative Humidity

Another crucial factor influencing the development of BSFL is relative humidity. Higher relative humidity percentages correspond to a lower mortality rate among the BSFL [26]. With a low mortality rate, a higher number of larvae remain alive [26], thereby reducing the likelihood of a decrease in the conversion rate due to a decrease in the number of BSFL in the substrate.



Source: <https://kuriosity.sg/collections/temperature-air-wind-gas-soil/products/digital-temperature-sensor-ds18b20>

Fig. 28. Temperature Humidity Sensor DHT11 (left) and DHT22 (right)  
Source: Adapted from [43]

[43, Fig. 28] shows the **DHT11 and DHT22 sensors** that were tested. Both sensors contain a humidity sensing element comprising of two electrodes which is separated by a moisture-absorbing substrate. When there is an increase in humidity, the substrate will absorb the water vapor, leading to a decrease in resistance between the electrodes [51]. The experiment was conducted by having two humidity sensors and a cup filled with a saltwater mixture sealed inside an airtight plastic container as shown in [Fig 29]. The sensors remained inside for approximately 24 hours, and by the end of the process, the anticipated readings from the sensors should display 75 % RH [52].



Fig. 29. Top View of relative humidity sensors inside a container (top left), Front view relative humidity sensors inside a container (bottom left), To further prevent exposure to external environments (right)

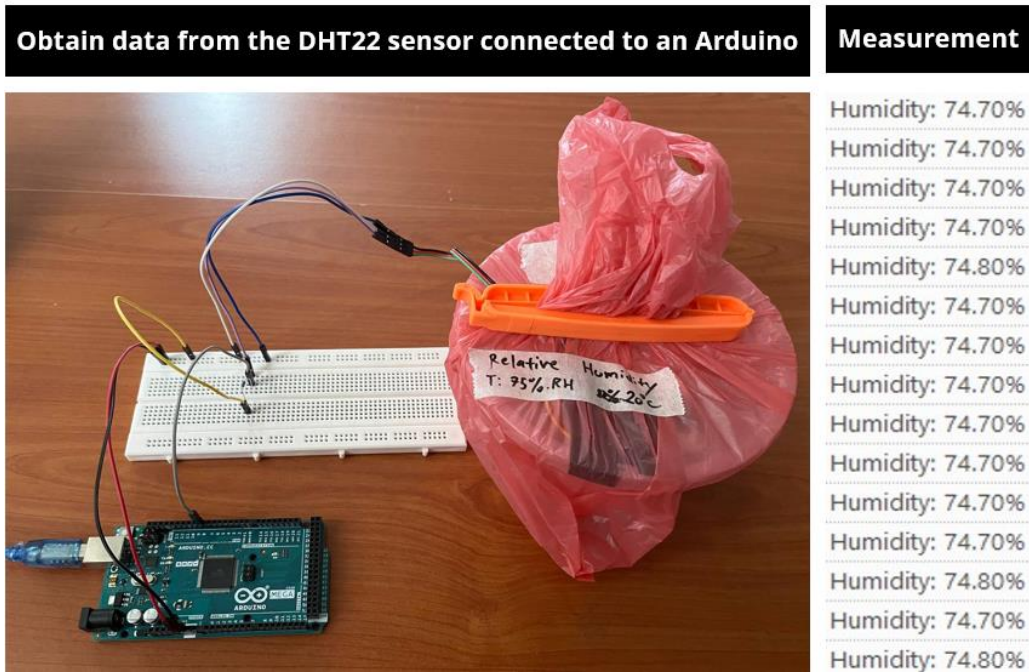
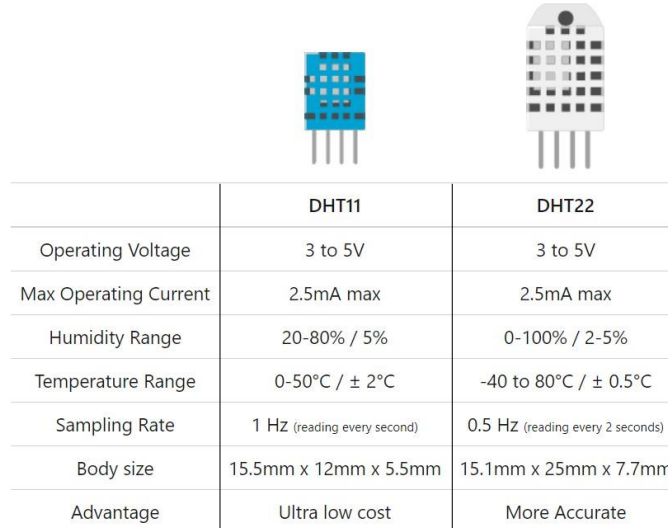


Fig. 30. Readings from the DHT22 Humidity Sensors

[Fig. 30] shows the readings from the DHT22 sensors. While the readings didn't precisely reach 75% RH, the sensor outperformed the DHT11 Sensor. Upon powering the DHT11 sensor, the readings hovered around 15% RH, suggesting a potential fault in the sensor. Therefore, further testing is

necessary to accurately determine the ideal humidity sensor for the reactor. However, considering that the DHT22 has better specifications than the DHT11 as shown in [51, Fig. 31], with a smaller error rate of  $\pm 2 - 5 \%$ , the DHT22 would ideally be the better choice.



	DHT11	DHT22
Operating Voltage	3 to 5V	3 to 5V
Max Operating Current	2.5mA max	2.5mA max
Humidity Range	20-80% / 5%	0-100% / 2-5%
Temperature Range	0-50°C / $\pm 2^\circ\text{C}$	-40 to 80°C / $\pm 0.5^\circ\text{C}$
Sampling Rate	1 Hz (reading every second)	0.5 Hz (reading every 2 seconds)
Body size	15.5mm x 12mm x 5.5mm	15.1mm x 25mm x 7.7mm
Advantage	Ultra low cost	More Accurate

*Fig. 31. Specification Comparison between DHT11 and DHT22*

Source: Adapted from [51]

## 4.6 Carbon Dioxide Emissions

As a result of metabolic activity, particularly during respiration, organisms such as the BSFL will release CO<sub>2</sub> into the atmosphere [28]. Without proper circulation, and should the CO<sub>2</sub> be allowed to accumulate over time, the survival rate of the larvae would likely be negatively affected. If the number of larvae in the substrate reduces, the conversion rate of the substrate would also likely deteriorate.



Source: <https://sandboxelectronics.com/?product=mh-z16-ndir-co2-sensor-with-i2cuart-5v3-3v-interface-for-arduinoorraspberrypi>

Fig. 32. 10,000ppm MH-Z16 NDIR CO<sub>2</sub> Sensor

Source: Adapted from [53]

[53, Fig. 32] shows the **MH-Z16 NDIR CO<sub>2</sub> Sensor** that was tested. This CO<sub>2</sub> sensor operates by detecting variations in the infrared radiation between the infrared lamp and the receiver inside of the tube. The difference is the result of the infrared light being absorbed by the CO<sub>2</sub> molecules in the air inside the tub. The difference is also proportional to the number of CO<sub>2</sub> molecules in the air sample tube [54].

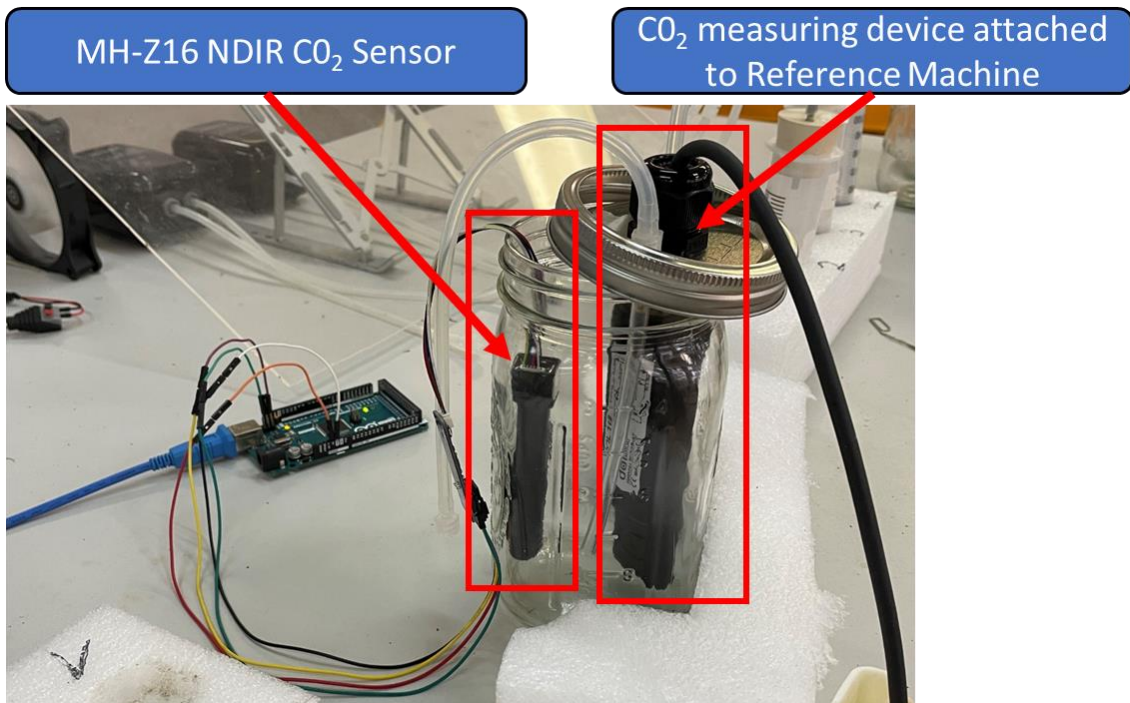


Fig. 33. MH-Z16 CO<sub>2</sub> Sensor inside a Glass Jar with another CO<sub>2</sub> measuring device attached to reference machine

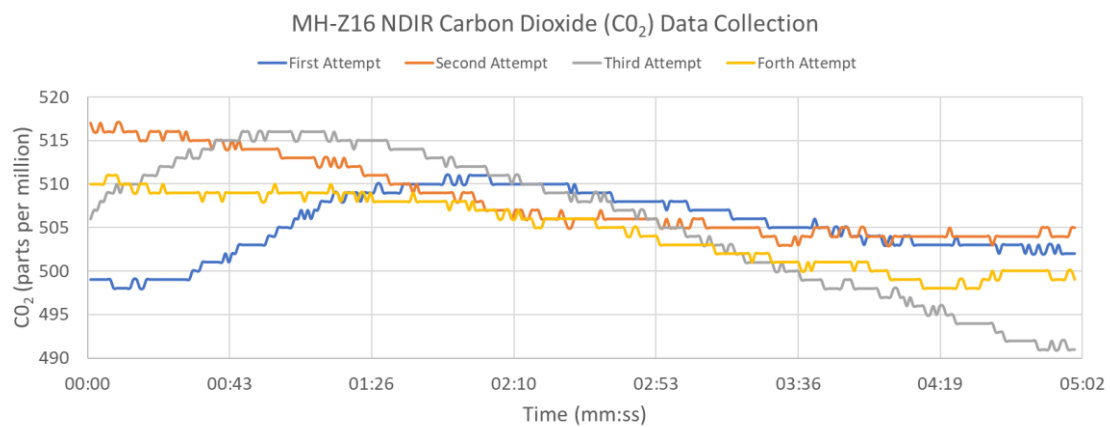
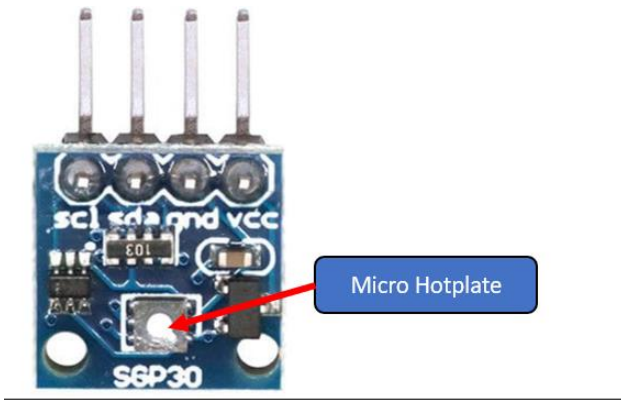


Fig. 34. Data from MH-Z16 CO<sub>2</sub> Sensor inside of Glass Jar

The CO<sub>2</sub> sensor was tested by placing it inside a glass jar as shown in [Fig. 33] together with another CO<sub>2</sub> measuring device and readings from both sensors were taken over a duration of five minutes. To assess the accuracy and consistency of the readings, the experiment was conducted four times. From these four trials, the average reading was determined to be 506.04 ppm. This average reading was then compared to the average reading obtained by the reference sensor, which was 500 ppm. As such, this sensor appears to be functioning reliably and providing results within its specified error range of  $\pm 100$  ppm.



Source: [https://kuriosity.sg/products/air-quality-sensor-sgp30?\\_pos=1&\\_sid=3bf3812b7&\\_ss=r](https://kuriosity.sg/products/air-quality-sensor-sgp30?_pos=1&_sid=3bf3812b7&_ss=r)

*Fig. 35. SGP30 Air Quality Sensor*

Source: Adapted from [55]

[55, Fig. 35] shows another type of CO<sub>2</sub> sensor, **SGP30 Air Quality Sensor**, that was experimented with. This sensor, equipped with a temperature-controlled micro hotplate, is capable of outputting equivalent CO<sub>2</sub> in ppm as well as total volatile organic compounds (TVOC) in ppb [56]. Additionally, for further refinement of the readings, this sensor can interface with any external humidity sensor to provide additional humidity compensation [56]. Between the **SGP30** and **MH-Z16 NDIR** CO<sub>2</sub> sensor, the SGP30 sensor, with its unique serial ID, was initially identified as the preferred option due to the need for multiple sensors measuring the same parameters to be installed inside the reactor.

To facilitate the comparison of CO<sub>2</sub> changes resulting from the bioconversion process, it is necessary to install at least two sensors. One sensor will be positioned at the inlet, where the fans are located, and another at the outlet, near the chimney. With at least two sensors, the difference between the readings can provide a much more precise assessment of the amount of CO<sub>2</sub> produced because of the bioconversion process. However, it was only through functional testing that it was discovered that the SGP30 cannot operate alongside another SGP30 sensor. Despite both sensors being verified to have unique serial IDs, when both sensors were connected to the same SDA and SCL pins on the Arduino, the Arduino board was unable to detect either sensor. Therefore, to use either type of CO<sub>2</sub> sensors, additional research is required to identify a method that would enable the microcontroller board to detect multiple sensors on the same SDA and SCL lines.

## 4.7 Ammonia

$\text{NH}_3$  gas, like  $\text{CO}_2$ , is produced as a result of the metabolic activity during the bioconversion process [25]. Without proper circulation and should the  $\text{NH}_3$  gas be allowed to accumulate over time, the survival rate of the larvae would likely be negatively affected. If the number of larvae in the substrate reduces, the conversion rate of the substrate would also likely deteriorate.



---

Source: <https://continental.sg/product/gas-sensor-mq137-ammonia-nh3/>

*Fig. 36. MQ137 Ammonia Gas Sensor*

Source: Adapted from [57]

[57, Fig. 36] shows the **MQ137 Ammonia Gas Sensor** module that was tested. This sensor was initially chosen because it was readily available and capable of detecting ammonia [58]. However, before the functional test could be conducted, it was discovered that the "MQUnifiedsensor" library, which enables the Arduino board to read MQ sensors, did not include support for the MQ137 sensor. Without the necessary library support, calibration of the MQ137 sensor needs to be performed with the help of its datasheet. However, due to time constraints, calibration was not performed, and consequently, the MQ137 sensor will not be utilized in the one-third scale prototype reactor.

## 4.8 Methane

$\text{CH}_4$  gas, like  $\text{CO}_2$  and  $\text{NH}_3$ , is produced as a result of the metabolic activity during the bioconversion process [25]. Without proper circulation and should the  $\text{CH}_4$  gas be allowed to accumulate over time, the larvae survival rate would likely be negatively affected. If the number of larvae in the substrate reduces, the substrate conversion rate would also likely be adversely affected.



Source: <https://www.dfrobot.com/product-683.html>

Fig. 37. Gravity: Analog CH<sub>4</sub> Gas Sensor

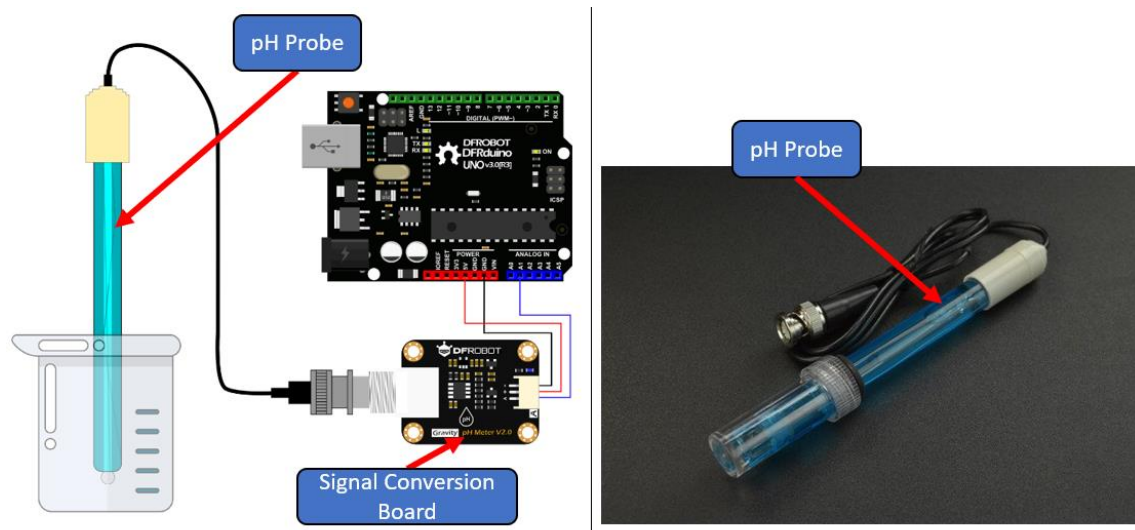
Source: Adapted from [59]

[59, Fig. 37] shows the **Gravity: Analog MQ4 Methane Gas Sensor** module that was tested. This sensor was initially chosen because it was readily available, from the BSFL research facility at Block S4A, and capable of detecting methane [58], [59]. With the support from the "MQUnifiedsensor" library, the Arduino was successful in detecting methane gas in the research facility. However, to assess the sensor's accuracy, it must undergo testing against another methane measuring device to validate its readings. Due to time constraints, as well as the limited stock of this stock in the research facility, only one of this sensor shall be implanted inside the one-third scale prototype reactor. For future experiments, it is advisable to include multiple  $\text{CH}_4$  measuring devices in the reactor to facilitate a more robust comparison of  $\text{CH}_4$  gas changes resulting from the bioconversion process.

## 4.9 pH Value

The pH level, a value that reflects the exact acidity or alkalinity of a solution, plays a crucial role in influencing the survival and growth of the BSFL [25], [28]. Although the larvae have been found to

have a survival rate of 88–96 % within the range of 2–10, it has been observed that at pH values higher than 6, the larval growth rate or body weight is higher compared to when the pH is at 2 [26], [28]. Should the pH value of the substrate fall outside the ranges of 2–10, which is very unlikely, there is a possibility that the number of surviving larvae will decrease due to the unfavorable conditions, leading to a slower substrate conversion rate [25]. A useful discovery is that the BSFL can modify the pH value of the waste stream towards a higher, more alkaline range [26], [28]. Therefore, if the municipal food waste provided has a lower pH value, the BSFL could raise the pH content in the substrate without requiring external interventions, thereby minimizing the impact on the larval growth rate [26], [28].



Source: [https://wiki.dfrobot.com/Gravity\\_\\_Analog\\_pH\\_Sensor\\_Meter\\_Kit\\_V2\\_SKU\\_SEN0161-V2#More\\_Documents](https://wiki.dfrobot.com/Gravity__Analog_pH_Sensor_Meter_Kit_V2_SKU_SEN0161-V2#More_Documents)

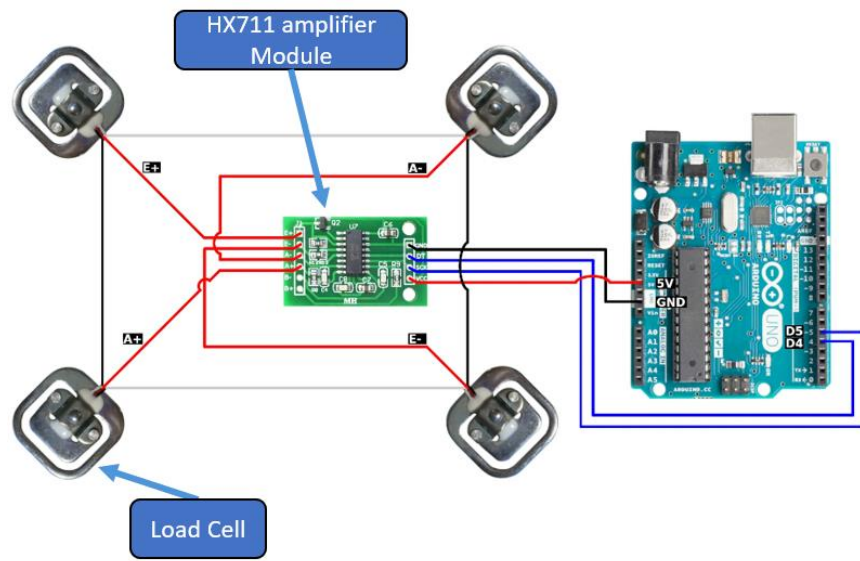
*Fig. 38. Gravity Analog pH sensor*

Source: Adapted from [60]

[60, Fig. 38] shows the **DFRobot's Gravity: Analog pH sensor** that was tested. The pH sensor is included in a pH meter kit that comes with two standard buffer solutions (pH 4.0 and pH 7.0), simplifying the calibration process. Utilizing the software library and employing the two-point calibration method, the pH sensor can be readily calibrated and confidently utilized, while accounting for its measurement accuracy of  $\pm 0.1$ . As such, after performing the calibration with the two standard buffer solution, this sensor is ready to be used in the one-third scale prototype reactor.

## 4.10 Mass of the Substrate

The mass of the substrate is a useful indicator of the bioconversion process (A. Fuhrmann, personal communication, April 1, 2024). During the bioconversion, as the larvae feed, they will convert the waste into their body mass, effectively turning themselves into a resource that is rich in protein and fat [26]. Tracking the substrate mass will not determine the rate of bioconversion, rather it can only be an indicator (A. Fuhrmann, personal communication, April 1, 2024), considering that data from the sensors will not be able to differentiate between substrate reduction and larval growth.



Source: <https://circuitjournal.com/50kg-load-cells-with-HX711>

Fig. 39. Four 50 Kg Load with HX711 Amplifier Module

Source: Adapted from [61]

[61, Fig. 39] shows the **50kg Load Cells with HX711 amplifier module** that was tested. Each load cell comprises of four strain gauges arranged in a Wheatstone bridge configuration [62]. When an external force is applied, there will be a deformation of the structure of the object, resulting in a change in the resistance of the strain gauges [62]. Since the resistance is proportional to the force applied by the load, the gauges, with their circuit design, allow for the calculation of the weight of the objects or loads [62]. During the final testing, the load cell unexpectedly fails to operate as intended. As such, due to limited time constraints, this sensor will not be used inside the one-third scale reactor.

## 5. Hardware and Software Integration

To enable the optimization of the internal conditions within the one-third scale prototype reactor, the questions listed in Section 3.3 needs to be answered. While awaiting the construction of the one-third scale prototype reactor, attempts were made to gain insights and gather valuable data by conducting two experiments in the BSFL research facility at Block S4A. The first experiment – Phase 1 was conducted in an open-air configuration while the second experiment – Phase 2 utilized a closed configuration. The open-air configuration was chosen to acquire initial insights into the variability of the substrate. In contrast, the closed configuration was intended to collect additional data, verify the integration of all sensors, ensure data storage capability, and identify additional variability in different environmental conditions, such as the introduction of relatively constant airflow from a fan. Phase 2 was performed with the assistance of a separate bioconversion reactor (which is henceforth referred to as standalone reactor), shown in [Fig. 40]. Utilizing the array of sensors detailed in Section 4, an **Arduino** microcontroller was selected due to its versatility and capability to interface with various sensors, making it ideal for connecting multiple types of sensors together.



Fig. 40. Standalone reactor for BSFL bioconversion by ETH Zurich, Singapore-ETH Centre, NUS funded by the National Research Foundation of Singapore at Block S4A

With the data and insights acquired from Phase 1 and Phase 2, the information will be used to determine the number of sensors for each parameter and the placement of the various sensors in the

one-third scale prototype reactor, in Phase three. In addition, the data will be useful in identifying possible faulty numerical outputs from the sensor, which will then inform how much data filtering is required.

## 5.1 Hardware Integration

[Tab. 8] shows the various sensors and the corresponding number of sensors that were used in each phase. Phase 1 mainly utilized sensors that would be placed directly into the substrate while Phase 2 comprises sensors that would measure both conditions in the substrate as well as environmental conditions within the reactor. The data obtained from phase 1 are expected to show less variation across different bioconversion reactors since those sensors directly measure the properties of the solution they are immersed in. In contrast, the data from Phase 2, particularly from sensors measuring environmental conditions, is expected to yield different readings when placed in the one-third scale prototype reactor due to the significant differences in size and materials. Nevertheless, obtaining data from both trials is immensely valuable and can reveal hidden insights that may have remained undiscovered without conducting the trials.

*Tab. 8. Overview of the working Sensors and the their quantity planned to be used in each phase*

Parameter	Sensors	Phase 1 (Open Configuration)		Phase 2 (Standalone Reactor)		Phase 3 (One-third scale prototype reactor)	
		Employ	QTY	Employ	QTY	Employ	QTY
Moisture Content of the Substrate	Capacitive Soil Moisture	✓	X6*	✓	X6	✓	X3
Temperature in the Substrate	DS18B20 digital Temperature sensor with waterproof probe	✓	X6	✓	X6	✓	X3
pH Value of the Substrate	DFRobot's Gravity: Analog pH sensor	✓	X3	✓	X1	✓	X3*
Internal Air Temperature	DS18B20	-	-	✓	X2	✓	X2
Relative Humidity	DHT22	-	-	✓	X1	✓	X1
Gas Emission (CO <sub>2</sub> )	SPG30	-	-	✓	X1	-	-
Gas Emission (CH <sub>4</sub> )	MQ4	-	-	-	-	✓	X1

Note: \* the number of sensors actually used was not the same due to technical problems faced during testing  
Sensors in orange denote that they are contact sensors and are placed in the substrate during testing. "QTY" stands for Quantity.

### 5.1.1 Phase 1

[Fig. 41] depicts the timeline of phase 1, starting from February 9<sup>th</sup> to February 19<sup>th</sup>. Phase 1 consists of two stages conducted at different points in time. The first stage involved using the capacitive soil moisture sensor and the DS18B20 sensor with waterproof probe to measure moisture and temperature in the substrate, respectively. In the second stage, the analog pH sensor was utilized to measure the pH value of the substrate. The duration of the first stage was about five and a half days while the duration of the second stage was initially set to last for about six days. However, due to an incorrect connection for one of the pH sensors, the data collected for that sensor during the first two days was unusable. Therefore, analysis of the pH data will commence on February 16<sup>th</sup>, after the error has been rectified.

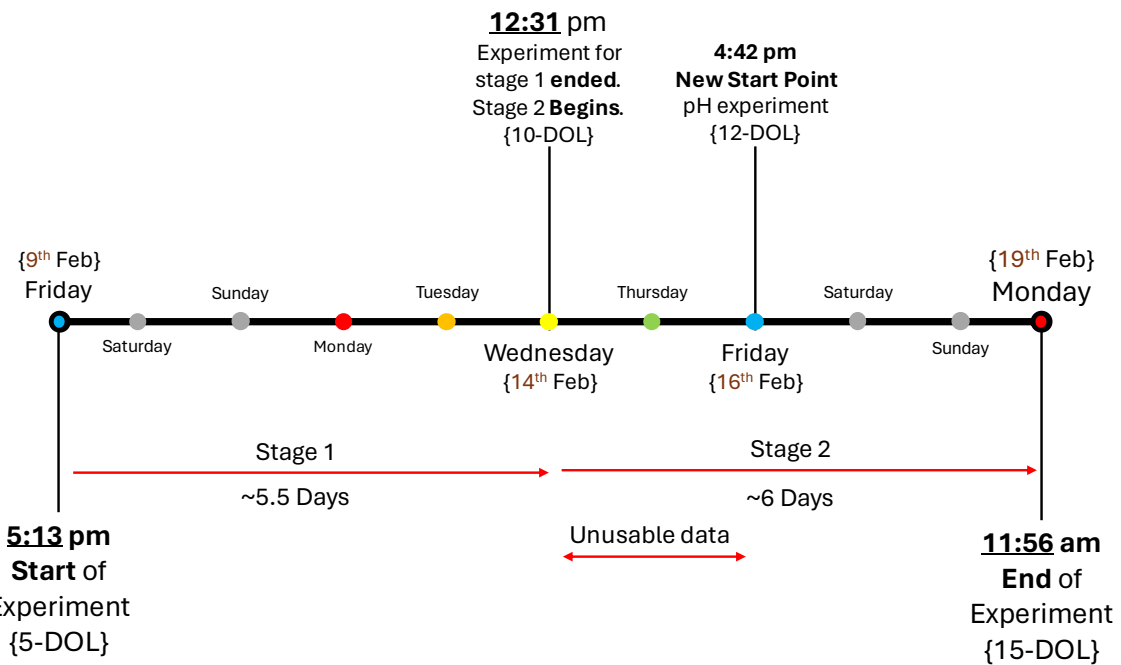


Fig. 41. Timeline of Phase 1



*Fig. 42. Plastic Container in the center of large bin (left) and Plastic Container before start of experiment (right)*  
Note: Food Waste and 5-DOL are distinguished by dark yellow and dark brown coloration, respectively, within the boundary

[Fig. 42] shows the open-air configuration at the beginning of the experiment. The materials utilized, including the large bin, food plastic container, roughly 10,000 5-DOL, 100 g of peanut skin, and notably, the 8 kg food waste, were all sourced from the BSFL research facility at Block S4A. The food plastic container was placed inside the large bin to contain the larvae that might escape due to adverse conditions, such as high temperature, ensuring that they remain within the designated area. Before pouring the 5-DOL into the center of the food waste, 100 g of peanut skin was first spread over the 8 kg of food waste, outside the boundary, shown in [Fig. 42]. The reason for using the peanut skin to form the boundary is to ensure that the larvae do not escape at the beginning of the experiment (A. Fuhrmann, personal communication, March 8, 2024). During a discussion conducted on March 8, 2024, Adrian, a researcher in charge of the BSFL research facility, shared that over time, the food waste will become saturated with moisture due to the microbial activity. With increasing moisture level, the BSFL will attempt to escape this unfavorable condition which is not desirable as the rate of the bioconversion process will not be optimal. Due to the absence of nutrients in peanut skin, the BSFL will avoid or refrain from feeding in the substrate area that has been covered with peanut skin. The effect of the peanut skin limited to the initial feeding stage, as it will eventually blend into the substrate after a few days due the decomposition. At that point, the BSFL will not be able to distinguish between peanut skin and food waste. To store data from the sensors, a micro-SD card was selected

given its size and universality. To interface the micro-SD card with the Arduino, a data logging shield, shown in [Fig. 43], was used. To use the data logging shield, an SD card adapter is required. One of the benefits of this shield is the option to utilize the Real-Time Clock (RTC) feature, which timestamps all data with the current time. To unlock this feature, a CR1220 coin cell battery is required. To ensure that the data collection unit, consisting of an Arduino board mounted with a data logging shield, remains clean and protected, the unit was placed on top of an elevated platform.

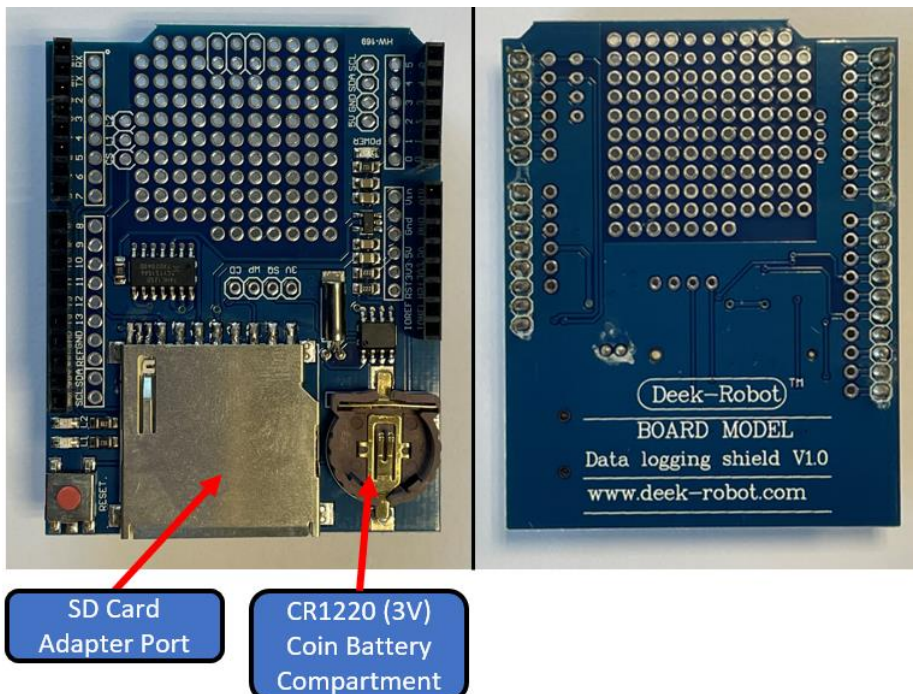


Fig. 43. Arduino Uno compatible Data Logging Shield V1.0

To assess the variability of the moisture and substrate temperature parameter, four capacitive soil moisture sensors and six DS18B20 sensors with waterproof probes were positioned at different central location in the substrate as depicted in [Fig. 44] and [Fig. 45]. Initially, the plan was to use six capacitive sensors, however, during the actual testing, two of the Arduino's analog pins were discovered to be faulty. Because the readings, measured from the two analog pins, consistently output values of -127, the number of capacitive moisture sensors were reduced from six down to four. To confirm whether the middle location would provide a representative interpretation of the substrate, the placement of the capacitive sensor was rearranged to the configuration in [Fig. 44]. With regards to mounting, each row has one aluminum profile bar which provides the means to attach all the

sensors and ensure that they do not sink to the bottom of the substrate. The capacitive sensor and DS18B20 digital temperature sensors were mounted next to each other, at the location depicted in [Fig. 44], to adhere to the desired placement of the sensors.

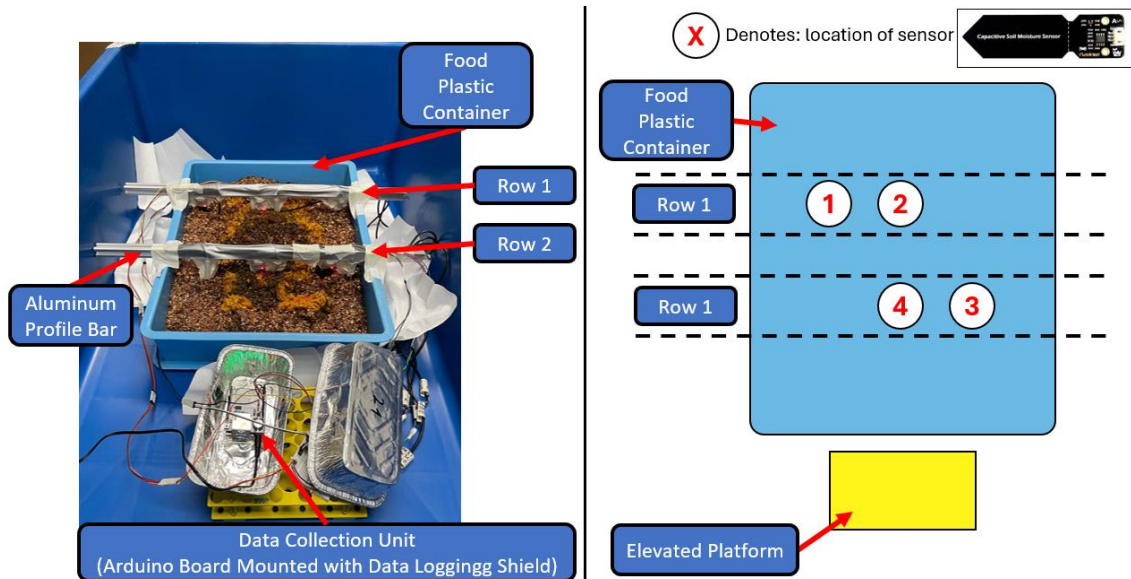


Fig. 44. Plastic Container with sensors mounted (left) and Placement of Capacitive Soil Moisture Sensors in container (right)  
Note: Diagram (right) is not drawn to scale

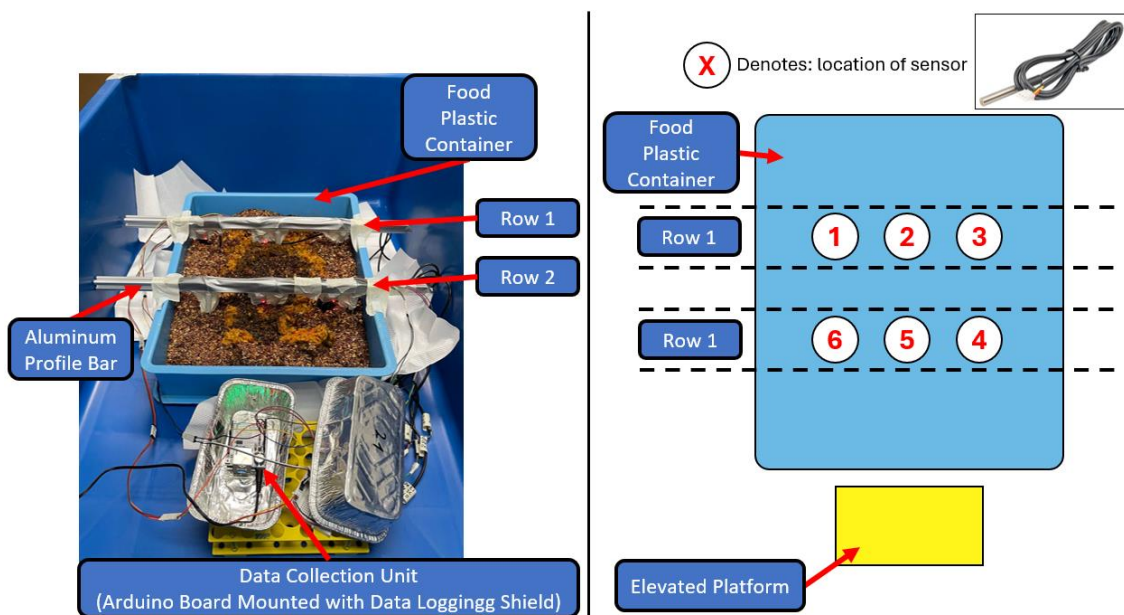


Fig. 45. Plastic Container with sensors mounted (left) and Placement of DS18B20 Sensors in container (right)  
Note: Diagram (right) is not drawn to scale

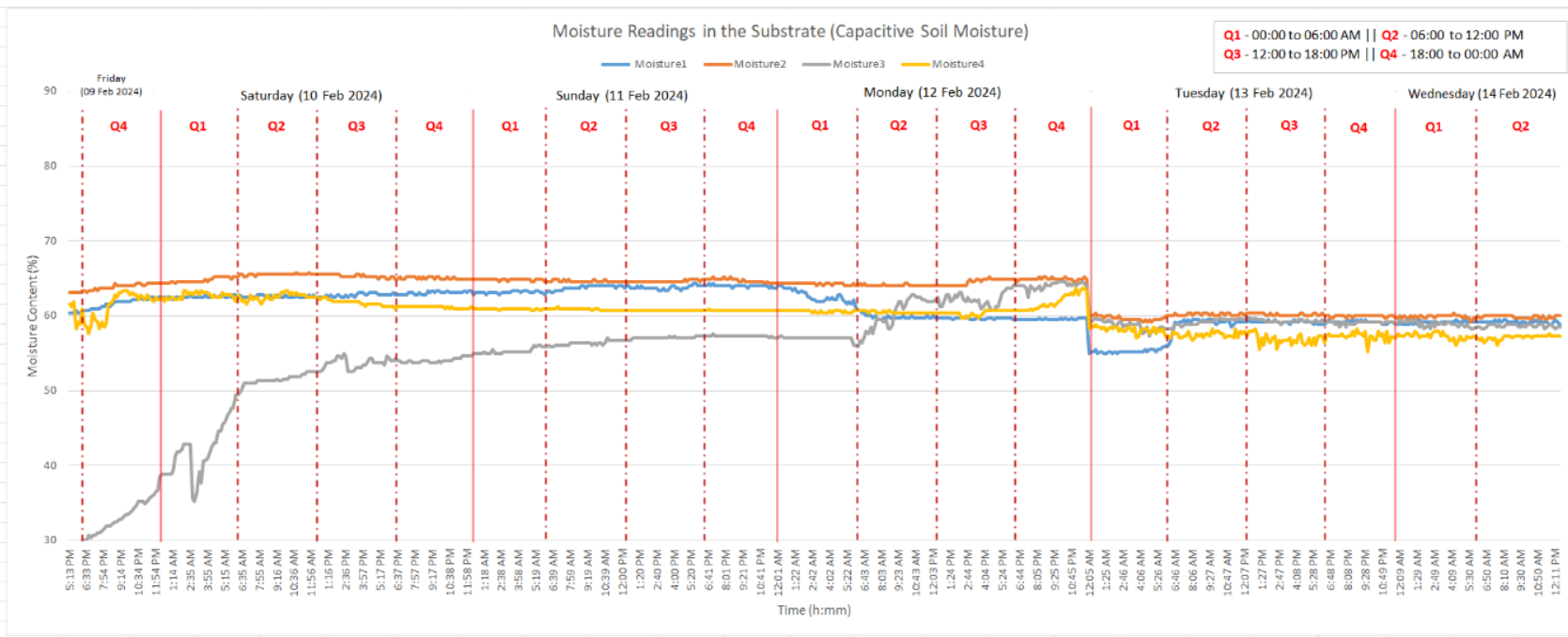


Fig. 46. Data from the four Capacitive Sensor in open-air configuration setup (Plotted on a Line Graph)

By using the equation ( $y = -3.03033x + 505.39$ ) derived in Section 4.1, the graph for moisture content of the substrate is plotted, as shown in [Fig. 46].

According to observations from [Fig. 46], among the four sensors, only the sensor positioned at location three did not initially start at the same moisture level as the others. However, after 48 hours, its readings have risen to approximately the same moisture level as the other sensors. After February 12<sup>th</sup>, there is a sudden drop in readings from all four sensors. The likely reason for this could be attributed to the sensor's accuracy range. However, as information regarding the accuracy of this sensor is unavailable, additional tests will need to be performed to verify whether the drop in temperature is within the expected error range. From [Fig. 46], it appears that the moisture level at the four locations is uniform with less than 5 % variance.

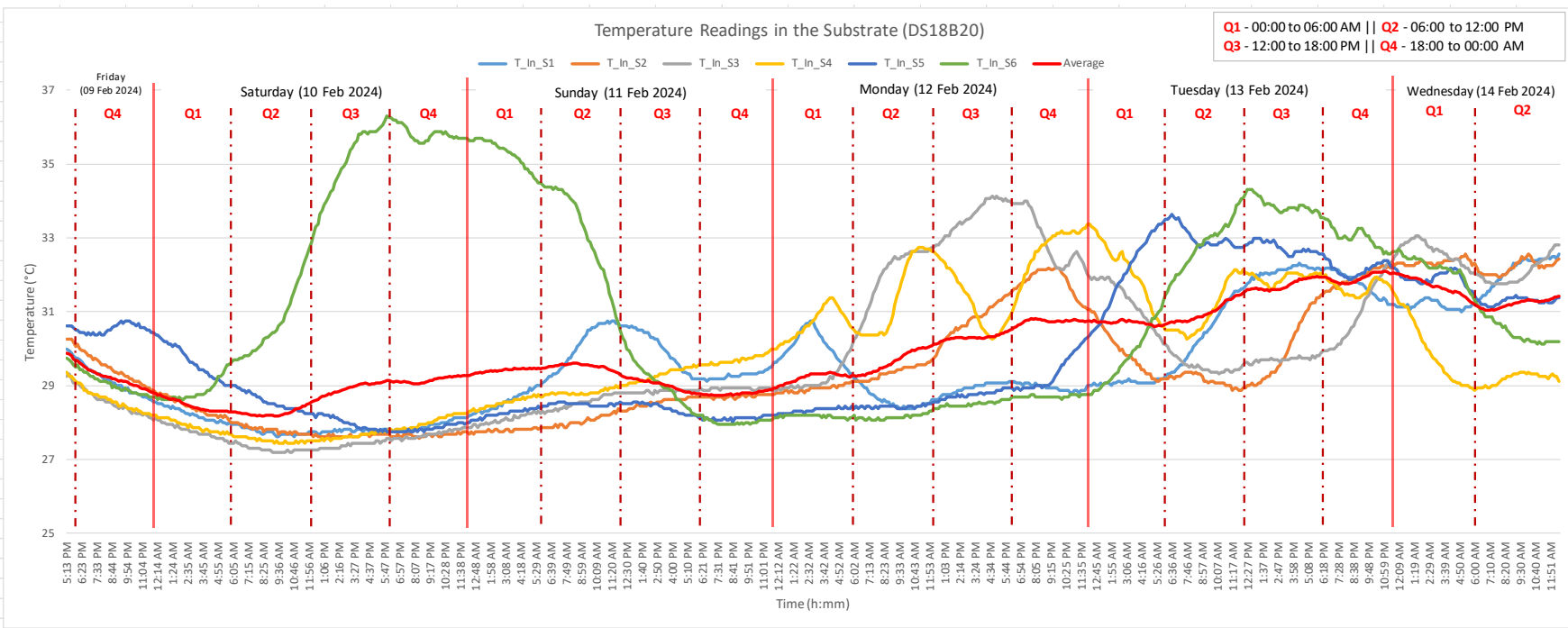


Fig. 47. Data from Six DS18B20 Temperature Sensor in open-air configuration setup (Plotted on a Line Graph)

According to observations from [Fig. 47], among the six sensors, only the sensor positioned at location five shows a spike in temperature readings on the second day (Sunday). The remaining sensors display relatively uniform temperatures, differing by less than 2 °C. After February 11<sup>th</sup>, the distribution between each sensor increases to above 2 °C, reaching up to about a 5 °C difference. To determine the location that can provide a representative interpretation of the substrate, the following steps were taken: Firstly, the difference between the average readings and the readings provided by each sensor was summed up respectively. Then, the respective average value of these summations was calculated, and the lowest value identified would be considered to offer a representative interpretation of the substrate.

After calculation, it is shown that the sensor placed at **location two** has the lowest difference of 0.819 °C variance. The sensor placed at **location one** has the next lowest difference with less than 0.823 °C variance and the sensor at **location five** is in third with less than 0.982 °C variance. Conversely, the sensor at **location six** shows the highest average difference of 2.093 °C. Therefore, the DS18B20 temperature sensor with waterproof probe should be placed at location two, and a safety margin of 2°C for the substrate temperature can be considered.

To assess the variability of the substrate pH value parameter, three analog pH sensors were positioned at three different locations in the substrate as depicted in [Fig. 48]. The analog pH sensor at location three was supposed to be in the middle, but due to a measurement error during mounting, the sensor ended up further to the right.

At the end of stage 2, the pH reading at location three was deemed usable because its output value exceeded the pH scale limit of 14.

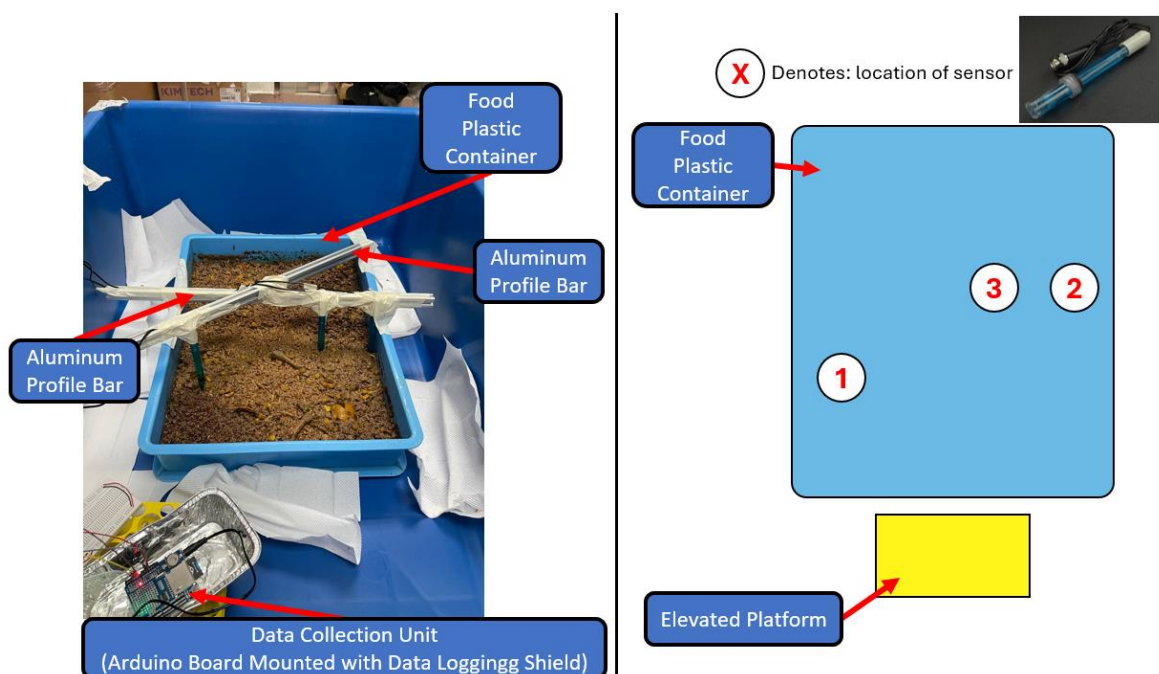


Fig. 48. Plastic Container with sensors mounted (left) and Placement of Analog pH Sensor in container (right)

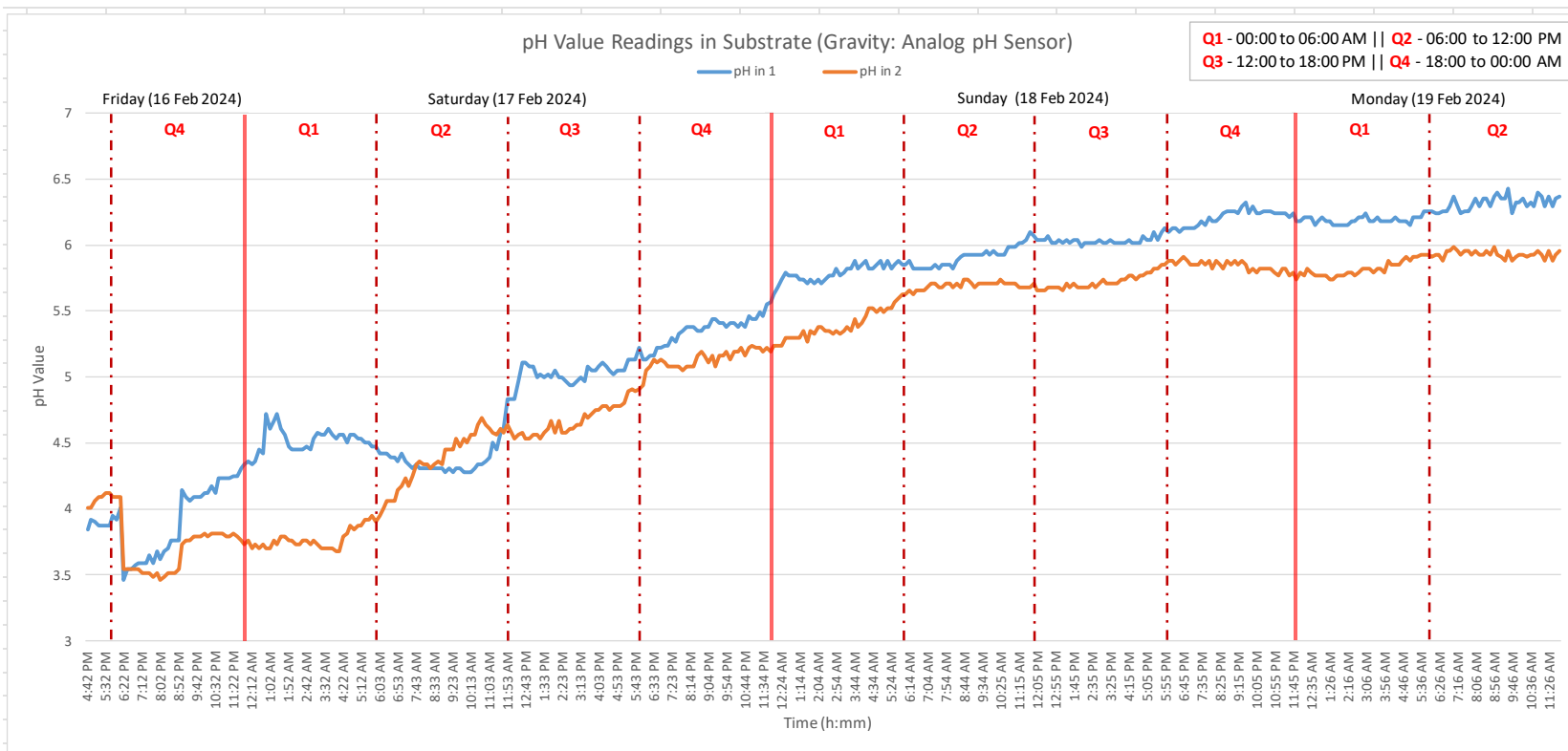


Fig. 49. Data from two Gravity: Analog pH Sensor in open-air configuration setup (Plotted on a Line Graph)

According to observations from [Fig. 49], the pH value shows a positive trend over time. This trend is consistent with studies that found that the BSFL are known to adjust the pH value of the waste stream towards a higher, more alkaline range [26], [28]. It is important to note that the rate at which the pH value of the waste stream changes will vary depending on factors such as type of food waste (A. Fuhrmann, personal communication, April 5, 2024). Hence, instead of monitoring the rate of change, a useful indicator for the end of the bioconversion process can be identified when the pH value levels out. (A. Fuhrmann, personal communication, April 5, 2024). From [Fig. 49], it appears that the pH value at the two locations is fairly uniform with less than 0.5 variance.

### 5.1.2 Phase 2

[Fig. 50] depicts the timeline of phase 2, starting from March 21<sup>st</sup> to March 27<sup>th</sup>. The duration of the second phase was planned to run for about seven days. As mentioned in Section 5, this experiment is conducted for the purpose of collection of additional data, verify the integration of all sensors, ensure data storage capability, and identify additional variability in different environmental conditions. The materials utilized, including the food plastic container, roughly 10,000 5-DOL, 300 g of peanut skin, and the 8 kg food waste, were all sourced from the BSFL research facility at Block S4A. Unexpected events led to an interruption in the data collection a few hours into the experiment, resulting in the loss of experimental data for this phase.

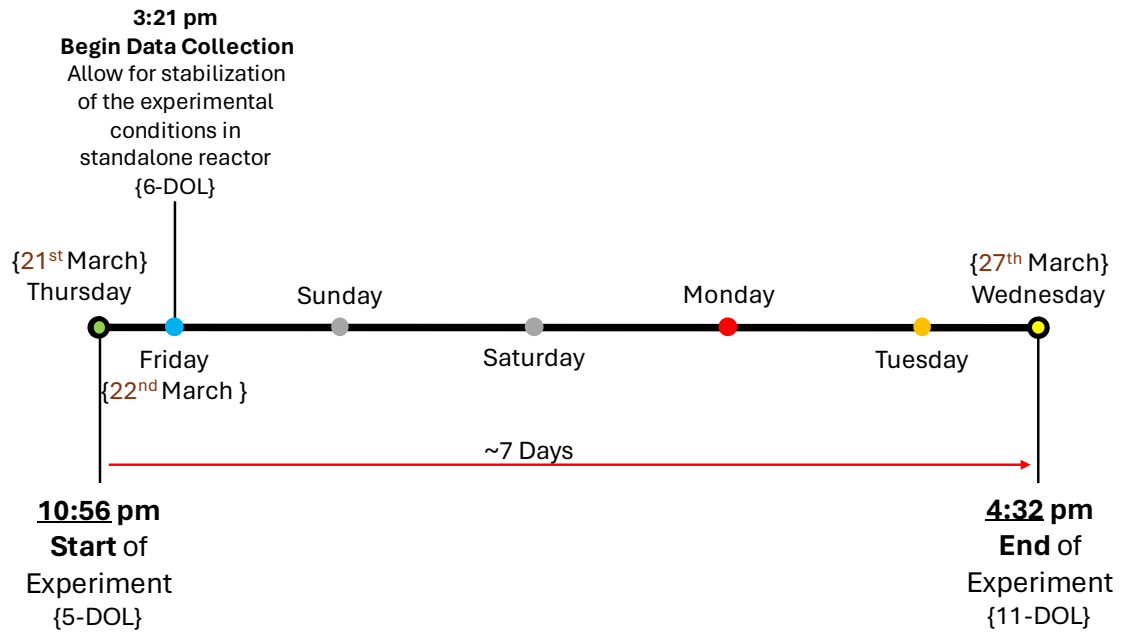


Fig. 50. Timeline of Phase 2

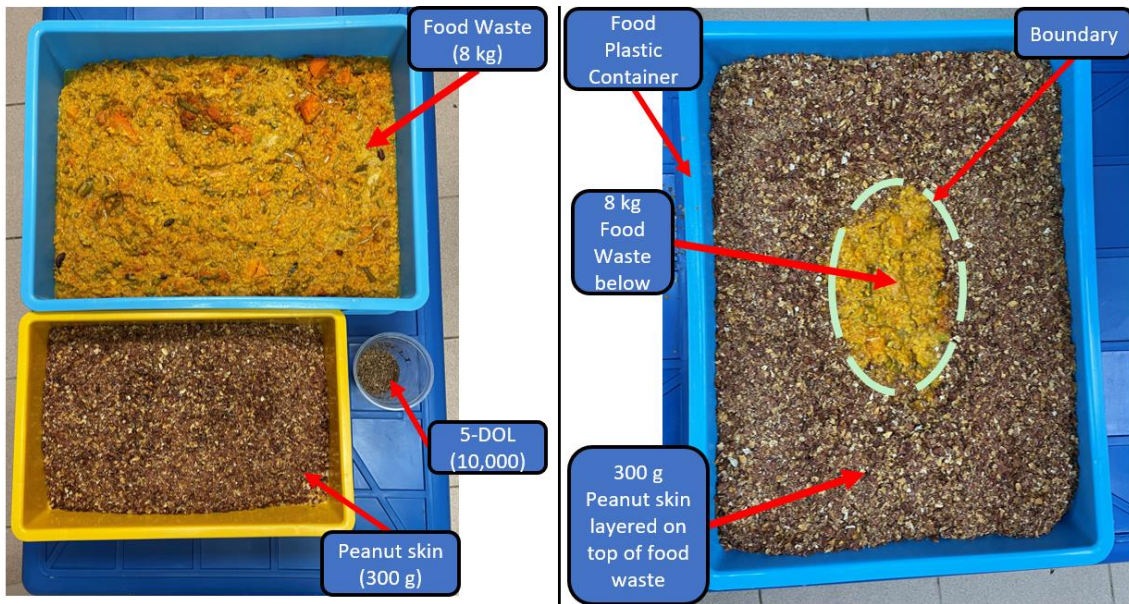


Fig. 51. Food waste, 5-DOL and Peanut Skin (left) and Top view after pouring the peanut skin over the food waste (right)

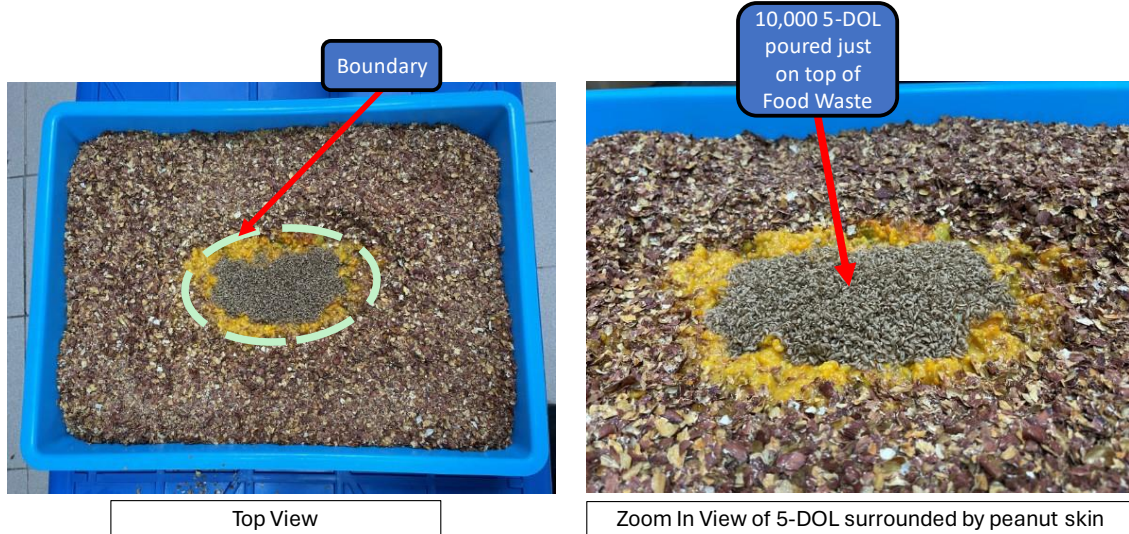


Fig. 52. Top view after pouring the 5-DOL over food waste in the center (left) and Larvae sitting above food waste (right)

[Fig. 51] and [Fig. 52] show the experiment set up phase for preparing the substrate prior to the insertion of sensors. To ensure that the BSFL do not escape during the initial feeding stage of the bioconversion process, a boundary form with peanut skin was used.

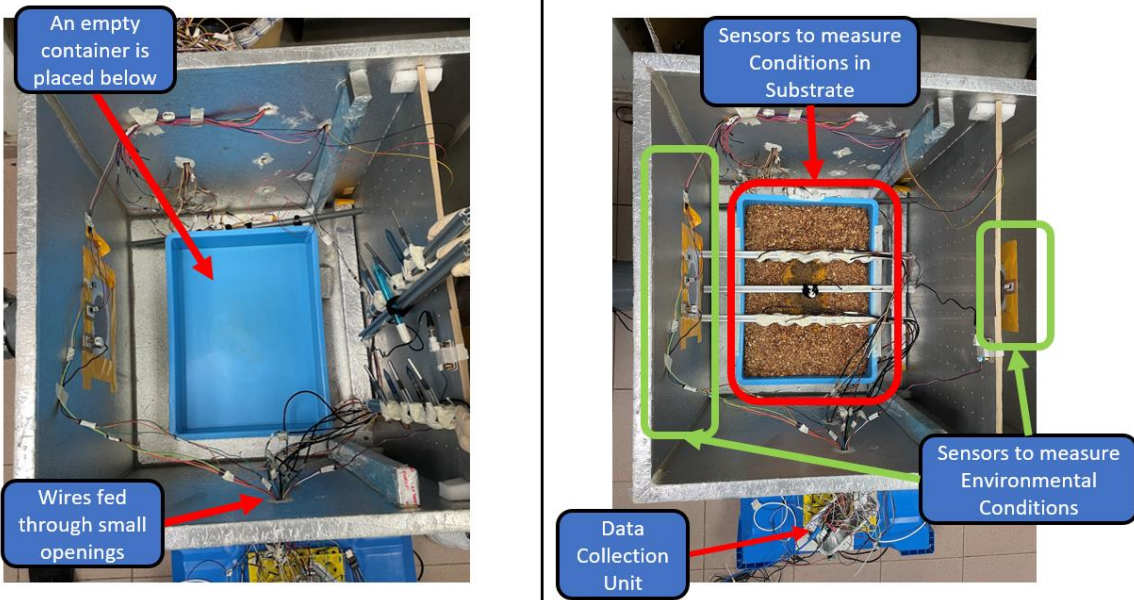


Fig. 53. Top view before food container with substrate is placed inside standalone reactor (left) and Overview of the general locations of the various electronics (right)

Due to the design of the standalone reactor, as seen in [Fig. 53], small openings which have cable glands fitted on the outside serve as the only entry points for wires to enter. This is likely to ensure a proper sealing of the reactor. Before placing the plastic container containing the substrate, presented in [Fig. 52], inside the reactor, an empty container, as seen in [Fig. 53] was used as an elevated platform. This is to allow the wires of various sensors to be able to connect to the data collection unit sitting outside of the reactor as seen on the right side of [Fig. 53].

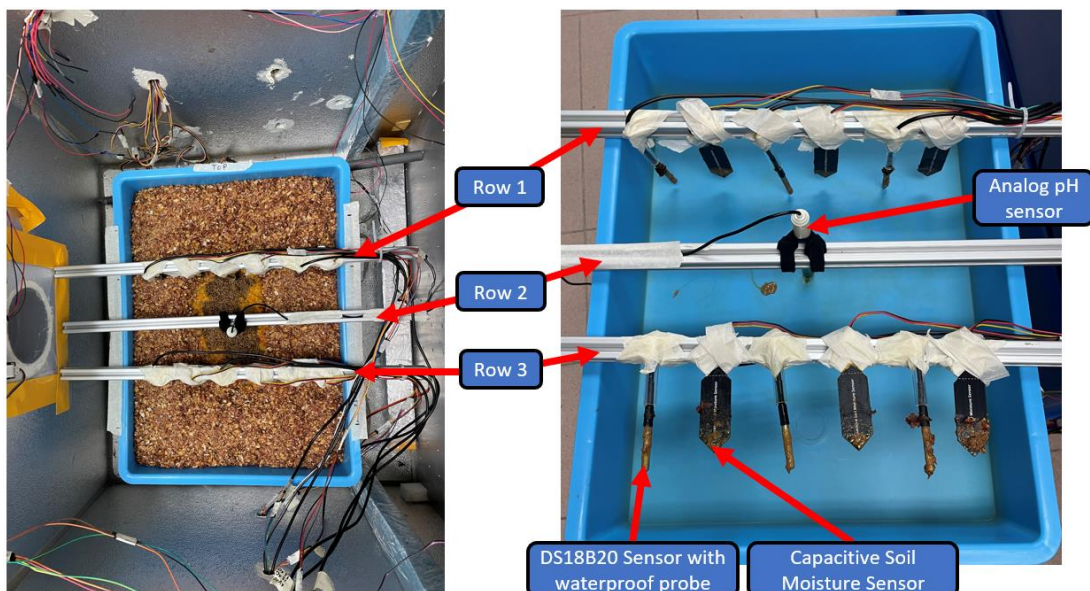
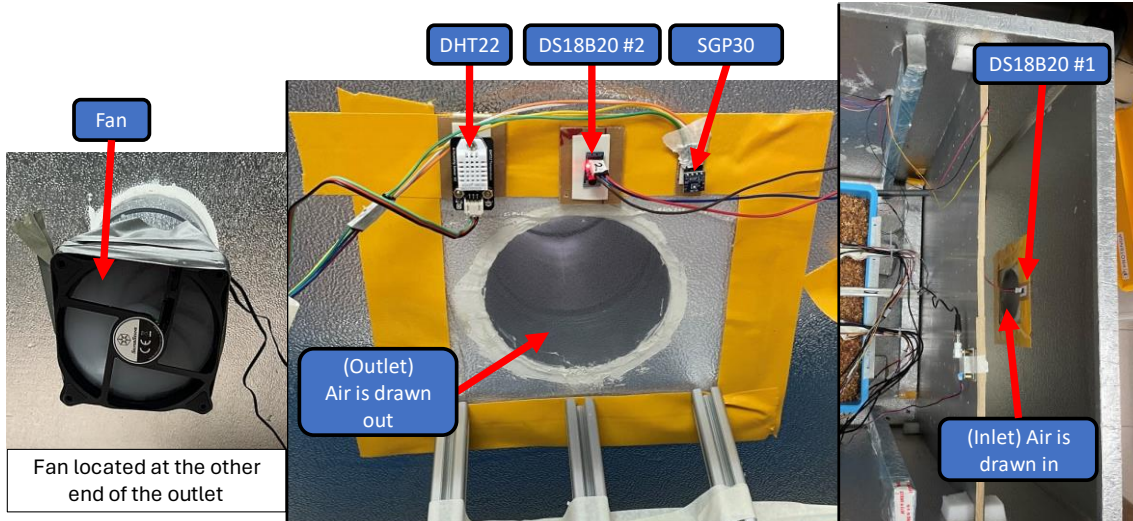


Fig. 54. Location of sensors to measure conditions in the substrate in the standalone reactor

To assess the variability of moisture, substrate temperature, and substrate pH, respectively, the following sensors were employed: six capacitive moisture sensors, six DS18B20 temperature sensors waterproof probes, and one analog pH sensor as seen in [Fig. 54]. The placement of the sensors is similar to that in Phase 1, enabling comparison between the open and closed configurations. Only one pH sensor is used due to the limited availability of long wires.



*Fig 55. Fan mounted on the outside of reactor (left), Location of sensors to measure environmental conditions inside standalone reactor, outlet (middle), inlet (right)*

[Fig. 55] shows the 3 types of sensors that are being used to measure environmental conditions inside the standalone reactor. A DS18B20 sensor is installed at both the inlet and outlet to facilitate monitoring and comparison of temperature changes throughout the system. A single SGP30 sensor is used as an Arduino is unable to recognize multiple SGP30 as discussed in Section 4.6. A single DHT22 is used due to the limited availability of long wires at hand. The sensors were affixed to the yellow tape region using double-sided tape to preserve the integrity of the standalone sealed reactor. To establish an airflow that draws air inward from the inlet, over the substrate, and outward through the outlet, a small fan was positioned on the outside of the outlet. This fan was utilized as it was already mounted at the outlet of the standalone reactor. Furthermore, since the requirement was to generate airflow, the specific selection of the fan was not critical.

To store data from the sensors, like in Phase 1, a micro-SD card was selected given its universality. To interface the micro-SD card with the Arduino, an Arduino Mega board was paired with

a specially designed protoboard instead of utilizing the data logging shield, as depicted in [Fig. 56].

This decision aimed to test the functionality of the protoboard before its final integration in Phase three.

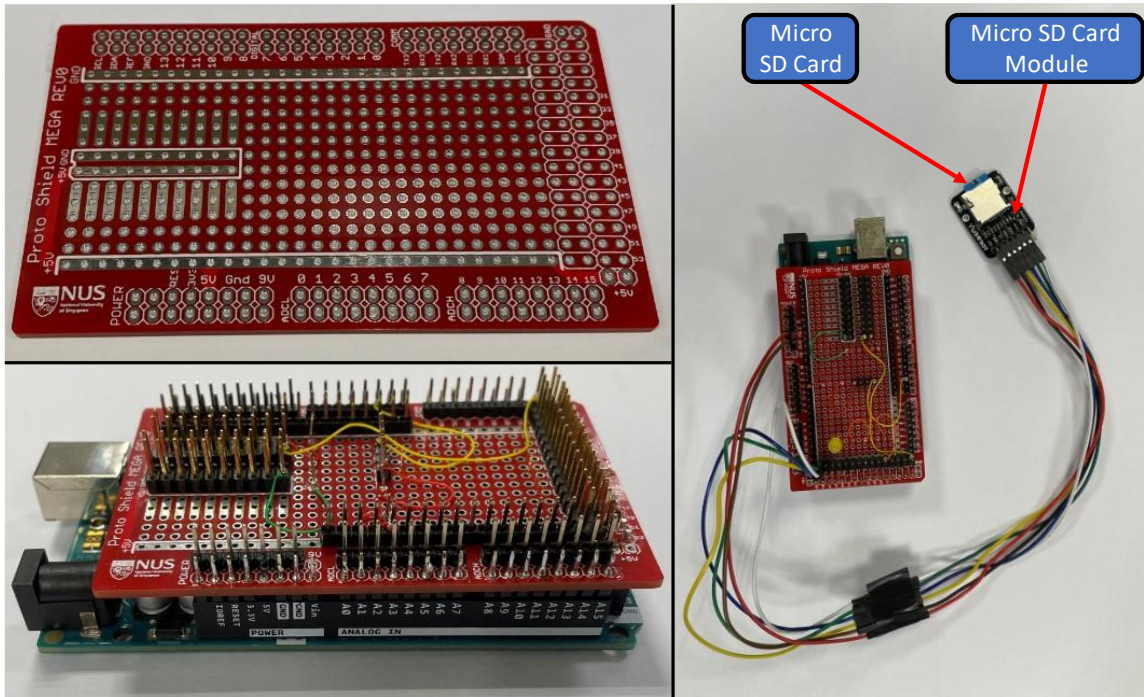


Fig. 56. NUS Protoboard shield for Arduino Mega before soldering (top left), Components soldered onto protoboard (bottom left) and Micro SD Card Module connect to shield

Before the weekend, on the afternoon of Friday, March 22nd, the data collection was intentionally paused for less than half an hour. This interruption was to conduct an inspection of the data collection process by checking for any consistent measurement readings of invalid output values from the sensors. Should there be a constant flow of invalid output, the reason would likely be attributed to a loose connection in the circuit. Upon inspecting the data stored in the SD card and confirming the functionality of the data collection process, it was observed that the majority of sensor readings are valid, as evidenced by their frequent fluctuations. Moreover, since the initial plan was to analyze the data after allowing some time for the experimental conditions in the standalone reactor to stabilize, this interruption did not significantly affect Phase 2.

Unfortunately, due to unforeseen circumstances, a disturbance occurred only 18 hours later, leading to an interruption in the data collection process. Consequently, the data recording ceased operation and no data was recorded.

The data interruption might have been discovered sooner had the data storage been on a cloud server rather than an SD Card. Transferring data to a real-time cloud service and storage platform like ThingSpeak using a wireless communication module such as a nRF24L01 module could have saved the experiment. However, after several unsuccessful attempts to establish a connection from the nRF24L01 module to ThingSpeak, likely due to the stringent security measures of the NUS Wi-Fi network, this approach was abandoned. Depending on the cost, an alternative solution to overcome this limitation would be to acquire an a SIM card that has data capabilities.

Drawing from this experience, and recognizing the necessity for regular experiment checks, an indicator was soldered onto the specially designed protoboard as seen in [Fig. 57]. With this indicator, should the Arduino fail to store data into the SD Card, the light emitting diode (LED) will glow, signaling a problem with data collection process.

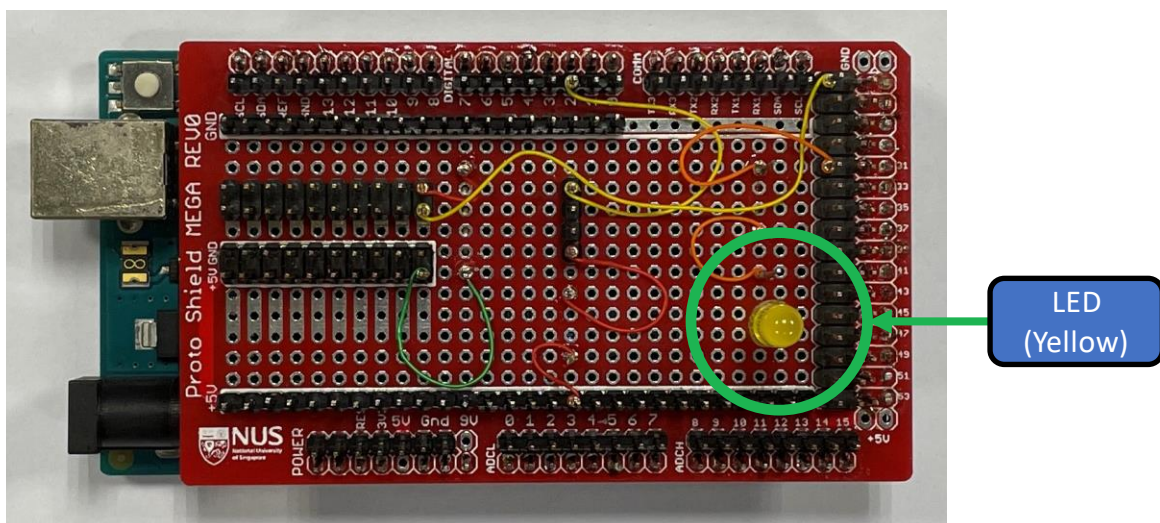


Fig. 57. Modifications made to Protoboard Shield

### 5.1.3 Phase 3 (Full System Assembly Test)

[Fig. 58] illustrates the ongoing timeline of phase three, which commenced on April 4<sup>th</sup> and is anticipated to conclude by April 15<sup>th</sup>. The duration of the third phase is expected to span approximately 12 days. Having designed and fabricated the individual scope of work (Section 3.3), integration between the various sub-system was done to assemble the one-third scale prototype envisioned in [Fig. 9]. During this phase, all electronic components, including the fans, self-cut multistrand (multicore) wires, and various sensors identified in Section 4.0, will be incorporated together, and installed into the one-third scale prototype of the proposed solution.

The bioconversion process using the prototype is still ongoing. Therefore, at the time of submitting this thesis, the data is not yet available. The full results will be documented at a later time.

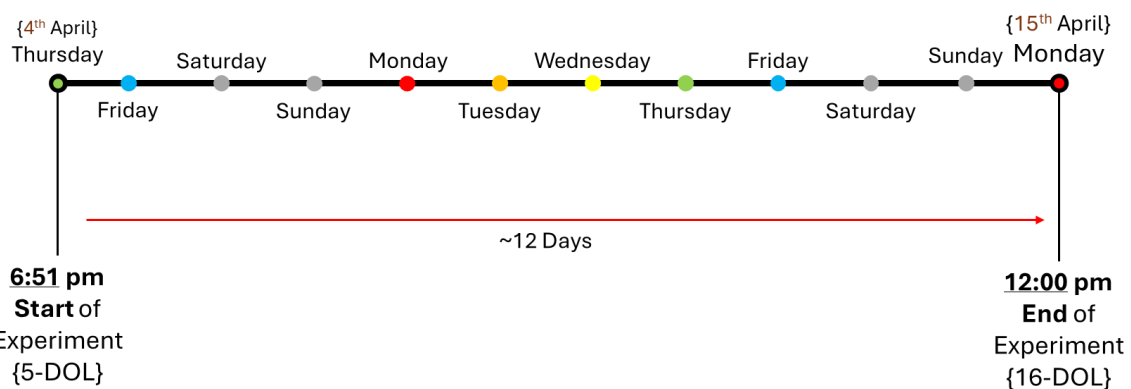


Fig 58. Phase 3, Ongoing Experiment Timeline (Subject to Change)

Since the proposed solution is to treat and recycle Singapore's heterogeneous food waste in a non-laboratory environment, to simulate the reactors being deployed in a decentralized manner, the experiment was decided to be conducted at the engineering area, at block E2A. Before commencing the experiment, the food waste was prepared at the research facility, and then it was packaged for transportation from Block S4A to Block E2A.

### 5.1.3.1 Preparation at the BSFL Research facility

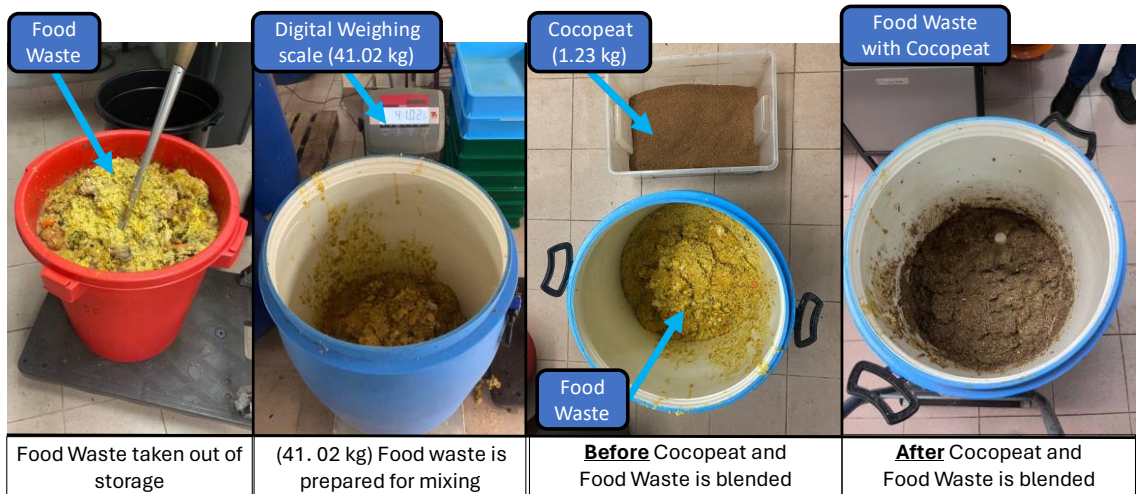


Fig 59. (From left to right) Unprepared Food Waste, Food Waste on weighing scale, Before Food Waste is mixed with cocopeat, After Food Waste is mixed with cocopeat

[Fig. 59] illustrates the process leading up to the preparation of the food waste for use. In accordance with the pre-experiment discussion, it was decided that, considering resource constraints and as this is the inaugural use of the one-third scale reactor, a reduced quantity of food waste, targeting 6.5 kg from the initial 8 kg, will be allocated for each food plastic container. To ensure adequate food waste in each of the six containers, an extra 2 kg was added as a safety margin. Once 41 kg of food waste was measured, to achieve uniformity, it was blended with 1.23 kg of cocopeat using a high torque drill fitted with a modified mixing attachment, designed specifically for blending and mixing purposes.

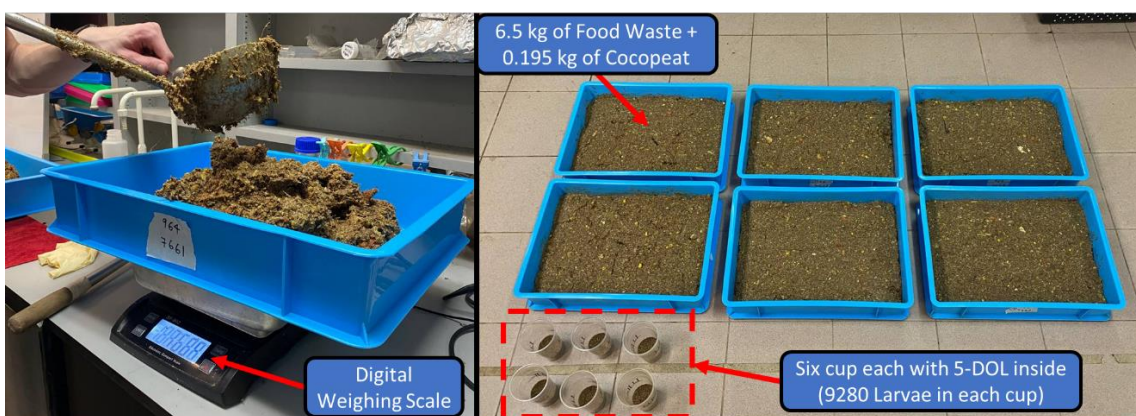


Fig. 60. Food Plastic Container being weigh on weighing scale (left) and Substrate ready for BSFL (right)

To ensure precise measurements of about 6.695 kg of substrate (comprising 6.5 kg of food waste and 0.195 kg of cocopeat) for each food plastic container, a digital weighing scale was employed, as depicted in [Fig. 60]. Instead of initiating the bioconversion process by pouring the 9280 5-DOL at the research facility, it was decided to perform this step back at the engineering area.



Fig. 61. Height of the substrate measured with a ruler (left) and Substrate wrapped in clear plastic (right)

Before wrapping the food plastic containers with clear plastic wrap, as seen in [Fig. 61], to prevent accidental spillage during transportation, a ruler was used to measure the height of the substrate for documentation purposes. However, since the measurement was taken visually using a ruler, there may be some margin of error.

### 5.1.3.2 Installation and Assembly of the Electronics Components into Prototype

As mentioned in the concept design (Section 3.2), depending on specific parameters, certain sensors will be embedded within the substrate, while others will be positioned either around the containers or somewhere inside the reactor. [Fig 62] shows an overview of where the sensors will be located within the prototype. The sensors are grouped into two categories namely, sensors to measure **conditions in the substrate** (indicated in Red) and sensors to measure **environmental conditions in the reactor** (Indicated in Green). The output signal from all the sensors will be sent to the Arduino Mega, located inside an Electronics Storage box, placed at the designated electronics compartment in the prototype.

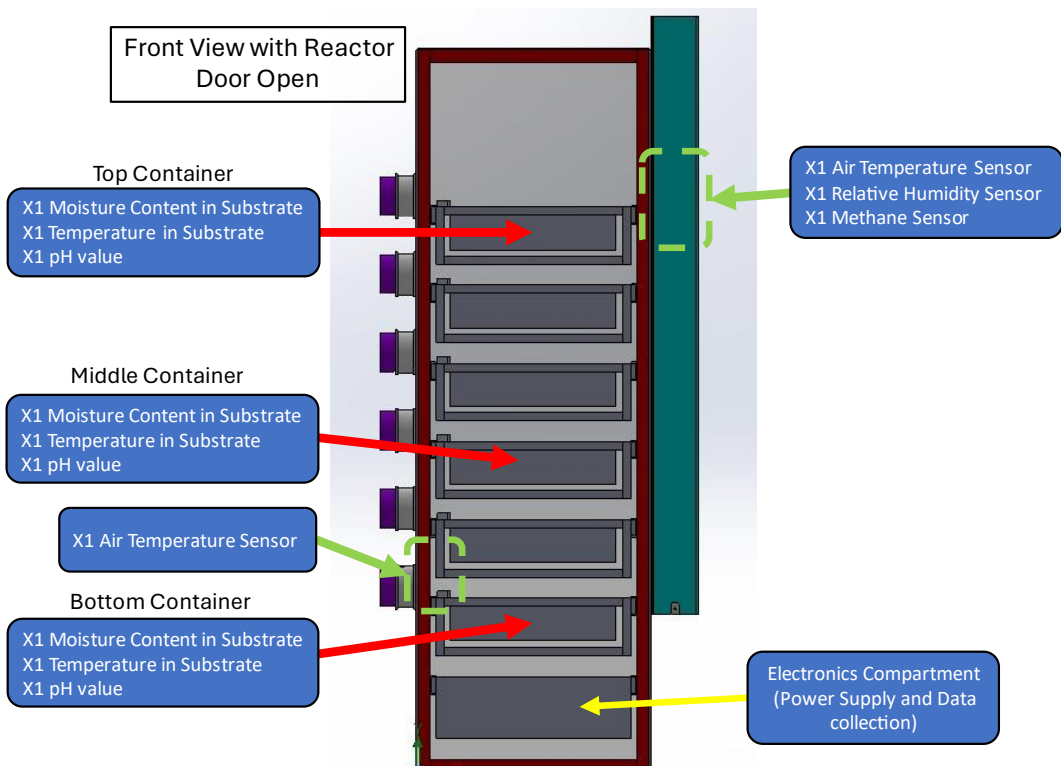


Fig. 62 General locations for sensors in the one-third scale prototype

To ensure a reliable connection between each electrical device and the Arduino board positioned at the bottom of the reactor, it is crucial that the wires are not only long but also well-insulated. Given the large number of electrical devices involved, a strategic approach was taken. Instead of using individual long wires for each pin of the electrical device, various types of multistrand (Multicore) cables were employed. For the fans, which require only four connections (Power, Ground,

PWM, and Tachometer output), a 4-wire multistrand cable was utilized. On the other hand, for the sensors responsible for measuring conditions in the substrate and environmental factors, an 8-wire multistrand cable was cut and used respectively. Since each sensor operates at 5 V, they will share a single power cable, thereby reducing the number of wires connecting back to the Arduino board. This concept is similar to the ground connection. Female Dupont Terminals were then crimped onto each end of the Multistrand cable, and a protective layer of heat shrink tubing was applied, as shown in [Fig. 63]

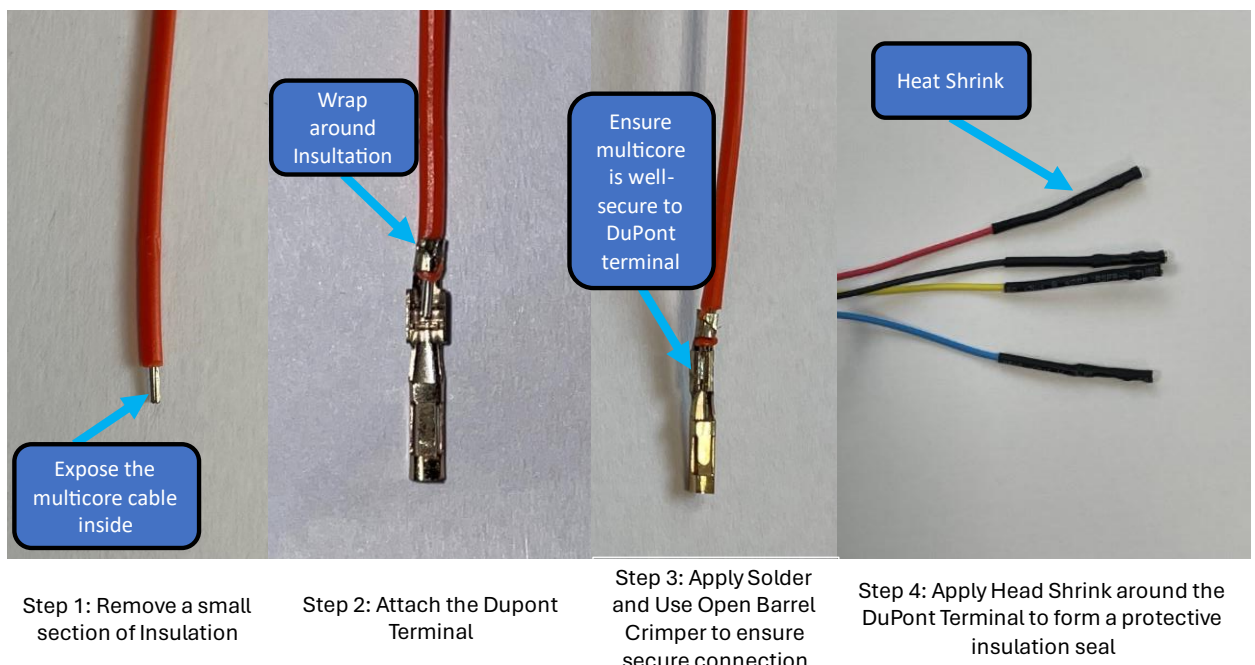


Fig. 63. (left to right) Female Dupont Connections to ensure reliable connection from sensors to Arduino board

Furthermore, to guarantee a stable and consistent 5V power supply, a DC-DC Step-down buck converter was incorporated into the system. This ensures not only a steady 5V supply to the sensors but also prevents significant heating of the Arduino board due to generated heat. [Fig. 64] and [Fig. 65] give an overview of all the Electronics components that is being implemented inside the reactor. [Fig. 64] consists of the wiring to the various sensors while [Fig. 65] consists of the wiring to the 12 V fan.

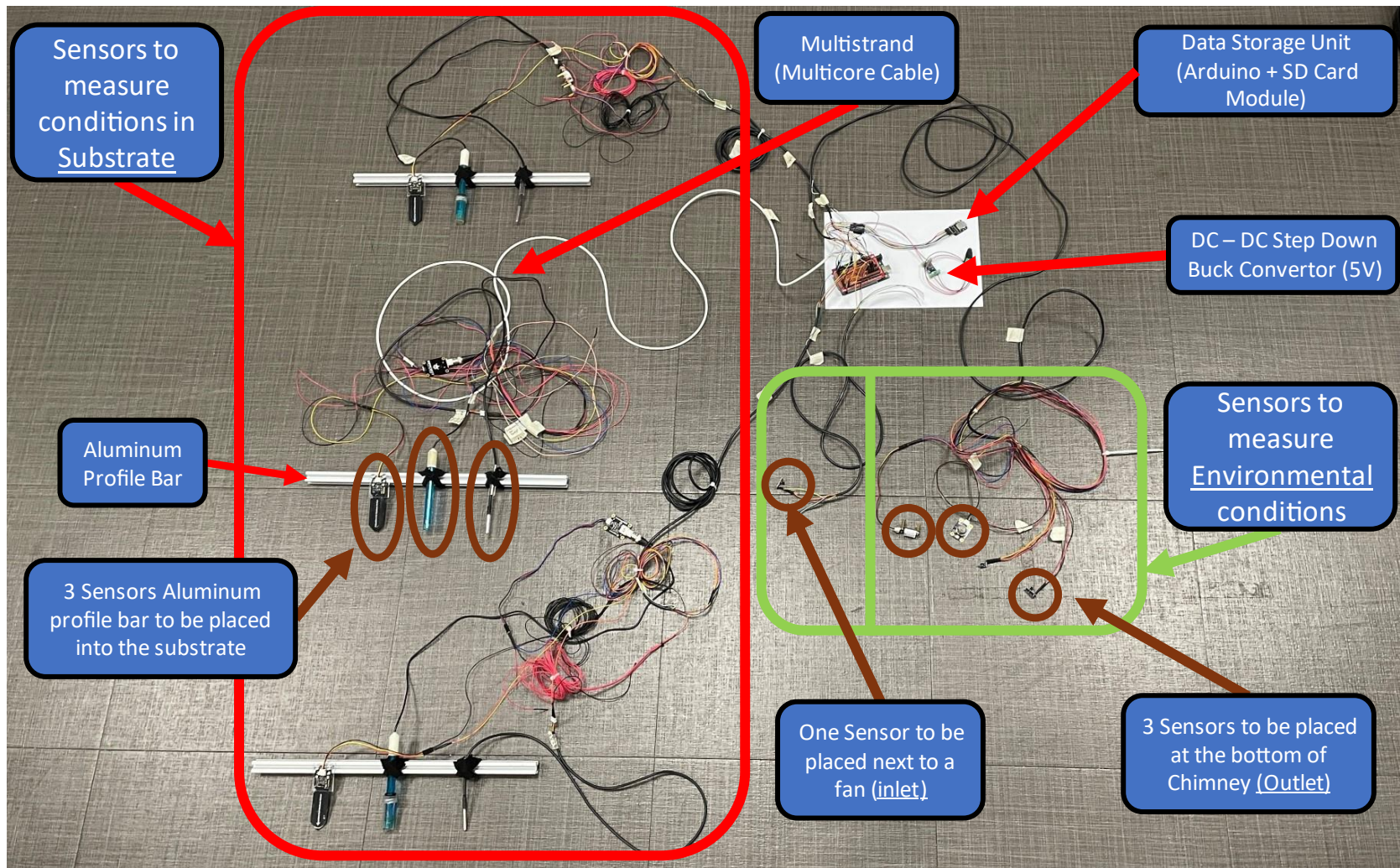


Fig. 64. Overview of the all the Electronics components Part #1 (Exclude the fans)

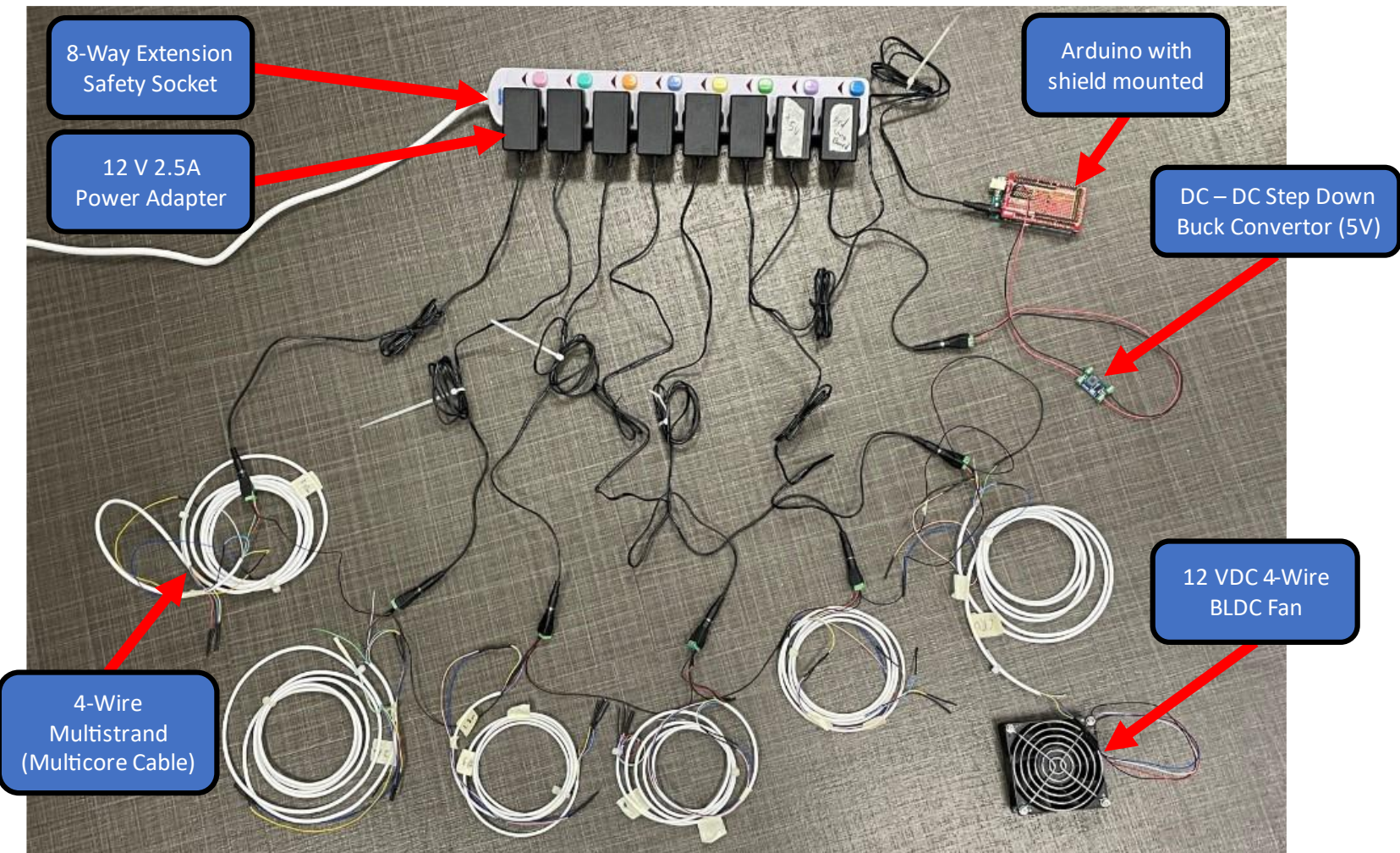
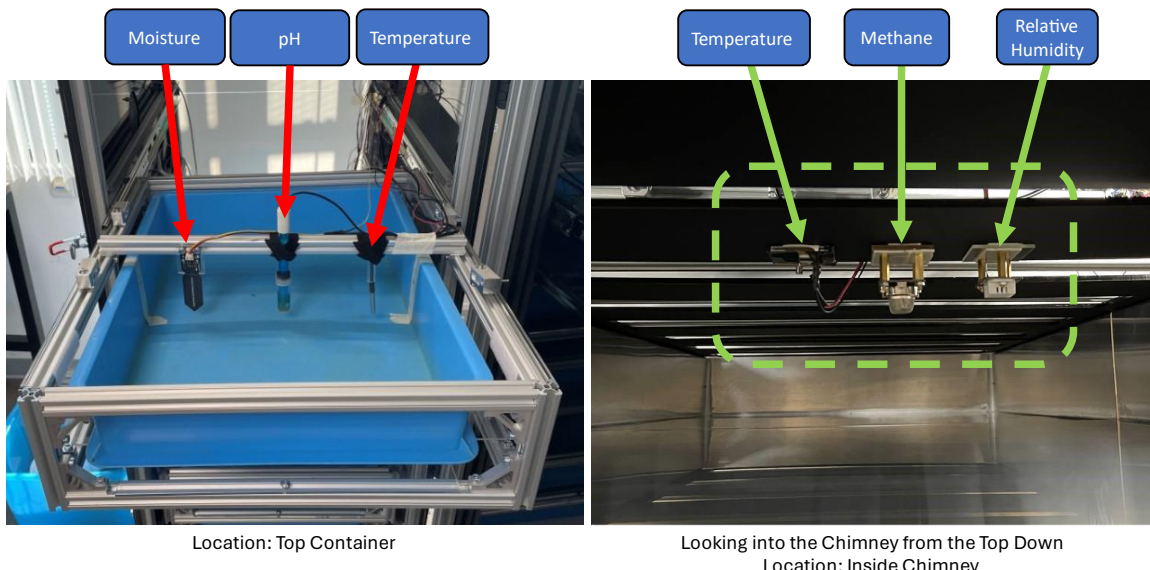


Fig. 65. Overview of the all the Electronics components Part #2 (Exclude sensors)

With one Arduino board, one 5V step-down buck converter, and six fans all requiring power, a single 8-way extension safety socket was utilized. This socket enables the entire prototype to be powered down with a single flip of the switch, located at the wall socket. Because each fan has a current rating of 2 A, a dedicated power adapter is required for each fan, as depicted in [Fig. 65]. With the selected power adapter, the maximum current that can be drawn is 2.5 A at the output, which is higher than the fan's current rating. (Please refer to Appendix F for the calculations to support the current fans configuration) Therefore, the circuit adheres to electrical safety limits and is unlikely to pose any fire hazards.



*Fig. 66. Sensors mounted on aluminum profile at Top Container (left) and Sensors mounted inside the chimney (right)*

[Fig. 66] shows the placement of the various sensors in the prototype. The DS18B20 temperature sensor with a waterproof probe is positioned at its current location primarily because it is situated farthest from the fan. Given that the system will utilize temperature readings to regulate fan speed, it was decided to position the sensor in a location less susceptible to direct airflow impact. For the capacitive sensors, while the findings from phase 1 imply that the middle position could offer a representative reading of the entire substrate, it's important to note that phase 1 was conducted without airflow. Therefore, the validity of this assumption in the current reactor setup needs to be verified through further experimentation. Considering that the system does not take the moisture

readings to perform any action, such as regulating fan speed, the moisture sensor was placed at its current position as seen in [Fig. 66]. For the sensors measuring environmental conditions, they were positioned in their current locations to ensure that the wires do not affect their readings. This setup ensures that the airflow remains undisturbed and unaffected by the presence of any wires.

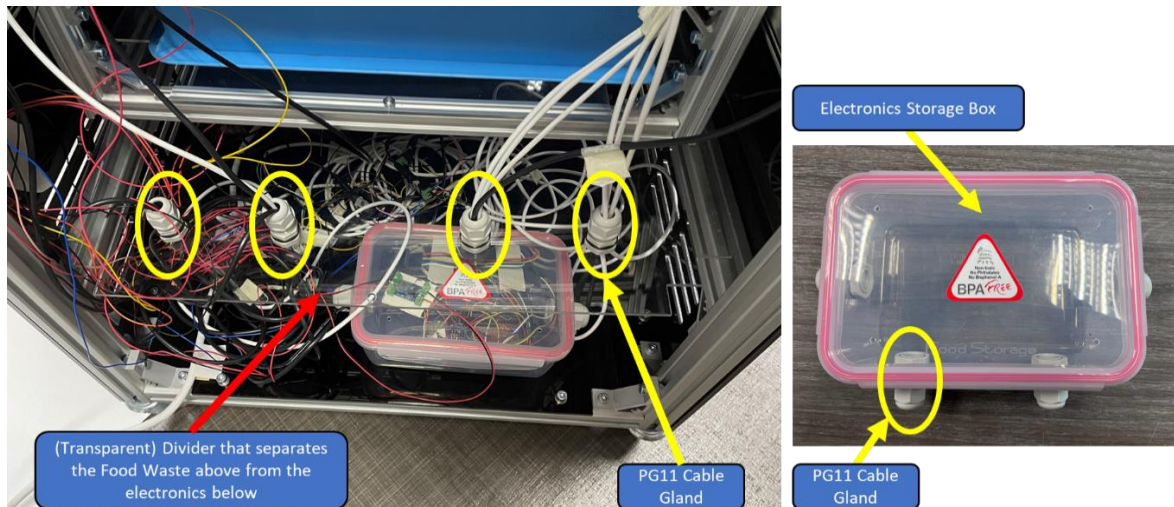


*Fig. 67. Electronic compartment view from the back of reactor, Electrical considerations to protect the electronics below from the substrate above*

To ensure that the BSFL or the substrate does not accidentally fall into the electronic compartment, a divider made with 3mm acrylic was fabricated and installed just below the bottom container, as seen [Fig. 67]. Additionally, to safeguard against any accidental liquid contact with the electronics below, particularly the Arduino Board, the Arduino is housed within the electronics storage box for enhanced protection from external elements, in conjunction with the use of a cable gland.

It is important to incorporate added protections for the Arduino considering that there are also air vents on both the left and right sides of the reactors, as seen in [Fig. 68]. While these vents are advantageous for preventing heat buildup within the electronics compartment, they also create openings that could allow small insects or rodents to easily access the interior. To address this issue, wire mesh was attached over the air vents as an additional measure as seen in [Fig. 68].



Air Vents to allow airflow in and out to dissipate Heat  
*Fig. 68. Side view of Prototype where air vents are located (left) and Installation of wire mesh (right)*

[Fig. 69] shows a pictorial diagram of various electronic components used in the prototype. The diagram depicts only one sensor for each parameter, but it does not imply that only one sensor for each parameter is being utilized in the Phase three experiment. The system operates with two primary functionalities. Firstly, it collects data or signals from various sensors and stores them into an SD Card through the SD Card module. Secondly, it utilizes this data to adjust the PWM signals sent to the fans, thereby regulating the fan speed.

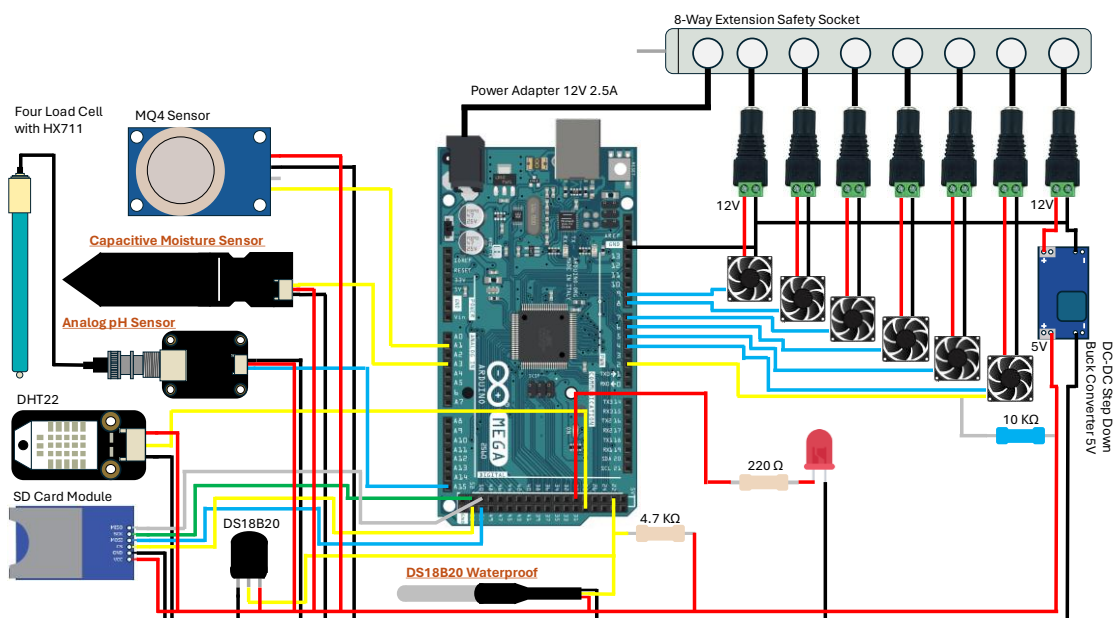


*Fig. 69. Pictorial Diagram of Electronic Circuit showing the connections of the Sensors, Fans and 5 V Power supply*  
Note: Sensors with their names underlined and in brown denote that they measure conditions in the substrate

[Tab. 9] list the components utilized during the full system assembly test in the one-third scale prototype. Similar to [Fig. 69], the table only shows one sensor for each parameter, but it does not imply that only one sensor for each parameter is being utilized in Phase three experiment.

*Tab 9. Overview of the Electrical Components and their Pinouts*

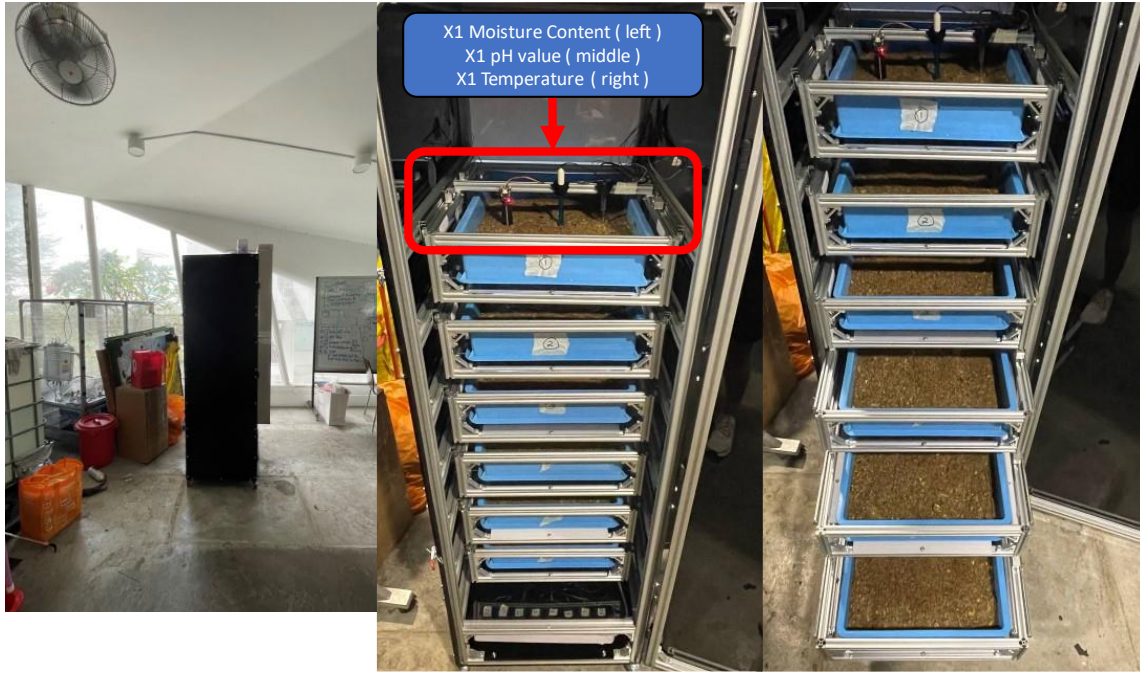
	Component	Pins Required	Pin Number on Arduino (Respectively)
Data Recording	Micro SD Module	MISO, MOSI, SCK, CS, VCC, GND	D50, D51, D52, D53
Sensors measuring conditions in Substrate	Capacitive Soil Moisture	AOUT, VCC, GND	A3
	DS18B20 (Waterproof)	DQ, VCC, GND	D22
	Gravity Analog pH	AOUT, VCC, GND	A13
Sensors measuring environmental conditions in reactor	DS18B20	DQ, VCC, GND	D22
	DHT22	DATA, VCC, GND	D29
	MQ4	AOUT, VCC, GND	A1
Aeration	BLDC 12V Fan	TACH, PWM, VCC, GND	D2, D4

Note: Component in purple denotes that it is inside the electronics storage box. "D" Denotes a digital pin while "A" denotes an analog pin on the Arduino. VCC and GND are connected to the 5 V from the Step-down buck converter rather than from the Arduino

### 5.1.3.3 Placing the containers with substrate into the prototype

Phase 3 experiment is currently being conducted at the prototyping area at building E2A, Level 1.

1. Although it is located outdoors, it is sheltered from the weather conditions to a certain extend as seen in [Fig. 70]



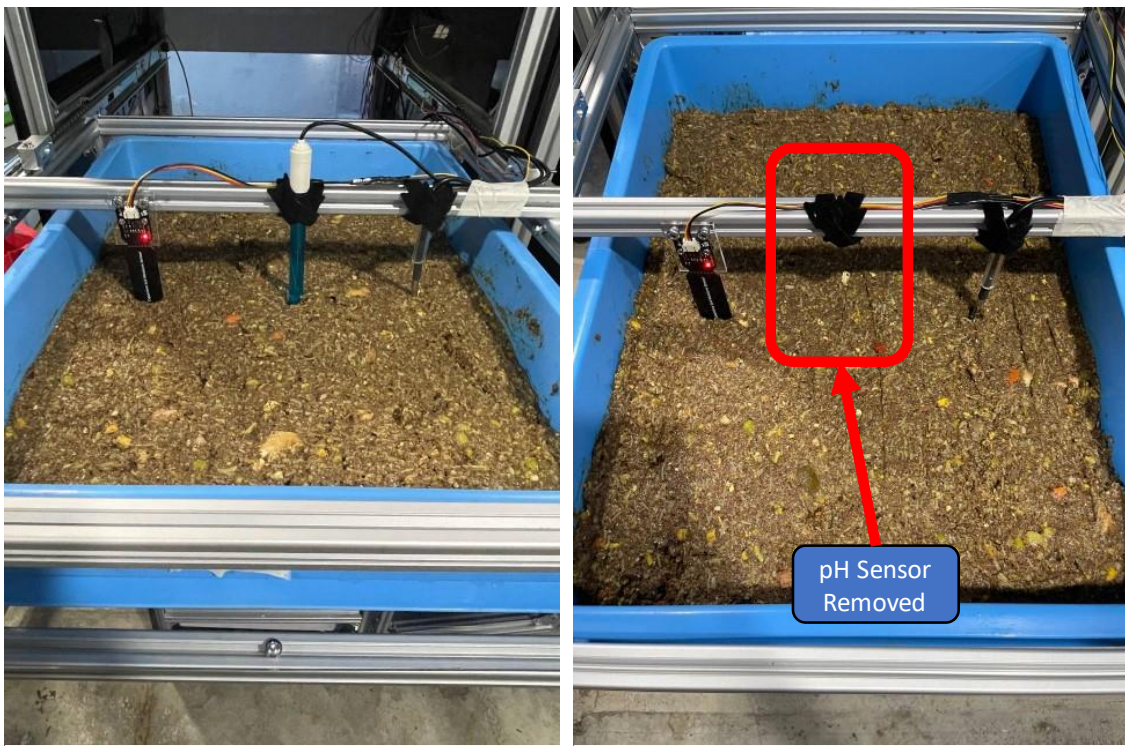
Location: Prototyping Area at Building E2A, Level 1

Front View of the reactor during the bioconversion process

Each level containing substrate

Fig. 70. Location of Phase 3 Experiment (left), View of the bioconversion process, door open (middle), Each level containing substrate (right)

During the installation of the sensors that measures conditions in the substrate, a discovery was made regarding the limited clearance between each container. This became evident from the second container downward to the sixth at the bottom, where the mounting of the pH sensor was impractical due to the restricted space. Instead of adjusting the angle of pH probe, the decision was made to entirely remove the pH sensor as shown in [Fig. 71]. Hence, only one pH sensor, located at the top container will be used to gather readings.



Location: Top Container

Location: Middle and Bottom Container

Fig. 71. pH sensor removed from middle and bottom container

## 5.2. Software Integration

[Fig. 72] illustrates a flowchart of how the various sensors shown in [Tab. 7] can be incorporated together. The flowchart is divided into 3 sections.

Most of the sensors are in the middle section, where conditions inside the reactor will be monitored and environmental parameters within can be adjusted via the fans.

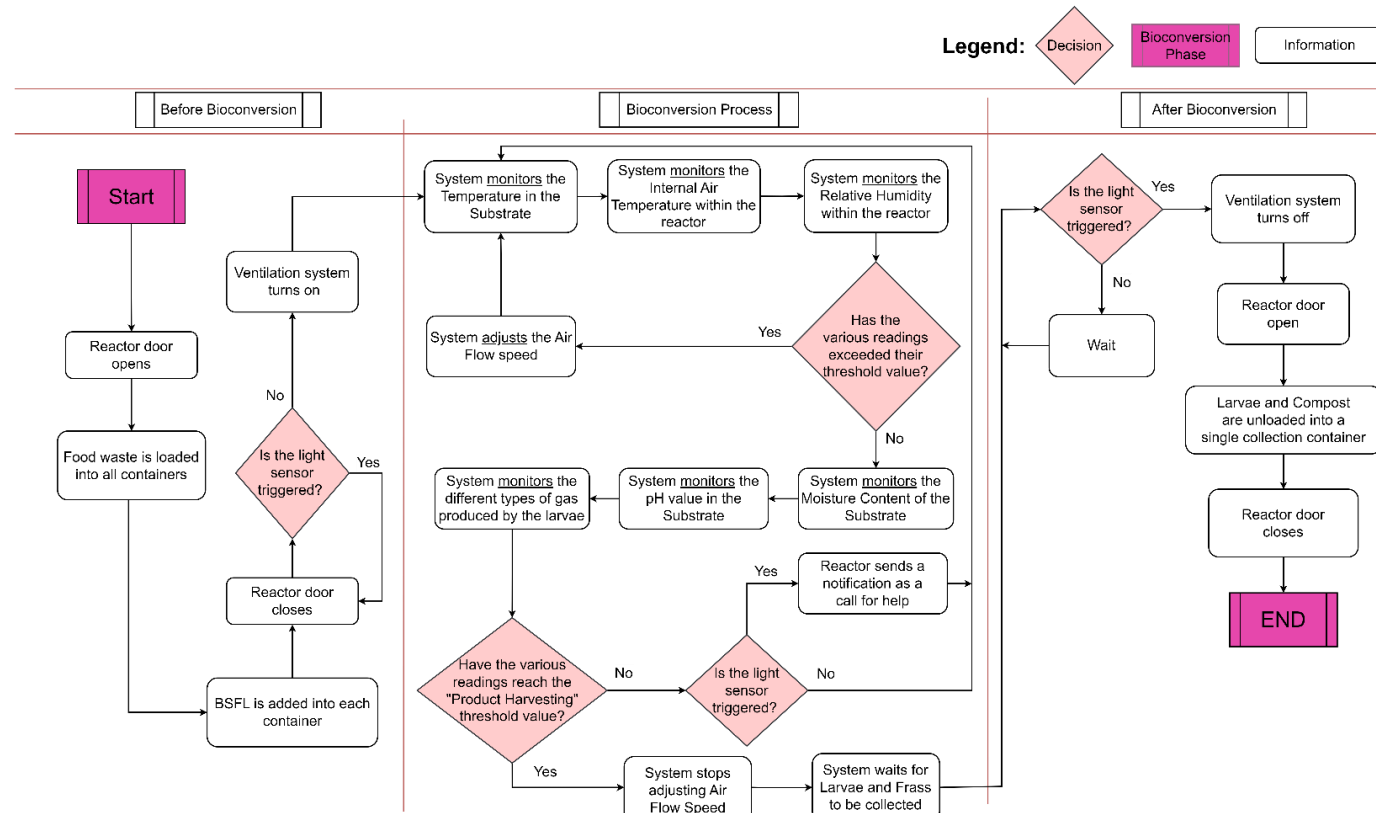


Fig. 72. Flowchart of the Various Sensors Integrated Together

Note: Light Sensor will not be used in the one-third scaled reactor as the need to measure the intensity of light within the reactor is not required at this stage of the prototyping.

Before the BSFL loader leaves the reactor, if there is a gap in the door where light can reach the light sensor, the ventilation system in the reactor will not activate. This should prompt the BSFL loader to inspect the system. Throughout the bioconversion process, parameters such as temperature and relative humidity will be periodically checked to assess the need for adjusting the airflow rate within the reactor. Additionally, to determine the optimal harvest time, the system can monitor parameters such as moisture content and pH value of the substrate. When these measurements reach specific threshold values, indicating that the BSFL has ceased feeding, an alert can be sent to the BSFL harvester, via a wireless communication module, to collect the larvae (pupae stage) for harvesting.

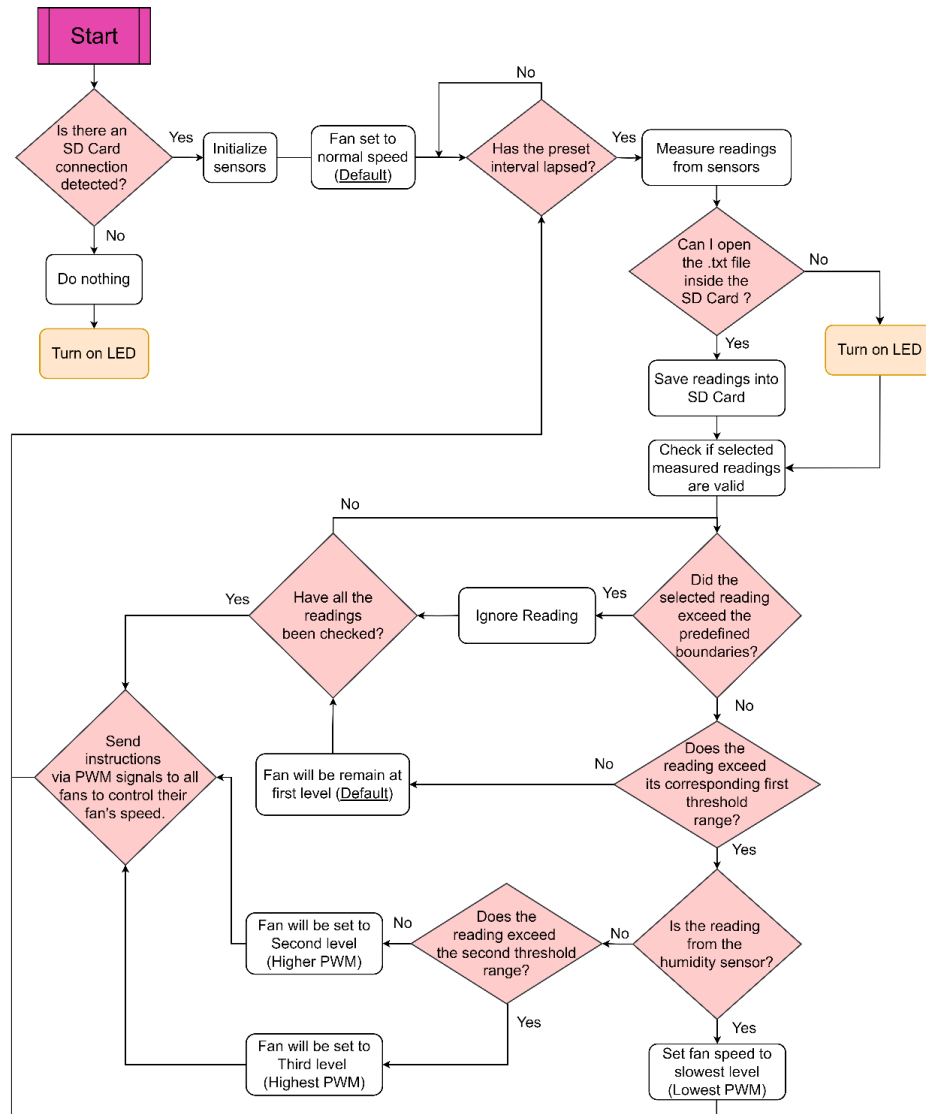


Fig. 73. Overview of Logical Flow for Storing of data and Regulating Air flow rate

One challenge encountered when utilizing the micro-SD card is the potential for interruptions in the data collection process, exemplified by the absence of data in the Phase 2 experiment. While it may be desirable to leave the experiment unattended for extended periods until it is ready for harvest, regular inspections are necessary. To facilitate the inspection process, the code has been programmed so that if the LED lights up, it will indicate a problem with the SD card connectivity.

Furthermore, in the event of an unexpected failure of the SD card at odd hours, it should not negatively impact the BSFL who are residing inside the reactor. Therefore, the code has been rewritten to ensure that if the data collection process fails, the system can continue to operate, albeit at its default settings, ensuring that the fans will continue to run at the default speed.

## 6. Conclusion and Future Work

In conclusion, utilizing the current hardware and software setup, the electronics team has developed a system capable of managing the internal conditions within the reactor to a certain extent throughout the bioconversion process. If the humidity value falls below a threshold, or if the temperature readings in the air and substrate exceed adjustable thresholds, the fan will adjust its speed accordingly, thereby influencing the internal conditions. The current optimization process is by no means efficient due to the limited testing performed and data available. However, through continued testing and the inclusion of additional sensors measuring parameters such as CO<sub>2</sub>, NH<sub>3</sub>, and mass of the food waste, significant enhancements in the optimization process are anticipated. The current implementation should suffice as a proof-of-concept prototype.

Regarding the number and placement of sensors for each parameter, definitive conclusions have not yet been reached. However, according to the findings from phase 1, particularly temperature measurement in the substrate, the middle region appears to be the optimal location, showing the least variance with only **0.819 °C** and **0.982 °C** variance. Furthermore, regarding the pH value in the substrate, the two pH analog sensor demonstrated a consistent trend of increasing pH values, suggesting a shift towards alkaline conditions, which aligns with existing studies on the behavior of the BSFL [26], [28]. With a variance of less than 0.5 (within the error range) between the two sensors, it indicates that despite the sensors being spaced apart, the consistency in their readings suggests that the pH sensor could be effectively placed somewhere along the middle region of the substrate.

In terms of data storage procedures, while the SD card offers simplicity and universal compatibility, it would be notably advantages to integrate a wireless communication device to allow the system to upload its data quickly to a cloud server. By incorporating this feature, any discrepancies or unexpected data loss can be promptly addressed by the user or researcher, enabling swift action to resolve the issue before the problem escalates. While overcoming the stringent security of NUS-Wifi with a simple purchase of a SIM card may seem feasible, the subsequent challenge lies in the

ongoing requirement to pay for and maintain a monthly subscription to a telecommunications service provider.

For future endeavors, there are several areas worth exploring. Firstly, the choice of microcontroller warrants consideration. The Arduino Mega was chosen for its expanded number of pins and compatibility with various electronic sensors. However, a primary issue arises due to the size constraints of the Arduino board. While the board can accommodate the increased number of sensors, connecting all these wires to a single small board becomes challenging. An additional concern that became apparent during experimentation is the inability of the board to detect multiple sensors if they utilize the same communication protocol. Exploring the adoption of a programmable logic device (PLC) instead of an Arduino board is worth considering, given its industrial application.

Secondly, it is with regards to the mounting of the various sensors in the reactor. The method currently in use involves using tape and Velcro to attach them to an aluminum profile bar. However, it would be more beneficial to design a linear mechanism for the sensors that measure substrate conditions, allowing for easy height adjustment. This could potentially involve utilizing a rack and pinion design for greater flexibility and accuracy in positioning the sensors.

Thirdly, it concerns the wiring. In the current design, there is a significant risk of wires coming into contact with the substrate located below when the food plastic container is pushed back into the reactor. Furthermore, the excess wire needed to accommodate the additional length for pulling the container out of its resting position increases the likelihood of these cables getting caught along the side of the sliding mechanism. To address this issue, it is important to explore alternatives beyond relying solely on a flexible spiral cable organizer. While this solution is effective for managing cables, it may not be suitable for situations involving movement, as it could lead to unwanted wire bending. Therefore, it is advisable to consider implementing a mechanism that can temporarily store the wires in a separate compartment.

## References

- [1] "Environment," Latest Data, <https://www.singstat.gov.sg/find-data/search-by-theme/society/environment/latest-data> (accessed Sep. 22, 2023).
- [2] "Waste statistics and overall recycling," National Environment Agency, <https://www.nea.gov.sg/our-services/waste-management/waste-statistics-and-overall-recycling> (accessed Sep. 22, 2023).
- [3] "Food Waste Management," National Environment Agency, <https://www.nea.gov.sg/our-services/waste-management/3r-programmes-and-resources/food-waste-management>. (accessed Sep. 22, 2023).
- [4] "Food waste," Towards Zero Waste Singapore, <https://www.towardszerowaste.gov.sg/foodwaste/> (accessed Sep. 22, 2023).
- [5] "Food Waste Management Strategies," National Environment Agency, <https://www.nea.gov.sg/our-services/waste-management/3r-programmes-and-resources/food-waste-management/food-waste-management-strategies> (accessed Sep. 22, 2023).
- [6] "Waste management infrastructure," National Environment Agency, <https://www.nea.gov.sg/our-services/waste-management/waste-management-infrastructure> (accessed Sep. 22, 2023).
- [7] "Solid waste management infrastructure," National Environment Agency, <https://www.nea.gov.sg/our-services/waste-management/waste-management-infrastructure/solid-waste-management-infrastructure> (accessed Sep. 22, 2023).
- [8] "Zero waste nation," Towards Zero Waste Singapore, <https://www.towardszerowaste.gov.sg/zero-waste-nation/> (accessed Sep. 22, 2023).

- [9] A. Tan, "Singapore aims to send one-third less waste to Semakau Landfill by 2030: Amy Khor," The Straits Times, <https://www.straitstimes.com/singapore/environment/spore-aims-to-send-one-third-less-waste-to-semakau-landfill-by-2030-ammy-khor> (accessed Nov. 13, 2023).
- [10] T.-H. Tsui and J. W. C. Wong, "A critical review: emerging bioeconomy and waste-to-energy technologies for sustainable municipal solid waste management," *Waste Dispos. Sustain. Energy*, vol. 1, no. 3, pp. 151–167, Nov. 2019, doi: 10.1007/s42768-019-00013-z.
- [11] V. Amicarelli, G. Lagioia, and C. Bux, "Global warming potential of food waste through the life cycle assessment: An analytical review," *Environ. Impact Assess. Rev.*, vol. 91, 2021, doi: 10.1016/j.eiar.2021.106677.
- [12] R. Sharma, M. Sharma, R. Sharma, and V. Sharma, "The impact of incinerators on human health and environment," 0, vol. 28, no. 1, pp. 67–72, 2013, doi: 10.1515/reveh-2012-0035.
- [13] "The science behind incineration," Towards Zero Waste Singapore, [https://www.towardszerowaste.gov.sg/science\\_behind\\_incineration/](https://www.towardszerowaste.gov.sg/science_behind_incineration/) (accessed Sep. 22, 2023).
- [14] "Waste-to-energy incineration plants," National Environment Agency, <https://www.nea.gov.sg/our-services/waste-management/waste-management-infrastructure/semakau-landfill/waste-to-energy-and-incineration-plants> (accessed Sep. 22, 2023).
- [15] "Integrated Sustainability Report 2021/2022," National Environment Agency, <https://www.nea.gov.sg/integrated-sustainability-report-2021-2022/review-of-fy2021/enabled-by-a-high-performance-and-future-ready-nea/walking-the-talk> (accessed Sep. 22, 2023).
- [16] "The case for Zero waste," Towards Zero Waste Singapore, <https://www.towardszerowaste.gov.sg/zero-waste-masterplan/chapter1/case-for-zero-waste> (accessed Sep. 22, 2023).

- [17] R. Syme, "A review of domestic waste management policy and law in Singapore," *Asia Pac. J. Environ. Law*, vol. 24, no. 1, pp. 90–119, 2021, doi: 10.4337/APJEL.2021.01.04.
- [18] "Foreword," Towards Zero Waste Singapore, <https://www.towardszerowaste.gov.sg/zero-waste-masterplan/foreword/> (accessed Sep. 22, 2023).
- [19] "Food," Towards Zero Waste Singapore, <https://www.towardszerowaste.gov.sg/zero-waste-masterplan/chapter3/food/> (accessed Sep. 22, 2023).
- [20] S. Jain, S. Jain, I. T. Wolf, J. Lee, and Y. W. Tong, "A comprehensive review on operating parameters and different pretreatment methodologies for anaerobic digestion of municipal solid waste," *Renew. Sustain. Energy Rev.*, vol. 52, pp. 142–154, Dec. 2015, doi: 10.1016/j.rser.2015.07.091.
- [21] National University of Singapore, "Food waste at East Coast Lagoon Food Village to be turned into energy and fertiliser under pilot project," NUSnews, <https://news.nus.edu.sg/food-waste-at-east-coast-lagoon-food-village-to-be-turned-into-energy-and-fertiliser-under-pilot-project/> (accessed Nov. 16, 2023).
- [22] A. Kumar and S. R. Samadder, "Performance evaluation of anaerobic digestion technology for energy recovery from organic fraction of municipal solid waste: A review," *Energy*, vol. 197, p. 117253, Apr. 2020, doi: 10.1016/j.energy.2020.117253.
- [23] "NEA Commences Next Stage Of Tuas Nexus Integrated Waste Management Facility To Develop Integrated Sludge Processing And Food Waste Treatment Facilities," National Environment Agency, <https://www.nea.gov.sg/media/news/news/index/nea-commences-next-stage-of-tuas-nexus-integrated-waste-management-facility-to-develop-integrated-sludge-processing-and-food-waste-treatment-facilities> (accessed Nov. 17, 2023).

- [24] M. Mannaa, A. Mansour, I. Park, D.-W. Lee, and Y.-S. Seo, "Insect-based agri-food waste valorization: Agricultural applications and roles of insect gut microbiota," *Environ. Sci. Ecotechnology*, vol. 17, p. 100287, Jan. 2024, doi: 10.1016/j.ese.2023.100287.
- [25] S. A. Siddiqui et al., "Black soldier fly larvae (BSFL) and their affinity for organic waste processing," *Waste Manag.*, vol. 140, pp. 1–13, Mar. 2022, doi: 10.1016/j.wasman.2021.12.044.
- [26] D. Purkayastha and S. Sarkar, "Sustainable waste management using black soldier fly larva: a review," *Int. J. Environ. Sci. Technol.*, vol. 19, no. 12, pp. 12701–12726, Dec. 2022, doi: 10.1007/s13762-021-03524-7.
- [27] B. Dortmans, S. Diener, V. Bart, and C. Zurbrügg, "Introduction into BSF biowaste processing," *Black soldier Fly Biowaste processing: A step-by-step guide*, 2nd ed, Dübendorf: eawag, 2017, ch. 2, sec. 2.1 pp. 5-7
- [28] M. Salam et al., "Effect of different environmental conditions on the growth and development of Black Soldier Fly Larvae and its utilization in solid waste management and pollution mitigation," *Environ. Technol. Innov.*, vol. 28, p. 102649, Nov. 2022, doi: 10.1016/j.eti.2022.102649.
- [29] B. Dortmans, S. Diener, V. Bart, and C. Zurbrügg, "Introduction into BSF biowaste processing," *Black soldier Fly Biowaste processing: A step-by-step guide*, 2nd ed, Dübendorf: eawag, 2017, ch. 2, sec. 2.2 pp. 7
- [30] C. Tan, "Researchers develop blueprint for Sustainable Food System using black soldier flies," *The Straits Times*, <https://www.straitstimes.com/singapore/researchers-develop-blueprint-for-sustainable-food-system-using-black-soldier-flies> (accessed Nov. 17, 2023).
- [31] C. Lalander, S. Diener, C. Zurbrügg, and B. Vinnerås, "Effects of feedstock on larval development and process efficiency in waste treatment with black soldier fly (*Hermetia illucens*)," *J. Clean. Prod.*, vol. 208, pp. 211–219, Jan. 2019, doi: 10.1016/j.jclepro.2018.10.017.

- [32] "CNA explains: Where does Singapore get its food from?," CNA,  
<https://www.channelnewsasia.com/singapore/cna-explains-where-does-singapore-get-its-food-2709161> (accessed Sep. 22, 2023).
- [33] "30 by 30," Our Food Future, <https://www.ourfoodfuture.gov.sg/30by30/> (accessed Sep. 22, 2023).
- [34] "Food Import & Export," Singapore Food Agency, <https://www.sfa.gov.sg/food-import-export/import-export-transshipment-of-live-poultry-livestock> (accessed Nov. 16, 2023).
- [35] "Our targets," Singapore Green Plan 2030, <https://www.greenplan.gov.sg/targets/> (accessed Sep. 22, 2023).
- [36] B. Dortmans, S. Diener, V. Bart, and C. Zurbrügg, "Introduction into BSF biowaste processing," Black soldier Fly Biowaste processing: A step-by-step guide, 2nd ed, Dübendorf: eawag, 2017, ch. 4, sec. 4.1 pp. 39
- [37] A. Parodi et al., "Bioconversion efficiencies, greenhouse gas and ammonia emissions during black soldier fly rearing – A mass balance approach," J. Clean. Prod., vol. 271, p. 122488, Oct. 2020, doi: 10.1016/j.jclepro.2020.122488.
- [38] K. V. Beskin et al., "Larval digestion of different manure types by the black soldier fly (Diptera: Stratiomyidae) impacts associated volatile emissions," Waste Manag., vol. 74, pp. 213–220, Apr. 2018, doi: 10.1016/j.wasman.2018.01.019.
- [39] B. Dortmans, S. Diener, V. Bart, and C. Zurbrügg, "Introduction into BSF biowaste processing," Black soldier Fly Biowaste processing: A step-by-step guide, 2nd ed, Dübendorf: eawag, 2017, ch. 4, sec. 4.1.2 pp. 41-43
- [40] "Managing Hawker Centres and Markets in Singapore," National Environment Agency,  
<https://www.nea.gov.sg/our-services/hawker-management/overview> (accessed Nov. 17, 2023).

- [41] K. Ganapathy, "Pilot project to use Hawker Centre food waste to generate electricity, produce fertiliser," CNA, <https://www.channelnewsasia.com/singapore/food-waste-nea-nus-nparks-east-coast-park-electricity-fertiliser-2319196> (accessed Nov. 17, 2023).
- [42] J. Y. K. Cheng, S. L. H. Chiu, and I. M. C. Lo, "Effects of moisture content of food waste on residue separation, larval growth and larval survival in black soldier fly bioconversion," *Waste Manag.*, vol. 67, pp. 315–323, Sep. 2017, doi: 10.1016/j.wasman.2017.05.046.
- [43] "Temperature, Air, Wind, Gas and Soil Sensors," Kuriosity, <https://kuriosity.sg/collections/temperature-air-wind-gas-soil> (accessed Nov. 18, 2023).
- [44] "How Soil Moisture Sensor Works and Interface it with Arduino," Last Minute Engineers, <https://lastminuteengineers.com/soil-moisture-sensor-arduino-tutorial/> (accessed Nov. 19, 2023).
- [45] "Interfacing Capacitive Soil Moisture Sensor with Arduino," Last Minute Engineers, <https://lastminuteengineers.com/capacitive-soil-moisture-sensor-arduino/> (accessed Nov. 19, 2023).
- [46] "Digital Luminosity Lux Light Sensor BH1750," Kuriosity, <https://kuriosity.sg/collections/light-line-ir-colour/products/digital-luminosity-lux-light-sensor-bh1750> (accessed Nov. 18, 2023).
- [47] "Arduino with BH1750 Ambient Light Sensor," Random Nerd Tutorials, <https://randomnerdtutorials.com/arduino-bh1750-ambient-light-sensor/> (accessed Nov. 19, 2023).
- [48] "Digital temperature sensor DS18B20 waterproof with JST header," Kuriosity, <https://kuriosity.sg/collections/temperature-air-wind-gas-soil/products/digital-temperature-sensor-ds18b20-waterproof-with-jst-header> (accessed Nov. 18, 2023).
- [49] "Interfacing DS18B20 1-Wire Digital Temperature Sensor with Arduino," Last Minute Engineers, <https://lastminuteengineers.com/ds18b20-arduino-tutorial/> (accessed Nov. 19, 2023).

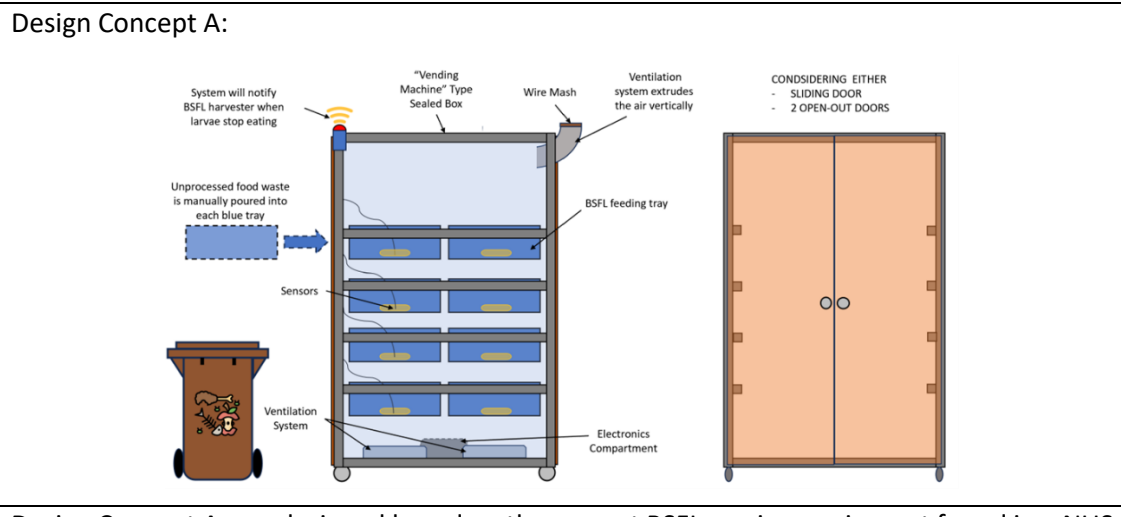
- [50] “Digital Temperature Sensor DS18B20,” Kuriosity, <https://kuriosity.sg/collections/temperature-air-wind-gas-soil/products/digital-temperature-sensor-ds18b20> (accessed Nov. 18, 2023).
- [51] “Interfacing DHT11 and DHT22 Sensors with Arduino,” Last Minute Engineers, <https://lastminuteengineers.com/dht11-dht22-arduino-tutorial/> (accessed Nov. 19, 2023).
- [52] engineer2you. *Arduino humidity sensors: Testing and calibration* (2020). Accessed: April 03, 2024. [Online Video]. Available at: <https://www.youtube.com/watch?v=6va7Et6ppz0>
- [53] “10,000ppm MH-Z16 Ndir CO2 sensor with I2C/UART 5V/3.3V interface for Arduino/Raspeberry Pi,” Sandbox Electronics, <https://sandboxelectronics.com/?product=mh-z16-ndir-co2-sensor-with-i2cuart-5v3-3v-interface-for-arduinoraspeberry-pi> (accessed Nov. 18, 2023).
- [54] “How does an NDIR CO2 Sensor Work?,” CO2 Meter, <https://www.co2meter.com/eng/blogs/news/how-does-an-ndir-co2-sensor-work> (accessed Nov. 19, 2023).
- [55] “Air Quality Sensor SGP30,” Kuriosity, [https://kuriosity.sg/products/air-quality-sensor-sgp30?\\_pos=1&\\_sid=3bf3812b7&\\_ss=r](https://kuriosity.sg/products/air-quality-sensor-sgp30?_pos=1&_sid=3bf3812b7&_ss=r) (accessed Apr. 2, 2024).
- [56] “Interfacing SGP30 CO2 & TVOC sensor with Arduino,” How To Electronics, <https://how2electronics.com/interfacing-sgp30-co2-tvoc-sensor-with-arduino/> (accessed Apr. 2, 2024).
- [57] “Gas Sensor MQ137 ammonia NH3,” Continental Electronics, <https://continental.sg/product/gas-sensor-mq137-ammonia-nh3/> (accessed Apr. 2, 2024).
- [58] Winsen MQ Sensor, <https://www.winsen-sensor.com/mq-sensor.html> (accessed Apr. 2, 2024).
- [59] “Gravity: Analog ch4 gas sensor (MQ4) for Arduino,” DFRobot, <https://www.dfrobot.com/product-683.html> (accessed Apr. 2, 2024).
- [60] “Gravity Analog pH Sensor Meter Kit V2,” DFRobot, [https://wiki.dfrobot.com/Gravity\\_\\_Analog\\_pH\\_Sensor\\_Meter\\_Kit\\_V2\\_SKU\\_SEN0161-V2#More\\_Documents](https://wiki.dfrobot.com/Gravity__Analog_pH_Sensor_Meter_Kit_V2_SKU_SEN0161-V2#More_Documents) (accessed Apr. 3, 2024).

[61] I. Luuk, “Using Four Load Cells in a Single Circuit,” 50kg Load Cells with HX711 and Arduino. 4x, 2x, 1x Diagrams. - Circuit Journal, <https://circuitjournal.com/50kg-load-cells-with-HX711> (accessed Apr. 3, 2024).

[62] “Arduino with load cell and HX711 amplifier (Digital Scale),” Random Nerd Tutorials, <https://randomnerdtutorials.com/arduino-load-cell-hx711/> (accessed Apr. 3, 2024).

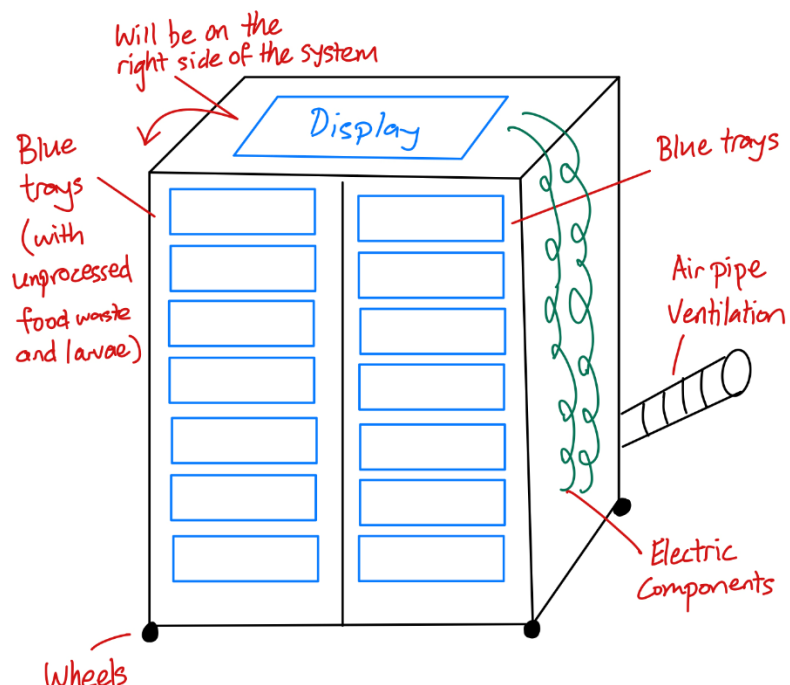
# Appendix

## Appendix A: List of Design Concepts



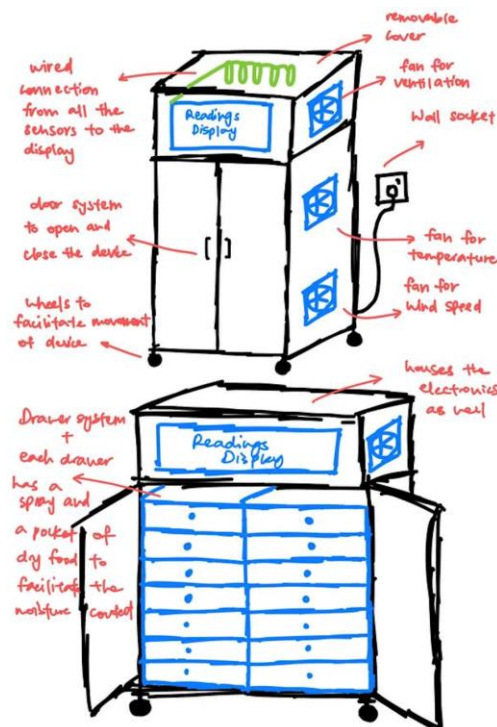
Design Concept A was designed based on the current BSFL rearing equipment found in a NUS research lab under ETH, researching on Food Waste Management and Sustainable Food Production in Urban System. The main difference of this design is the incorporation of a sealed environment and additional sensors to help regulate the air-flow. However, because of the simplic nature and lack of novelty behind this idea, Concept A was not selected.

Design Concept B:



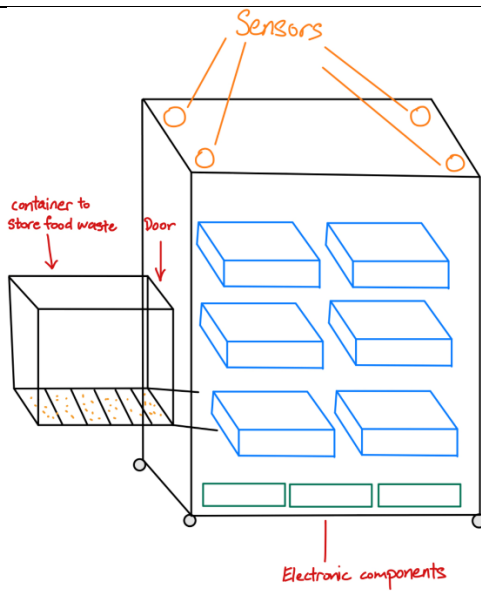
Design Concept B was also designed based on the existing BSFL rearing equipment. However, the main difference is that the height is significantly reduced. Lowering the height reduces the risk of injury for individuals handling the loading and unloading of food waste, minimizing the strain associated with these activities. However, this idea was shelved due to other considerations that arose during the course of the project.

#### Design Concept C:



Design Concept C was conceived as a cabinet-like structure, featuring a door and shelves of different heights, much like a traditional cabinet. The difference is that this design will be incorporating wheels and a ventilation system to regulate the air-speed inside the structure. However, this idea was shelved due to other considerations that arose during the course of the project.

#### Design Concept D:



Design Concept D is more unique in the sense that there is a convey-like system that will aid the food waste loader load and unload food waste. The food waste will be placed stored in a separate container and then fed into the opening on the left. The system will detect the presence of a container and rotate that container to an available spot dictated by the 6 blue containers. However, due to the complexity of the design, Design Concept D was not selected.

## Appendix B: Solution Principles

*Tab. 1. Morphological Chart*

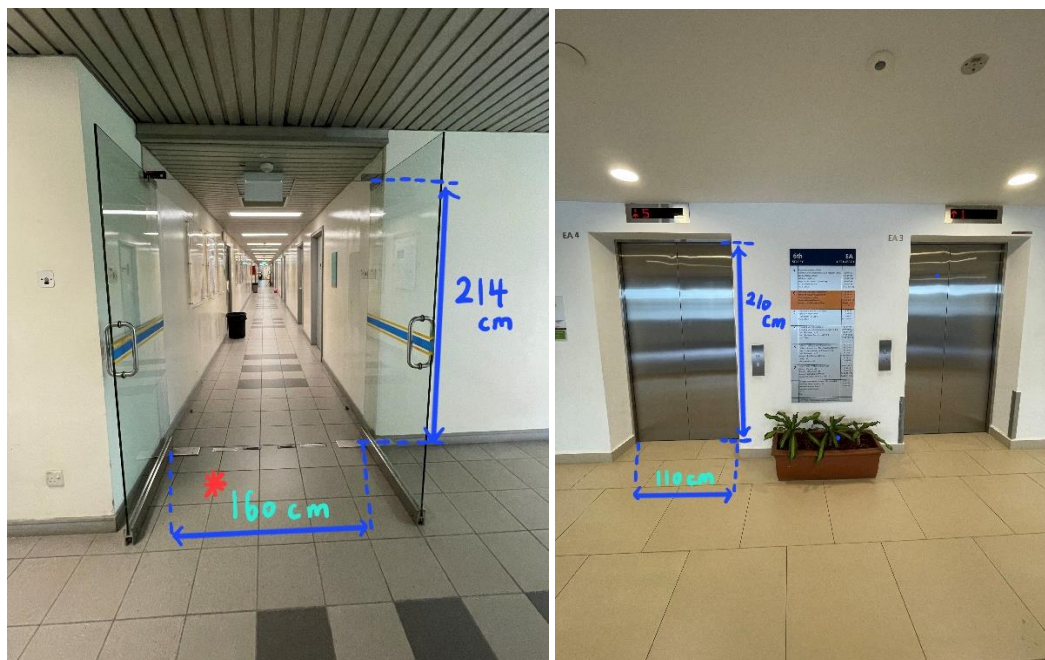
Function	Solution Principles			
<b>Supply Energy</b>	Electrical Grid	Battery Pack	Solar Power	Kinetic
<b>Control Unit</b>	Microcontroller	Microprocessor	Programmable logic controller	
<b>Receive User Input</b>	Human	Stylus Pen	External Plug in Device	
<b>Display Parameters</b>	Screen	Wireless Display	External Plug in Device	
<b>Measure Environmental Parameters</b>	Sensors	Camera	Sampling	
<b>Adjust Environmental Parameters</b>	Motor	Heater	Refrigerant	Evaporative Cooling
<b>Odor Prevention</b>	Chemical	Ventilation System	Containment	Purifiers
<b>Foreign Object Prevention</b>	Wire Mesh	Fabric	Animal Trap	Compression
<b>Bioconversion Alert</b>	Audio	Wireless	Text	LED

Table 2 shows the morphological chart of the various possible solution principles. The list of functions identified were based on assumptions as well as feedback provided by Fuhrmann Adrian. Adrian is in charge of the BSFL research facility that is researching on using BSFL in Food Waste Management and Sustainable Food Production in Urban System. One crucial feedback offered was the need to implement a mechanism to prevent foreign objections from entering the system. Since the reactor is planned to be set up in a decentralized manner around Singapore, the environment in which the reactor is to be operational will not be akin to a laboratory environment. There is a likelihood that other insects and rodents may detect the food waste within the reactor and attempt to enter it. Given the potential for external interference, it is crucial to take measures to safeguard the bioconversion process from being physically affected.

## Appendix C: Lift and Passageways Considerations in NUS

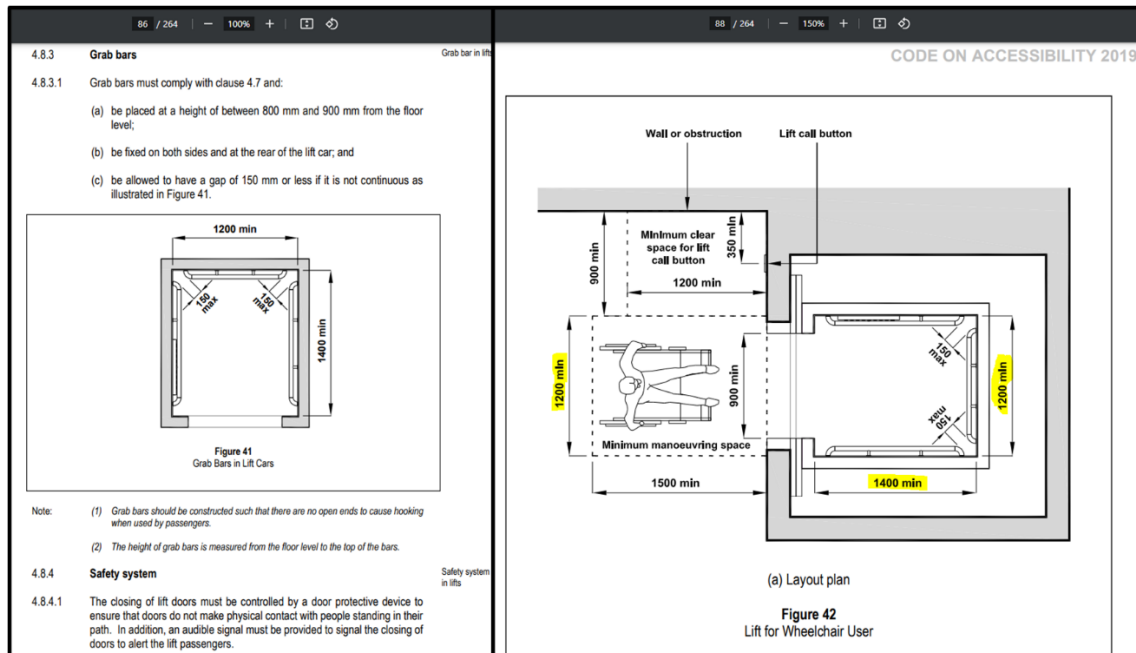
Because the BSFL reactor will be first designed on NUS campus, we need to at least ensure that the reactor can be moved around the Engineering Area of NUS. Considering that the project may need to be exhibited at the EA building, most of the measurements taken were along that direction. Due to its large size, we would also need to ensure that the size of the reactor will not be larger than the door openings of the various lifts along the direction mentioned.





As there were several lifts of different sizes in NUS, we needed to find out whether there is a minimum requirement for the various lifts in NUS and possibly in Singapore. As seen in the figure below, there is a minimum requirement for the various lift's dimensions. Where lifts are available in a building, at least one lift must be made accessible for wheelchair users. Using this piece of information, we could potentially get a sense of the design requirements for our reactor.

Source: <https://www1.bca.gov.sg/docs/default-source/universaldesign/accessibilitycode2019.pdf>



## Appendix D: Explanation for the Weight of the Reactor

As discussed in Section 2.5.2, the goal of the project is to have the reactors be deployed in a decentralized manner to treat the food waste at its source. Considering that some hawker centers can be found within buildings, the weight of the reactor needs to be lower than the maximum weight capacity of the respective lift in Singapore. To determine if there exist a standard maximum weight capacity for lifts in Singapore, we search various Singapore standards. However, to no avail as the maximum weight capacity for lifts fluctuates based on factors such as their dimensions, speed, and the dimensions of the lift shaft within the building, among others. (Source: <https://kleemannlifts.com/newsletter/choosing-right-passenger-lift-your-building>)

As a last resort, we decided to use a vending machine as a benchmark example as it has been designed to be deployable in numerous locations around Singapore. By using the Ben & Jerry's Ice cream vending machine as a possible example, since the company claim to have more than 300 ice cream vending machines deployed across Singapore, this could be a plausible point of reference for our reactor.

Source: <https://happyice.com.sg/frozen-vending-machine-draft/>



Technical Specification	
Model :	Model E
Weight:	280Kg
Dimension:	71.4 x 90 x 198 cm (Length x Depth x Height)
Input voltage:	230-240Ac
Rated current:	1A
Power:	200W
Vending interface:	MDB
Connectivity:	3G
<a href="#">Video: How it works</a>	

## **Appendix E: Explanation for the Dimensions of the Reactor**

The dimension of the reactor are in comparison with the dimension of a vending machine. As mentioned in Appendix C, the dimension of the reactor needs to be at least smaller than the various pathways and doorways around the Engineering Area of NUS. A vending machine is an ideal benchmark example as it has been designed to be deployable in numerous locations around Singapore. Hence, we decided that we ought to benchmark the dimensions of the reactor to a vending machine.

To ascertain the dimensions of a vending machine, we researched various Singapore standards. Ultimately, we did find a Singapore Standard SS 690:2022—Guidelines for Food Safety and Good Hygienic Practices for the Vending Industry. However, this standard was not specific to vending machines; rather, it applied to machines in general, with a requirement that they cannot occupy more than 3 square meters of void deck floor space. As such, it did not provide any exact dimensions for a standard vending machine. Various International and American standards were explored but still no luck.

## Appendix F: Calculations to support the use of 6 fans in one 8-way extension safety socket

SG Voltage: 230 V

Extension cord: 13A Max. [Limit]

---

Fan Supply voltage: 12V

Current : 2 A

---

Safety mark      3-Pin Plug      { V: 12 V  
Rating                                    I: 2.5 A

Power consumption : 30 W [Full 2.5A being Drawn]

Current Consume from a single 3-Pin Plug:  $\frac{30 \text{ W}}{230 \text{ V}} = 0.1304347 \text{ A}$

Since the Limit is 13A, assume 3A set aside for microcontroller & sensor,  
I will have  $\sim 10 \text{ A}$  Remaining.

Since the current rating of the fans (2 A) is below the maximum output current rated by the power adapter at 2.5 A, the power consumption from the fans will not reach 30 W. Consequently, after taking into consideration the microcontroller and 5V DC-DC Step Down buck converter, the total current drawn will remain below the 13 A limit of the 8-way extension socket.